Evolutionary Developmental Morphology of the Distal Humerus in Hominoids and Fossil hominins

by

Aileen Fernandez

A dissertation accepted and approved in partial fulfillment of the

requirements for the degree of

Doctor of Philosophy

in Anthropology

Dissertation Committee:

Stephen Frost, Chair

Frances White, Core Member

Scott Blumenthal, Core Member

Andy Karduna, Institutional Representative

University of Oregon

Spring 2025

DISSERTATION ABSTRACT

Aileen Fernandez

Doctor of Philosophy in Anthropology

Title: Evolutionary Developmental Morphology of the Distal Humerus in Hominoids and Fossil Hominins

Bipedalism is considered a key development in the *Homo* lineage that removed the necessity of using the upper extremity for locomotion, essentially freeing the hands for other tasks. Australopiths, early human ancestors exhibited skeletal features both cranial and postcranial, that researchers agree are indicative of bipedal walking. However, they also exhibit features considered to be primitive ape-like. The importance of these ape-like features has been subject to an ongoing debate because depending on whether they served a functional purpose can help us understand the evolutionary selective pressures that led to upright walking. It has broader implications on the origin of bipedalism as it is tied to larger evolutionary hypotheses related to *Homo.*

This dissertation will address this ongoing debate by investigating the morphology of the distal humerus as it is part of the elbow joint which is used differently depending on whether you are a bipedal or quadrupedal. This dissertation will: 1) examine the morphology of adult hominoids using a large and diverse sample, including one cercopithecid as an outlier specialized arboreal monkey, 2) use an ontogenetic approach to test hypotheses on plasticity and use of the distal humerus using a large sample of hominoids across several developmental stages, and 3) investigate variation in the distal humerus across a sample of australopith fossils.

CURRICULUM VITAE

NAME OF AUTHOR: Aileen Fernandez

GRADUATE AND UNDERGRADUATE SCHOOLS ATTENDED:

University of Oregon, Eugene
Lehman College CUNY, New York

DEGREES AWARDED:

Doctor of Philosophy, Anthropology, 2025, University of Oregon
Master of Science, Anthropology, 2018, University of Oregon
Bachelor of Arts, Anthropology and History, 2016 Lehman College

AREAS OF SPECIAL INTEREST:

Geometric Morphometrics

PROFESSIONAL EXPERIENCE:

Graduate Teaching Fellow, University of Oregon, 2017-2025

Natural History Research Experience (NHRE) Intern, Smithsonian, 2014

GRANTS, AWARDS, AND HONORS:

AABA IDEAS Program Student Scholar Award, 2024

Community for Minorities in Stem (CMiS) Excellence in Research Travel Award, 2024

Paleoanthropology Society Grant, 2018

Oregon SYLFF Fellowship for International Research, 2022

Graduate Teaching Fellowship, First Year School, 2016-2017

Lehman College Foundation Scholarship, Lehman College, 2011-2015

ACKNOWLEDGMENTS

I would first like to thank Dr. Stephen Frost who has been the best graduate advisor I could ask for. His incredible patience and relentless support encouraged me to never give up. Thank you to my committee members, Dr. Frances White and Dr. Scott Blumenthal, for their wisdom and advice. I also want to thank Dr. Andy Karduna, who gave me the opportunity to teach Human Anatomy in the Human Physiology department and introduced me to a passion I will carry with me into my future career.

This dissertation would not be possible if not for the generosity of Dr. Mike Plavcan, Dr. Carol Ward, Dr. Sergio Almecija, and Dr. Kelsey Pugh for providing me with their humeri surface scans when the COVID-19 pandemic halted access to all collection. Thank you to all the wonderful people I met while traveling overseas collecting data, Dr. Mathy Rotonda and Dr. Emmanuel Gilissen (Royal Museum for Central Africa, Tervuren), Dr. Pepijn Kamminga (Naturalis Biodiversity Center, Leiden), Dr. Colin Shaw and Markus Gisi (University of Zurich), Dr. Maria Judite Silva Cardoso and Dr. Maria Susana de Jesus (National Museum of Natural Science, Lisbon) and the Portuguese Research Infrastructure of Scientific Collections (PRISC). Thank you to all the wonderful people at the American Museum of Natural History including Dr. Nancy B Simmons for access to the great apes and cercopithecids. This dissertation was fully funded by the SYLFF fellowship.

I am incredibly grateful to Dr. William Harcourt-Smith who took me under his wing when I was an undergraduate at Lehman College. He welcomed me into his lab and taught me about my first passion, functional morphology and the ankle joint. His incredible mentorship led me to Dr. Frost at the University of Oregon and made me feel welcomed in the Paleo community. Thank you for being the type of advisor I would like to be someday.

Thank you to all my family and my friends for all their encouragement over the years. You are right, there is a light at the end of the tunnel. Finally, thank you to Tyler Halford, your love and support saw me through it all.

To my grandfather

Rafael Armando Fernandez

TABLE OF CONTENTS

LIST OF FIGURES

Figure Page

LIST OF TABLES

Table Page

CHAPTER I

INTRODUCTION

INTRODUCTION

Australopiths, early human ancestors from eastern, central, and southern Africa exhibit morphological features associated with bipedalism, upright walking (Ward, 2002, Harcourt-Smith and Aiello, 2004). Yet they also have postcranial features considered to be ape-like when compared to quadrupedal extant non-human primates (Stern and Susman, 1983; Susman et al, 1984; Lovejoy, 1988; Lovejoy and Latimer 1990; Lovejoy, 1990; Latimer, 1991). The importance of these ape-like features to early hominin locomotion is part of an ongoing debate as to the selective pressures that led to upright walking in humans. As a key evolutionary development modern humans are the only living species within the *Homo* lineage that are obligate bipeds. This shift is tied to larger evolutionary hypotheses important to studies of human evolution.

1.1 Background

1.2 Fossil Hominins

1.2.1 Pre-Australopith

The earliest evidence from Chad, central Africa, a fragmentary cranium of *Sahelanthropus tchadensis,* suggests adaptations for upright walking were present 6-7 million years ago (Ma) (Brunet et al., 2002). The basiocranium of *Sahelanthropus tchadensis* has an anteriorly and horizontally positioned foramen magnum, features associated with an upright posture (Brunet et al., 2002). Postcranial elements attributed to *S. tchadensis* include the partial femur TM 266-01-063 which lacks a proximal head and distal femoral condyles, preserving only the base of the neck and shaft and two previously unreported partial ulnae TM 266-01-050 and

TM 266-01-358 (Macchiarelli et al., 2020; Davers et al., 2022; Cazenave et al., 2024). Some have argued the partial femur has musculature markings indicative of bipedalism (Davers et al., 2022), while other find evidence from the preserved neck such as the angle exceeds the range of Plio-Pleistocene hominins, matching closer in range to values seen in pronograde quadrupedal Miocene hominoids like *Rangawapithecus* (139-139 degrees) and outside the top range of variation in modern humans (Aiello and Dean, 1990; MacLatchy et al., 2000; Köhler et al., 2002; DeSilva et al., 2013; Pina, 2016; Macchiarelli et al., 2020; Pina et al., 2021). The femur of *Orrorin tugenensis* (5.8-6.2 Ma) an early hominin from the Lukeino Formation, Tugen Hills, Kenya has a shallow trochanteric fossa and pronounced gluteal tuberosity, suggestive of large leg muscles associated with upright walking (Senut et al., 2001; Pickford et al., 2002). *Ardipithecus*, especially *A. ramidus* is better represented by cranial, dental and postcranial remains. *Ardipithecus kadabba* (5.2-5.8 Ma) from the Middle Awash Valley, Ethiopia was determined to likely be bipedal based on an isolated toe phalanx (Haile-Selassie, 2001). The complete 4th proximal pedal phalanx AME-VP-1/71 has a combination of features seen in extant apes and other extinct hominids like a strong plantar curvature at the shaft, is distally dorsoventrally compressed, and proximally mediolaterally compressed with strong constriction above the base (Haile-Selassie, 2001). *Ardipithecus ramidus* (4.4 Ma) represented from 110 specimens includes the partial skeleton known as "Ardi" ARA-VP-6/500 from the 4.4 Ma Lower Aramis Member, Middle Awash, Ethiopia (White et al., 1994; White et al., 2009). ARA-VP-6/500 also had a combination of postcranial features suggesting it was capable of facultative bipedalism. This partial skeleton presents a short and broad ilia with a separated anterior inferior iliac spine (AIIS) but also a fully abducted hallux, elongated hand phalanges and an elbow that fully extends but unlike extant suspensory apes (White et al., 2009). *Kenyanthropus* platyops (~3.5 Ma) from the

Lomekwi locality in west Turkana, Kenya KNM-WT 40000 is a highly fragmented cranium that lacks postcranial elements tentatively posited to be a separate genus from *Australopithecus afarensis*, a bipedal hominin from Hadar, Ethiopia with which it was contemporaneous (Leakey et al., 2001; Hammond and Ward, 2013).

1.2.2 Australopiths

The term "australopith" is an informal category that refers to different genera of early hominins that nearly all researchers agree were bipedal, including *Australopithecus, Paranthropus,* and typically *Ardipithecus*, but not *Homo* (Kimbel and Delezene, 2009; Wood, 2010; Strait, 2010; Mongle et al., 2019; Guil-Guerrero and Manzano-Agugliaro, 2024). The Afar Depression of Ethiopia has yielded over 400 fossil remains attributed to the genus *Australopithecus,* including some of the most well-known. The partial skeleton *Australopithecus afarensis* or "Lucy" A.L. 288-1 (~3.2 Ma) from Hadar, Ethiopia at the time of its discovery was one of the most complete partial skeletons found and one of the oldest (Johanson et al., 1978; Johanson and Edey, 1981). While discoveries like *Ardipithecus* presented a mosaic of "ape-like" and "human-like" features, Lucy further highlighted this distinctive morphology. To name a few of these features, A.L. 288-1 demonstrated a short and broad pelvis and a valgus angle, both associated with a higher center of gravity for bipedalism but also curved hand and pedal phalanges commonly associated with quadrupedalism (Ward and Hammond, 2016). The nearly complete skeleton the juvenile *Australopithecus afarensis* nicknamed "Selam" DIK-1-1 (3.3 M) presents a foot and lower limb indicating bipedalism but a scapula that is gorilla-like with curved phalanges (Alemseged et al., 2006; Green and Alemseged, 2012). The discovery of the large partial skeleton KSD-VP 1/1 commonly known as "Kadanuumuu" (3.58 Ma) thought to be male from the Korsi Dora vertebrate locality 1 in Woranso-Mille paleontological area of the Afar

region, Ethiopia supported further evidence of bipedalism in *Australopithecus* (Haile-Selassie et al., 2010). KSD-VP 1/1 is older than A.L. 288-1 by about 0.4 Ma but shares homologous features with *Australopithecus* like a prominent obturator externus tendon groove, a narrow auricular surface on the sacrum and broad sacral alae relative to centrum size (Haile-Selassie et al., 2010). Evidence of habitual bipedalism includes valgus knee, an upper thorax that is more *Homo*-like based on the preserved ribs that exhibit a costal angle indicative of a deep vertebral column than seen in apes, a clavicle comparable in length that falls within the *Homo* range, a relatively complete scapula falling within range of modern humans based on largely on axillary-spine angulation with no evidence of suspensory or climbing when compared to extant hominoids (Haile-Selassie et al., 2010). The Laetoli footprints (~3.6 Ma) from Tanzania captures the human-like stride and morphology of *Australopithecus* providing further evidence of bipedalism in this genus(Le Gros Clark, 1947; Leakey and Hay, 1979; Susman and Stern, 1982, 1991; Stern and Susman, 1983; Latimer, 1987; White and Suwa, 1987; Latimer and Lovejoy, 1990a. b; Harcourt-Smith and Aiello, 2004; Hatala et al., 2016). Sites in southern Africa unearthed *Australopithecus africanus* (2.1-3.3 Ma) and *Australopithecus sediba* (1.97-1.98 Ma). Attributed to *Australopithecus africanus* is the famous "Taung child" a skull of a juvenile 3-year-old from Taung, south Africa that was a biped with an anterior foramen magnum (Dart, 1925). *Australopithecus africanus* is also known from the StW 431 adult partial skeleton from Member 4 Sterkfontein which also has a combination of ape-like and derived human-like features (McHenry and Berger, 1998). Also attributed to *A. africanus* is the partial skeleton Sts 14 (~2.5 Ma) from Member 4 Sterkfontein thought to represent a juvenile presumably female individual (Broom and Robinson, 1950). based on unfused sacral elements and presence of an epiphyseal plate on the auricular surface (Broom and Robinson, 1950; Thackeray et al., 2002). Sts 14 was

found in close proximity to the cranium "Mrs Ples" Sts 5 but there is no evidence to confidently support they are the same individual (Thackeray et al., 2002). Reconstruction of the Sts 14 pelvis suggests it was short and broad as seen in *Australopithecus* and analyses on the angulation of the sacral elements suggests presence of lumbar lordosis associated with upright standing (Abitbol, 1995; Thackeray et al., 2002). The StW 573 (3.76 Ma) partial skeleton nicknamed "Little Foot" was recovered from Member 2 within the exposed Silberberg Grotto Sterkfontein one of the oldest fossil bearing deposits (Clarke and Tobia, 1995; Clarke, 1998; Granger et al., 2015; Stratford et al., 2017, Kramers and Dirks, 2017a,b). StW 573 has been argued to represent a different *Australopithecus* species distinct from *A. africanus* based on mostly cranial and dental differences (Clarke, 2008; Clarke, 2013). The proposal that there are multiple *Australopithecus* species at Member 2 and Member 4 at Sterkfontein (Kimbel and White, 1988; Lockwood and Tobias, 2002, Fornai et al, 2018) has been challenged by those who argue the fossils are instead representative of high degrees of morphological variation within the *Australopithecus* (Ahern, 1998; Grine, 2013; Fornai et al., 2015). The partial skeleton of StW 573 appears to have a pectoral girdle adapted for arboreal behaviors rather than human-like manipulation (Carlson et al., 2021). The initial discovery of the four articulating foot bones of StW 573 was described as appearing human-like in the hindfoot but ape-like and mobile in the forefoot with a highly mobile hallux (Clarke and Tobias, 1995). The fossil known as Malapa Hominin 2 or MH2 (Uw 88-57) (~ 2.0 Ma) *Australopithecus sediba* fossils from the Malapa, Gauteng Province in southern Africa share derived features in dentition, hand, feet and pelvis with fossils and *Homo* (Berger et al., 2010; Churchill et al., 2018). However, it's upper extremity appears to be more primitive suggesting adaptations for climbing were still present and maybe more so than *Australopithecus afarensis* (Berger et al., 2010; de Ruiter et al., 2013; Kivell et al., 2011; Kibii et

al., 2011; Zipfel et al., 2011; Rein et al., 2017; Churchill et al., 2018). Then there is the genus *Paranthropus* (2.7-1.2 Ma) found through eastern and southern Africa which stood out from *Australopithecus* when compared by having pronounced chewing apparatus like a large sagittal crest, wide zygomatic bones and large molars which some suggest due to its hard diet. The overall robustness of this genus and features of the skull along with its likely tough diet and its coexistence with other australopiths suggest it was bipedal despite limited postcranial remains (Arambourg and Coppens, 1968; Walker et al., 1986; Leakey, 1959; Constantino and Wood, 2007; Cazenave et al., 2020; Richmond et al., 2020).

1.2.3. Overview

. This dissertation addresses the ongoing debate by assessing the functional morphology of the distal humerus, a major component of the elbow joint actively used by extant quadrupedal apes. Extant non-human primates rely on the varying degrees of stability and flexibility in the elbow depending on their locomotor mode when traversing across the substrate (Rose, 1988, 1993). Additionally, the humerus is an element that is well represented in the fossil record by adult and juvenile Australopiths (Johanson et al, 1982a; Lovejoy et al, 1982b; White et al, 1993; Kimbel et al 1994; Alemseged et al, 2006; Kimbel and Delezene, 2009; Berger et al., 2010; de Ruiter et al., 2013; Kivell et al., 2011; Kibii et al., 2011; Zipfel et al., 2011; Rein et al., 2017; Churchill et al., 2018). Existing studies on the distal humerus have used 2D geometric morphometrics which provides limited insight into the functional geometry of the articular surfaces, lacking a large diverse hominoid sample or an ontogenetic approach (Bacon, 2000; Zelazny, 2019). My study adds to previous work by incorporating 3D geometric morphometrics which capture and visualized all aspects of shape (Slice, 2007). I will also provide novel insight

on the ontogeny of the distal humerus using a large hominoid to build a framework for assessing australopith growth patterns and plasticity.

The first objective of this dissertation addressed in Chapter II is to analyze morphological variation of the distal humerus in a diverse sample of adult extant hominoids. This part of my dissertation I will investigate differences in adult forms among genera and the influence of allometry and locomotion. Chapter III will use a large ontogenetic sample of extant hominoids to assess ontogenetic trajectories, or patterns of growth and shape change, over developmental stages as represented by dental eruption. Previous studies have found aspects of plasticity can be traced to pivotal ages that could be informative of locomotor patterns during life (Inouye, 1994; Richmond, 2007; Zollikofer et al., 2010; Turley and Frost, 2014; Turley et al, 2015; Cowgill et al, 2018; Raichlen et al., 2017; Sarringhaus et al., 2016; Simons et al., 2019). Chapter IV will incorporate fossil Australopiths for comparative study with the extant adult sample from Chapter II and taking into consideration findings from Chapter III to make evolutionary interpretation early hominin locomotion during life.

CHAPTER II

ADULT HOMINOID DISTAL HUMERUS

2.1 Introduction

In paleoanthropology the longstanding debate as to the functional role of climbing australopiths has important implications for understanding the adaptive pressures that led to obligate bipedalism in the *Homo* lineage as it intersects with broader evolutionary hypotheses (Washburn and Lancaster, 1968; Lovejoy, 1981; Hunt et al, 1996; Wheeler, 1991; Pontzer et al., 2009; Bramble and Lieberman, 2004). The two opposing viewpoints of this debate are those who suggest the ape-like features in australopiths are primitive retentions that no longer serve a functional role (Lovejoy, 1988; Lovejoy and Latimer 1990; Lovejoy, 1990; Latimer, 1991), while others see them as evidence that quadrupedalism like climbing was still a part of their locomotor repertoire (Stern and Susman, 1983; Susman et al, 1984). The degree of arboreality is important for understanding the evolutionary timing of bipedalism and reconstructing past behaviors.

This chapter investigates variation in the distal humerus among adult hominoids as it used differently between bipeds and quadrupeds. Adult hominoids have fused epiphyses and thus offer the opportunity to assess morphology after cessation of growth and shape difference influenced by other epigenetic factors.

2.1.1 Objectives

This study has three objectives aimed at testing hypotheses related to plasticity in the adult distal humerus of extant hominoids. The first is to evaluate the effects of static allometry, which is the intraspecific size related shape variation in adult distal humeral shape across hominoids (Cardini, 2025). Static allometry differs from other forms of allometry such as evolutionary allometry, size-related shape divergence in clades of closely related species, and

ontogenetic allometry, patterns of size and shape changes occurring throughout individual development (Cardini, 2025). After taking static allometry into account, I will test for differences in adult distal humeral shape among genera. I will also test for differences in shape related to locomotor category and substrate use as represented by percentage of time on the ground.

2.2 Background

2..2.1 Distal humeral morphology

This distal humerus contributes to the elbow, a compound synovial joint formed by the humeroulnar, humeroradial and proximal radioulnar articulations. The elbow is the interface between the arm and forearm that facilitates movements of flexion-extension and pronation-supination. Modern humans are considered obligatory bipeds that do not engage the upper extremity in locomotion outside of the crawling stage and a brief window during the onset of upright walking (Ruff, 2003a,b; Cowgill and Johnston, 2018). Whereas extant apes actively engage their forelimbs while locomoting quadrupedally (Napier, 1967; Tuttle, 1981; Demes et al., 1991; Inouye, 1994; Taylor, 1997; Richmond, 2007; Jabbour, 2008; Sarringhaus et al., 2014; Arias-Martorell, 2018). Among apes, locomotion can be further subdivided by substrate type such as terrestrial, on the ground which the degree of use varies by species, or arboreal, in trees which can be further categorized by support type, substrate size and height. Terrestrial genera include the African large-bodied *Gorilla* and the smaller *Pan* which are both specialized knuckle-walkers, for which the evolutionary origins remain unclear (Napier, 1967; Tuttle, 1972; Inouye, 1994; Doran, 1996; Richmond, 2007; Simpson et al., 2018; Orr, 2018; Vaesen et al., 2020; Tarrega-Sunders et al., 2021). Asian apes, like the large-bodied *Pongo* are specialized arboreal quadrumanous scramblers as they pull and shift their weight using all four limbs across the canopy (Cant, 1987; Hunt, 1991; Oishi et al., 2008; Alméjica et al., 2021). Smaller-bodied

Hylobates and *Symphalangus* are brachiators that specialize in suspensory locomotion swing between branches to propel long distances (Fleagle, 1974; Fleagle, 1976; Hunt, 1991; Gebo, 1996; Malone, 2007; Alméjica et al., 2021).

2.3 Materials and Methods

2.3.1 Sample specimens

The sample consists of 164 distal humeri of adult individuals across 7 hominoid genera including *Gorilla*, *Homo*, *Pongo*, *Pan, Hylobates,* and *Symphalangus* and the large-bodied cercopithecid *Nasalis* (Table 1). I treated the two closely related species *Pan paniscus* and *Pan troglodytes* separately. This is because *Pan paniscus* is significantly more arboreal than *P. troglodytes* and engages considerably more arboreal quadrupedalism but also knuckle-walks when on the ground (White, 1996, 2020). *Nasalis* is a cercopithecid that was included as a comparative reference since it is a pronograde monkey that is an arboreal quadruped and leaper. *Nasalis* inhabits mangroves and lowland rain forests where it locomotes mainly by clambering and leaping but is also a proficient swimmer and has been observed to engage is some brachiation (Napier and Napier, 1967; Kawabe and Mano, 1972; Meijaard and Nijman, 2000, Su and Jablonski, 2009). One hundred-nineteen (119) specimens were collected by the author across international museums including the American Museum of Natural History (New York), Naturalis Biodiversity Center (Leiden, Netherlands), Royal Museum for Central Africa (Tervuren, Belgium), Universität Zürich (Zurich, Switzerland), and Museu Nacional de História Natural e da Ciência (Lisbon, Portugal). Surface scans were collected using the Artec Space Spider structured light scanner and the 3D shining Einstar handheld scanner (Artec 3D; Einstar). Both scanners operate with high resolution up to 0.1mm and accuracy up to 0.5mm. An additional 45 surface scans of specimens from the American Museum of Natural History in New

York, the Cleveland Natural History Museum in Cleveland, Ohio, the National Museum of Natural History in Washington, D.C., the Museum of Comparative Zoology at Harvard University, the Royal Museum for Central Africa in Tervuren, Belgium and the Stony Brook Anatomy Collection at Stony Brook University were generously shared by Dr. Joseph Plavcan, Dr. Carol Ward, Dr. Sergio Alméjica and Dr. Kelsey Pugh. See also appendix A for sample details.

Table 1: Chapter II specimens. 164 surface scans of distal hominoid humeri was included in this study, with a total of 81 males, 78 females and 5 of unknown sex. Details for each specimen including species are provided in Appendix 1

Genus	**Male**	**Female**	**Unknown**	**Total**
Gorilla	17	14	0	31
Homo	13	17	0	30
Hylobates	8	10	1	19
Nasalis	4	0	0	5
Pan paniscus*	11	*7*	0	18
Pan troglodytes*	22	*18*	4	44
Pongo	5	*8*	0	13
Symphalangus	1	*3*	0	4
Total	**81**	***78***	**5**	**164**

2.3.2 Data collection

Three-Dimensional Procrustes coordinate data were collected using a 28-landmark configuration on the distal humeral articular surfaces, medial and lateral epicondyles (Figure 1). The protocol was adapted from Tallman (2010), however there are previous studies that have

also used similar landmark configurations to assess the morphology of the distal humerus (see, McHenry, 1976; Bacon, 2000; Lague, 2014; Rosas et al., 2015; Zelazny, 2019). My 28-landmark configuration was adapted to capture the projection of the medial trochlear border, the depth of the trochlear groove and zona conoidea, and the overall shape of the capitulum. Additionally, I wanted to capture the size and depth of the olecranon fossa and the relative positions of the medial and lateral epicondyles. The shape of the trochlear border varies among hominoids where in *Homo* it appears to be more medial and distally projecting than in apes creating a more angular appearance (Zelazny, 2019). Tallman (2010) found the trochlea in apes to be deeper and wider, while humans had a higher, narrow and more asymmetrical morphology. The depth of the trochlear groove is notably the zona conoidea has been posited to help stabilize the radial head and its articulation with the capitular surface (Rose, 1988; Rose, 1993; Zelazny, 2019) See Table 2 for a complete description of each landmark location.

Figure 1: Chapter II landmarking protocol. From left to right a right male *Gorilla beringei* specimen catalog number 115609 from the American Museum of Natural History (New York) is demonstrated with the complete 28 single-point landmark protocol on the distal humerus. (A) posterior view, (B) anterior view, and (C) inferior view.

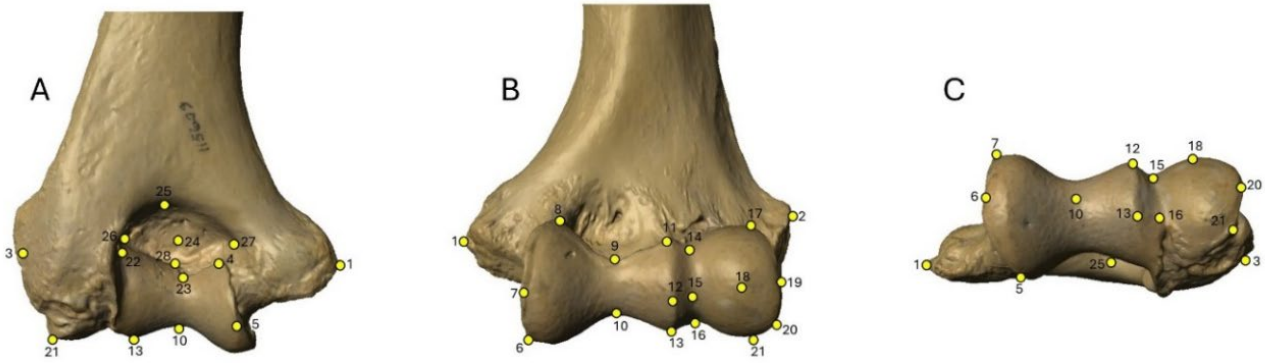

Table 2: Chapter II Landmark Description. Detailed description of landmark locations organized by region of the distal humerus.

Landmarks	Description
Medial Epicondyle	
1	most projecting point on the medial epicondyle
Laterale Epicondyle	
2	most projecting point on the lateral epicondyle
3	posterior aspect of the lateral epicondyle
Trochlea	
4	most posterior medial corner of the trochlea
5	most posterior projecting point of along the trochlear margin
6	most inferior projecting point of the trochlear margin
7	most anterior projecting point of the trochlear margin
8	most anterior midpoint projecting point of the trochlear margin
9	most superior anterior point of the trochlear margin
Trochlear groove	
9	deepest superior point of the trochlear groove
10	deepest inferior point of the trochlear groove
23	deepest point of the trochlear groove on the posterior aspect
Zona conoidea	
11	most superior point on the zona conoidea ridge
12	midpoint on the zona conoidea ridge
13	most inferior point on the zona conoidea ridge
14	deepest point parallel to lm 11
15	deepest point parallel to lm 12
16	deepest point parallel to lm 13

Table 2 (Continued)

Capitulum	
17	most superior lateral point of the capitulum margin
18	most projecting central point on the capitulum
19	point most in line with lm 18 along the capitulum margin
20	most inferior anterior point along the capitulum margin
21	most inferior point along the capitulum margin
22	most posterior point along the capitulum margin from the posterior aspect
Olecranon fossa	
24	deepest point in the olecranon fossa
25	most superior point along the olecranon fossa margin
26	most lateral point along the olecranon fossa margin
27	most medial point along the olecranon fossa margin
28	most inferior point along the midline of the olecranon fossa

2.3.3 Analytical methods

All analyses were performed in the *R* scientific computing language version 4.5.0 (R Development Core Team, 2025). The following packages were used: Geomorph version 4.0. (Adams and Otárola-Castillo, 2013; Adams and Collyer, 2018; Baken et al., 2021; Adams et al., 2025) for Generalized Procrustes analysis and Principal Component analysis. Geomorph is a software package that allows for all steps in 3D geometric morphometrics (Adams and Otárola-Castillo, 2013). Additionally, dplyr to treat the data for selecting and transforming the classifiers, the grouping variables, and ggplot2 version 3.5.2 (H.Wickham, 2016) and ggrepel version 0.9.6 (Slowikowski, 2024) were used for creating the resulting scatter plots.

2.3.3.1 3D Geometric Morphometrics

Geometric Morphometrics (GM) is a field of multivariate statistics that is concerned with all aspects of biological shape, including change, variation, group difference and possible influential external factors (Rohlf, 1990; Slice, 2007; Cook and Terhune, 2015). GM is different from traditional morphometrics because it uses the cartesian coordinates of homologous landmarks as variables which results in its capability to retain all geometric information throughout the research process and visualize it (Cook and Terhune, 2015; Mitteroecker and Gunz, 2009). This study directly deals with objectives investigating aspects of the distal humerus in hominoids as it relates to functional morphology and phylogeny that 3D GM can address.

2.3.3.2 Generalized Procrustes analyses

Generalized Procrustes analysis (GPA) was used to superimpose the landmark configurations. Specimens are scaled to the same unit centroid size, defined as the square root of the sum of squared distances of each landmark in a configuration to their average (Bookstein, 1991; Slice, 2007; Cooke and Terhune, 2015). Superimposition translates and rotates each specimen to minimize the squared distances between landmarks of each configuration and the consensus (Bookstein, 1991; Slice, 2007). Thus, after GPA and remaining differences in landmark coordinates represent differences in shape. With three-dimensional data, this step removes 7 degrees of freedom, 3 each for translation and rotation, and 1 for scale (Rohlf and Slice, 1991). GPA is an important step as it allows shape comparison after removing all non-shape variables and allows for multivariate testing (Slice, 2007; Klingenberg, 2020).

2.3.3.3 Principal components analysis

After superimposition a Principal components analysis (PCA) was performed on the dataset. A PCA holds no statistical power, rather it is an exploratory tool that performs a singular

value decomposition on data matrix (Rohlf, 1990; Bookstein, 1991; Slice, 2007; Klingenberg, 2020). This is achieved by centering the superimposed landmark configurations to the mean shape known as the consensus, so that the consensus lies at the origin, and the data are then rotated to orthogonal (i.e. uncorrelated) axes (called principal components) that each explains the most variance (Rohlf, 1990; Bookstein, 1991; Klingenberg, 2020). It also ordinates them so that the first PC explains the most variance, the second PC the next most, etc. (Klingenberg, 2020). The information is then extracted as eigenvalues which describe the percentage of variance in the data along those axes known as principal components (PC) (Table 3) (Klingenberg, 2020). PCA is a common tool in 3D GM as it helps simplify and visualize patterns of shape variation guiding subsequent tests of the underlying drivers (Slice, 2007).

2.3.3.4 Procrustes ANOVA and ANCOVA

To address my first objective a Procrustes analysis of variance, commonly known as an ANOVA was performed in Geomorph using procD.lm() (Collyer and Adams, 2018; Baken et al., 2021; Collyer and Adams, 2024; Adams et al., 2025). Procrustes ANOVA is preferred over a standard ANOVA due to its capabilities of properly handling high dimensional data (Klingenberg and McIntyre, 1998; Adams and Otárola-Castillo, 2013; Baken et al., 2021; Collyer and Adams, 2024). In this model shape, the Procrustes-aligned coordinates are the response, while log10 of centroid size is the predictor and directly tests the question as to how much of the shape variation is explained by log10 centroid size. Centroid size is log10 transformed due to biological size and shape often being allometric, so this is a way to normalize the size distribution and linearize the relationship so proceeding tests show the slope representing proportional shape change per change in size (Huxley, 1932; Zelditch et al., 2012).

To address my third objective, assessing the effects of locomotion and substrate use on distal humeral shape, I conducted a Procrustes analysis of covariance (ANCOVA). A Procrustes ANCOVA is used to test for shape differences among groups while considering covariates. I used it to evaluate the contribution of static allometry, genus, locomotion and their interaction to overall humeral shape variation across genera. Log_{10} transformed centroid size was included as a continuous covariate, and its interaction with both genus and locomotion to assess the extent of allometric and behavior-related effects (Adams and Otárola-Castillo, 2013).

2.3.3.5 *A Priori* Comparisons

To address my second objective, testing generic-level differences in distal humeral shape, I performed seven planned, one-degree-of-freedom contrasts on the Procrustes superimposed, centroid-size corrected. These contrasts were executed in Geomorph using procD.lm() with Randomized Residual Permutation in a Procedure and 999 (RRPP; Collyer and Adams, 2018; Baken et al., 2021; Collyer and Adams, 2024; Adams et al., 2025). Each genus was tested orthogonally against all others to quantify its unique contribution to shape variance.

2.4 Results

2.4.1 Principal Components Analysis

The first principal component (PC1) explains 23.1% and the second principal component (PC2) represents 8.7% of the variance in the data (Table 3). Convex hulls, shaded outlines that enclose all the data points for each genus, surround the distribution of each genus in the PCA plot. PC1 separates genera by size, with *Gorilla* at the negative end, *Hylobates*, *Symphalangus* and *Nasalis* at the positive end and all other genera overlapping in the middle (Figures 2 and 3). PC2 mostly separates taxa based on substrate use with more arboreal forms at the positive end, including *Pan paniscus* and *N. larvatus* and most other genera at the negative end. Most striking

is the separation of *Pan paniscus* from the closely related, but more terrestrial, *Pan troglodytes* (Figure 2 and 4). When plotting the same PCA scores by species (Figures 5), separation along PC2 becomes more evident with *Gorilla gorilla* positively displaced from *Gorilla beringei*. *Gorilla gorilla,* or western lowland gorillas, are comparatively more arboreal than the largely terrestrial eastern mountain gorillas, *Gorilla beringei* (Doran, 1997; Ruff et al., 2013). Along PC1 the size of the capitulum increases mediolaterally (Rose, 1988; Bacon, 2000) creating more surface area for the head of the radius for pronation and supination of the forearm (Figure 6). Along PC1 the olecranon fossa becomes wider mediolaterally indicating possibly increased depth. This shape differs in terrestrial knuckle-walkers where it has been observed they have a narrow and deep olecranon fossa which correlates stability and weigh (Napier, 1967; Tallman, 2010). Along the negative end of PC2 (Figure 7), driven by locomotion, the lateral epicondyle appears to elongate superior-inferiorly, a feature previously suggested to influence the moment arm for wrist extensors (Zelazny, 2019; Di Vincenzo et al., 2015).

Table 3: Chapter II proportion of total variance by each PC. The first two PCs explain the most variance of the data.

Proportion of Total Variance Captured by Each PC

Principal Component	Variance Explained (%)
PC1	23.51
PC2	8.68
PC3	6.84
PC4	6.20
PC5	5.88

Figure 2: Chapter 2 PCA of Hominoid humeri by Genus. of PC1 vs PC2 by genus. PC1 explains 23.1% of the variance and separates *Gorilla* from Hylobatids and *Pan*, *Pongo* and *Homo*, all which overlap. The separation along PC1 may be indicative of allometric differences, where *Pan*, *Pongo* and *Homo* appear to be intermediate. PC2 explains 8.7% of the variance and appears to separate genera based on use as *Nasalis*, the only cercopithecid is isolated from apes, and *Pan paniscus* shows more distinct separation from *Pan troglodytes*.

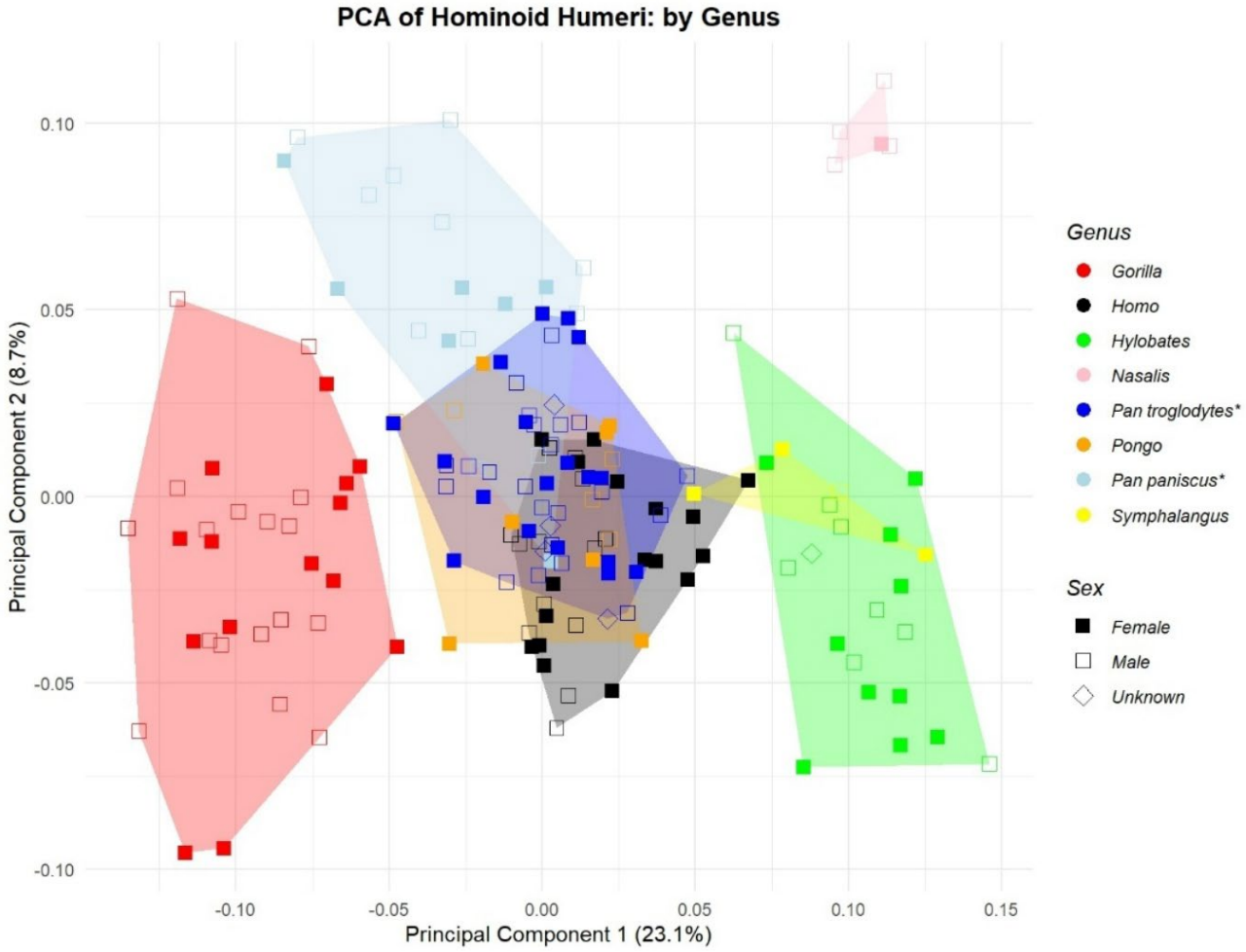

Figure 3: Boxplot of PC1 by genus. A boxplot representing the separation seen in PC1 vs genus when plotted demonstrating clear separation of *Gorilla* from all other genera, along with separation of the suspensory genera from the more terrestrial apes apart from *Pongo* which overlaps with *Pan* and *Homo*.

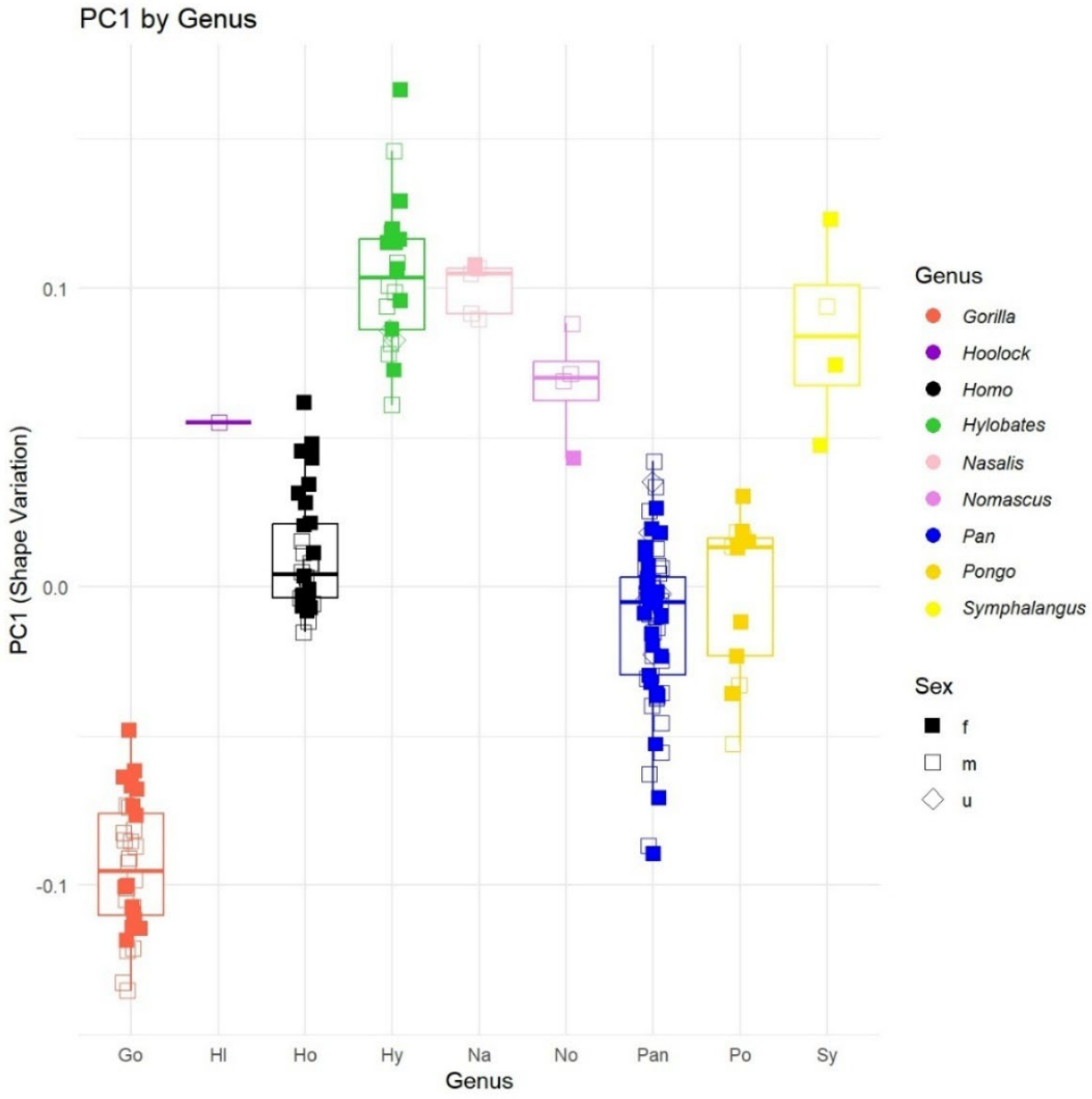

Figure 4: Chapter II Boxplot of PC2 by genus. Box plot of PC2 demonstrates separation of *Pan paniscus* from *Pan troglodytes* but modern humans overlap with *Gorilla* and *Hylobates. Pongo* and *Symphalangus also overlap with Pan troglodytes*.

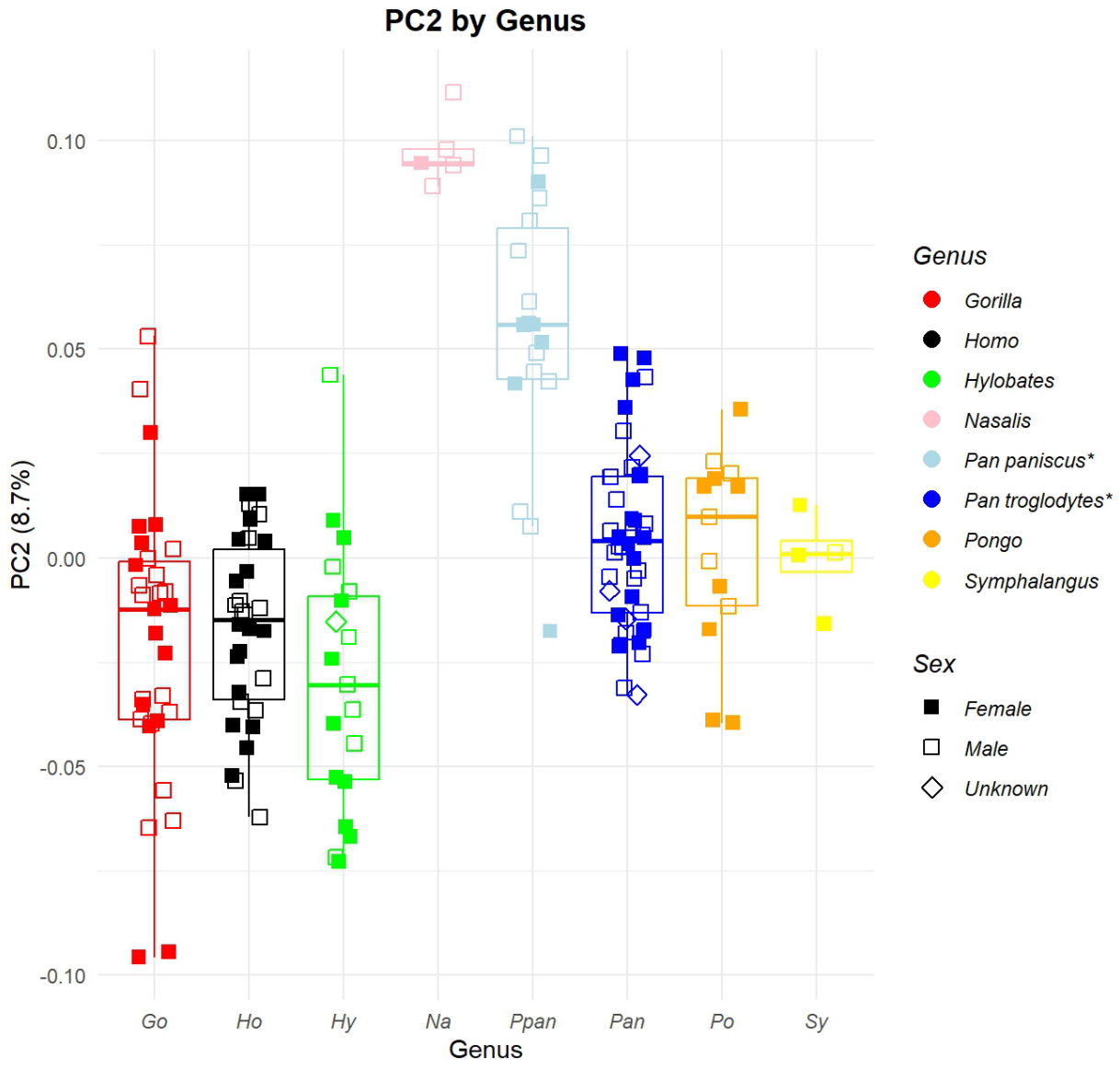

Figure 5: Chapter 2 PCA of Hominoid Humeri by Species. A species-level plot of PC1 vs PC2 indicates deeper differences within genera are present. Within *Gorilla* there is separation between the two closely related species like *Pan*, which again shows separation between *Pan paniscus* and *Pan troglodytes*. There is also greater separation between *Hylobates* and *Symphalangus*, the latter being a large-bodied siamang.

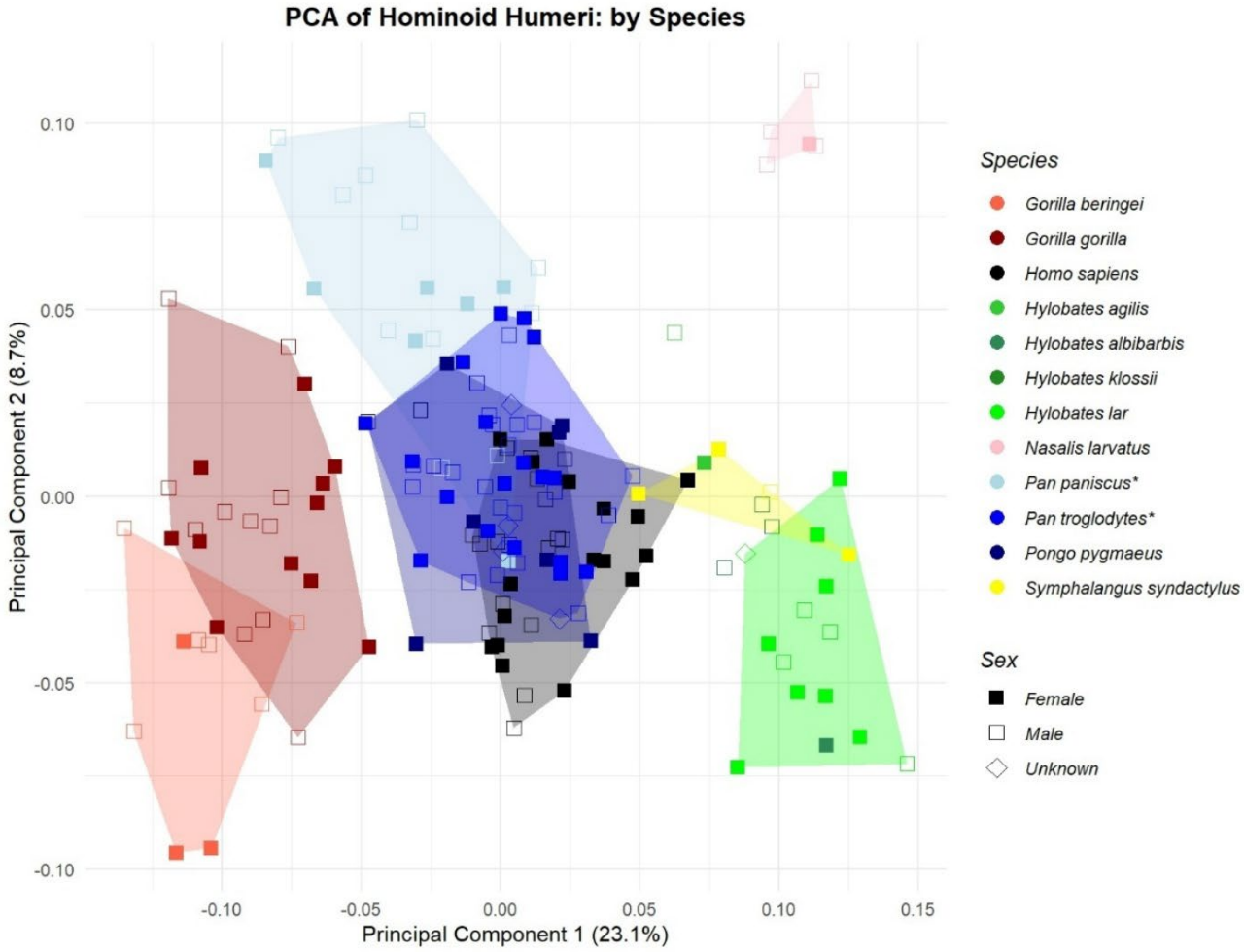

2.4.2 Procrustes ANOVA and ANCOVA

Procrustes-based ANOVA tested for the presence of shape variation correlated with size and for differences in shape among genera. Both indicated there is a significant relationship between distal humeral shape and size at an R^2 of 17.9%, and distal humeral shape and genus at an R^2 of 40.5%. However, in both tests the residuals were very high, at 82% for shape and $\log_{10}$

centroid size, and 59.5% for genus. This can be interpreted to mean that after considering size and genus, there are other factors potentially driving the variance in the data, and while size is a large driver of the variance, genus has a stronger effect.

The Procrustes-based ANCOVA tested shape against $\log_{10}$ centroid size, genus and their interaction using RRPP. The R^2 value indicated the main effect of size on shape accounts for about 17.9% of the total shape variance (Table 4). Genus accounts for about 23.6% of the total shape variance, while the interaction between the two terms explains on 2.9% of the total shape variance. These had a positive *p*-value indicating they were statistically significant except for the interaction between size and genus which appears to not be significant indicating all genera share parallel slopes. In essence this means that there is no evidence that any genus scales faster or slower than any other, only that they begin at different shapes.

Table 4: Chapter II Procrustes ANCOVA looking at shape and log10 transformed centroid size and its interaction with Genus and additionally locomotion. The table shows log size and genus are significant but the interaction between size and genus is less so, and the remaining variance is within the residual and likely locomotion.

Procrustes ANCOVA: Shape ~ $\log_{10}$(Size) * Genus * Locomotion

Term	Df	SS	MS	Rsq	F	Z	Pr(>F)
log_csize	1	0.512	0.512	0.179	47.596	6.000	0.001
genus	7	0.676	0.097	0.236	8.988	12.274	0.001
log_csize:genus	7	0.082	0.012	0.029	1.094	0.798	0.215
Residuals	148	1.591	0.011	0.556	NA	NA	NA
Total	163	2.862	NA	NA	NA	NA	NA

2.4.3 *A Priori* Comparisons

The planned *a priori* comparison demonstrates the greatest driver of the differences we see when comparing groups is between great apes, consisting of the genera *Gorilla, Pan, Pongo, and Homo* versus lesser apes consisting of the genera *Hylobates* and *Symphalangus* at a high R^2 value of 0.131 or 13%. Lower values are seen between closely related species like *Pan paniscus* (Ppan) versus *Pan troglodytes* (Ptro) with an R^2 value of 0.30 or 3%. This means little difference is detected in humeral shape between *P. paniscus* and *P. troglodytes* unlike between the great apes and lesser apes.

Table 5: Chapter II planned (*a priori)* comparison. contrasts table on genus demonstrates the significant contribution of each genus when orthogonally tested against all other groups.

Planned Genus Contrasts: 3-D distal-humerus shape

Contrast	Df	SS	MS	R^2	F	Z	p-value
Nas.vs.Apes	1	0.179	0.179	0.063	10.818	4.479	0.001
Hylo.vs.Symph	1	0.177	0.177	0.062	10.675	4.773	0.001
Lesser.vs.Great	1	0.375	0.375	0.131	24.444	6.238	0.001
Ho.vs.Great.Apes	1	0.149	0.149	0.052	8.905	4.670	0.001
Go.vs.Po_Ppan_Ptro	1	0.284	0.284	0.099	17.877	6.369	0.001
Ppan.vs.Ptro	1	0.086	0.086	0.030	5.045	4.030	0.001
Po.vs.Ppan_Ptro	1	0.117	0.117	0.041	6.926	5.215	0.001
Residuals	156	1.702	0.011	0.595	NA	NA	NA

Figure 6: Chapter II deformation along PC1. The deformation along PC1 shows an increase in the size of the capitulum and relief of the lateral trochlear border and depth of the trochlea groove along the negative end. It also shows a more anterior orientation of the medial epicondyle. On the positive end of the spectrum, the medial epicondyle is retroflexed posteriorly, while there is also an increase in the overall size of the trochlea and anterior inferior expansion of the medial trochlear border. On the negative end the olecranon fossa appears reduced medial-

laterally and increased superior-inferiorly, likely indicating decrease in depth, while the positive end appears opposite indicating increased depth.

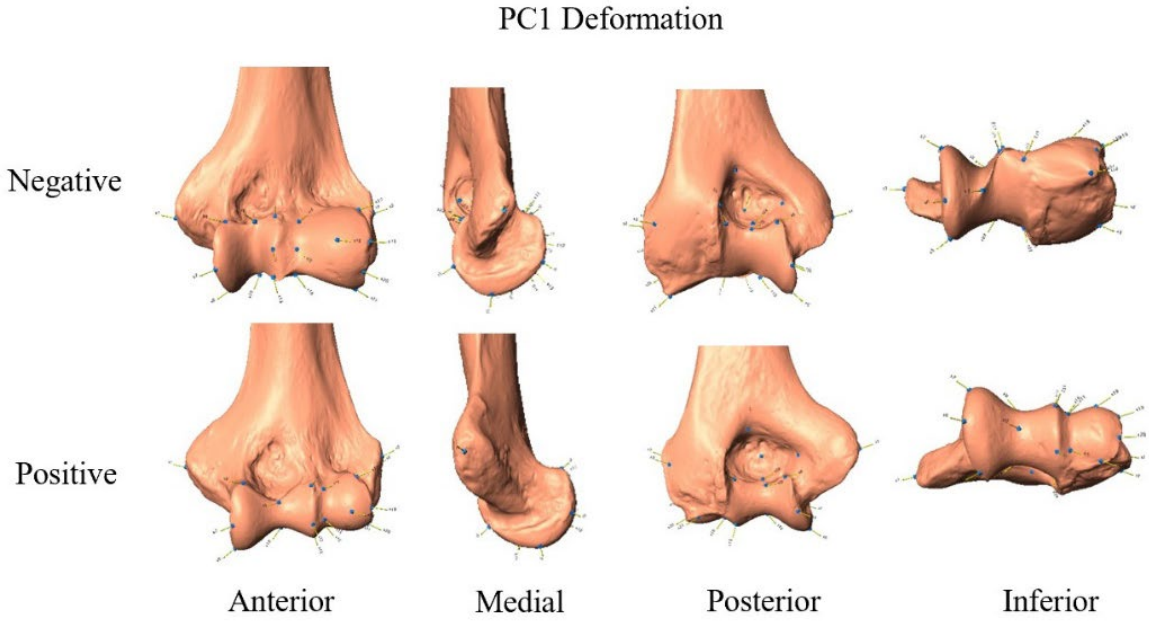

Figure 7: Chapter II deformation along PC2. The deformation along PC2 demonstrates the trochlear border becoming more anteriorly inferiorly projected. The lateral epicondyle is elongating superiorly, while the medial epicondyle shows some minor degree of retroflexion when compared to the shape change in PC 1.

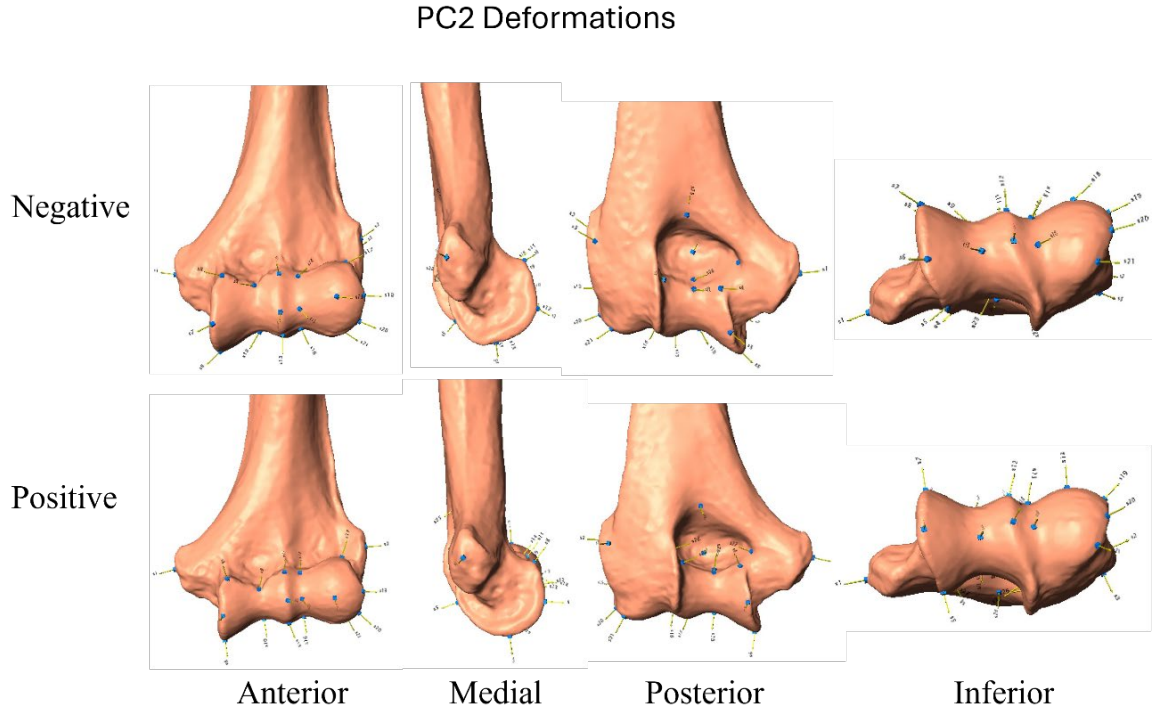

Discussion

The distal humerus is a key component of the elbow joint which is actively engaged during quadrupedal locomotion. Previous studies have proposed that variation in the hominoid elbow may reflect a trade-off between stability for terrestrial locomotion and flexibility for arboreal locomotion (Rose, 1988; Rose, 1983; Boren, 2014; Zelazny, 2019). Results from this study concur with previous findings which suggest that static allometry is an important influence on distal humeral shape, but not necessarily the most important (Tallman, 2010; Lague, 2014; Di Vincenzo et al., 2015; Zelazny, 2019). Findings also indicate significant differences in distal humeral shape among genera. Furthermore, when considering locomotor patterns and substrate use, both were significant but contributed little to the variance when compared to genus. The planned contrasts demonstrated significant results suggesting all genera appear different from one another, but the greatest contributor was between lesser apes (*Hylobates* and *Symphalangus*) and great apes (*Gorilla, Homo, Pan, troglodytes, Pan paniscus*). The least planned contrast was between *Pan troglodytes* and *Pan paniscus,* which could be due to their close relationship regardless of substrate preferences.

Differences in the morphology of the distal humerus across hominoids suggest that the mechanical demands at the elbow are not the same in all genera even within closely related species. The shape of the trochlea has been associated with stability of the elbow associated with loading through the forelimb during knuckle-walking (Knussman, 1967; Tuttle, 1969; Richmond and Strait, 2000; Tallman, 2010). Shape differences in this study concurred with previous findings that suggest features associated with stability as seen in *Gorilla* and *Pan* include a wide, broad and spool-shaped trochlea, pronounced trochlear keel, and a deep olecranon fossa (McHenry and Corruccini, 1975; Aiello and Dean, 1990; Rose, 1988; Larson, 1998; Tallman,

2010). The morphology of the olecranon fossa is thought to contribute to varying degrees of extension of the forelimb especially when paired with the trochlear notch of the ulna with which it articulates that allows flexion-extension (Knussman, 1967; Aiello and Dean, 1990; Tallman, 2010). Features associated with flexibility as seen in *Homo* include a narrow trochlea with a less pronounced spool shape and shallower trochlear groove and olecranon fossa (McHenry and Corruccini, 1975; Larson, 1998; Aiello and Dean, 1990; Tallman, 2010; Di Vincenzo et al., 2015). Similarly, Hylobatids and *Pongo* appear to have a moderate, shallow and somewhat broad trochlea with a shallow trochlear groove (McHenry and Corruccini, 1975; Rose, 1988; Aiello and Dean, 1990; Tallman, 2010; Di Vincenzo et al., 2015; Zelazny, 2019). The olecranon fossa, in *Homo* and hylobatids also appears to be shallower than in *Pongo* which is more intermediate suggesting more extension capabilities in the elbow (Rose, 1988; Aiello and Dean, 1990; Tallman, 2010; Di Vincenzo et al., 2015; Zelazny, 2019). Findings from this study that support these previous observations also suggest *Homo* when compared to terrestrial knuckle-walkers appear to share similarities closer to suspensory apes when it comes to the trade off of flexibility over stability in the elbow. While modern humans do not engage in suspensory brachiation, they do maintain an extended elbow posture when moving bipedally across the substrate (Harcourt-Smith and Aiello, 2004).

The morphology of the medial and lateral epicondyle is important to consider when assessing the distal humerus as they are important attachment sites for the flexors and extensors of the forelimb (Ibáñez-Gimeno et al, 2014). The medial epicondyle has been noted as pronounced, retroflexed and flared in knuckle-walkers likely related to actively engaged forearm flexors (Rose, 1988; Tallman, 2010; Di Vincenzo et al., 2015; Zelazny, 2019). The lateral epicondyle is also pronounced in *Gorilla* and *Pan,* moderate in *Pongo* and reduced in *Homo* and Hylobatids

(Tallman, 2010; Di Vincenzo et al., 2015; Zelazny, 2019). *Homo*, Hylobatids and *Pongo* appear to have a medial epicondyle that is reduced and less pronounced when compared to *Gorilla* and *Pan* (Tallman, 2010; Zelazny, 2019). *Nasalis*, as the only cercopithecid in the sample has a narrower, more gracile trochlea, a shallow trochlear groove, a less pronounced olecranon fossa, reduced epicondyles and a less developed zona conoidea which is thought to reflect arboreal quadrupedal loading (Su and Jablonski, 2009). Tallman (2010) found *Gorilla* and *Pan* to have a robust zona conoidea when compared to the more moderate relief in *Pongo* and reduced relief in *Homo* and Hylobatids, likely related to locomotor adaptations related for stability. Assessing the degree flexibility and stability in the elbow by looking at the morphology of the distal humerus can provide insight as to role of flexion-extension and pronation-supination in australopith locomotion. A comparative framework with extant hominoids could benefit from incorporating juveniles and using an ontogenetic approach to fill in gaps as to plasticity that may occur with use during life.

Conclusion

The result of this study demonstrates that the morphology of the distal humerus can be informative of the wide range of movements that are used differently between quadrupeds and bipeds. This study supports previous findings of static allometry influencing the distal humeral shape of adult hominoids (McHenry and Corruccini, 1975; Feldesman, 1982; Tallman, 2010; Lague, 2014; Zelazny, 2019). This means that it is worth considering how size may influence morphology when analyzing australopiths there appears to be a range of large australopiths like the Kadanuumuu KSD-VP- 1/1 specimen and small australopiths like *Australopithecus afarensis* or “lucy” (Johanson et al., 1978; Haile-Selassie, 2010; Tallman, 2010; Zelazny, 2019).

I also found distal humeral shape differs by genus likely due to how the elbow joint is engaged during locomotion regarding the flexibility vs stability trade off (Rose, 1988). This is important for future investigation as to the possible correlation between shape and phylogeny. In this study I noted that while locomotion may be a driver for shape change in the distal humerus of adult hominoids, it is worth taking an ontogenetic approach when the joint is still developing and still plastic. The differences between observed adult locomotor patterns and the more varied juvenile locomotor patterns in hominoids are important for observing possible shape changes in the distal humerus that will be actively engaged (Doran, 1992; Inouye, 1994; Remis, 1995).

It is important to note that while approximately equal numbers of individuals by sex were included in this study, some genera had fewer specimens than others including *Symphalangus* and *Pongo* which are difficult to obtain in museum collections. This may have also contributed to the consistent overlap with *Pan* and *Homo*. Future work will explore ontogeny in the distal humerus to assess patterns of shape change over developmental time. The goal will be to add novel information to our understanding of developmental plasticity either due to allometry, phylogeny or use. These studies provide an important contribution to evolutionary studies that continue to test hypotheses on early hominin locomotion that has led to our modern form and function.

CHAPTER III

ONTOGENY OF THE DISTAL HUMERUS IN EXTANT HOMINOIDS

3.1 Introduction

Juveniles of terrestrial African ape species have been observed to engage in more climbing and other arboreal behavior compared to their adult counterparts reflecting a shift in their locomotor behavior during development (Doran, 1992; Inouye, 1994; Remis, 1995). Between the closely related species of *Pan*, *P. troglodytes* is relatively terrestrial while *Pan paniscus* is more arboreal, living in trees while occasionally descending to knuckle-walk on the ground (White, 1996, 2020). Similarly, *Gorilla gorilla* (western lowland gorilla) is more arboreal than the closely related species *Gorilla beringei* (mountain gorilla) (Remis, 1999). Variation due to additional factors like group size, social rank and sex has been observed to influence substrate preference and positional behaviors (Remis, 1995, 1999). Hylobatids are suspensory apes living in the high canopy and like other apes experience a period of being carried by the parent prior to being fully weaned and becoming independent brachiators (Pusey, 1983; Goodall, 1986; Remis, 1995; Reichard and Sommer, 1997; Breuer et al., 2009).

In contrast to other apes, modern humans are born more altricial and go through various stages prior to the onset of bipedal walking that involves strengthening muscles, coordination and balance (Cowgill and Johnston, 2018). Bipedalism in modern humans begins on average at around ~ 12 months, or within 8-18 postnatal months (Karasik et al., 2012; Sutherland, Cooper and Daniel, 1980; Adolph and Franchak, 2017). However there is cultural variation that should be considered depending on the population that is studied (Karasik et al., 2015). Therefore, depending on whether locomotion is occurring quadrupedally or bipedally the forelimb is used differently throughout development.

Australopiths, early human ancestors that researchers agree were bipedal have a blend of ape-like skeletal features that has been the center of a longstanding debate as to their functional importance. Some suggest these features are primitive retentions that did not serve a locomotor purpose (Lovejoy, 1988; Lovejoy and Latimer 1990; Lovejoy, 1990; Latimer, 1991), while others propose the features are evidence quadrupedalism like climbing was still a part of their repertoire (Susman and Stern 1982; Susman, Stern and Jungers, 1983; Jungers et al., 1997; Ward, 2002). This debate has implications on the selective pressures that led to bipedalism in australopiths and eventually obligate bipedalism in modern humans (Washburn and Lancaster, 1968; Lovejoy, 1981; Hunt et al, 1996; Wheeler, 1991; Pontzer et al., 2009; Bramble and Lieberman, 2004). It questions whether once bipedalism was achieved did australopiths completely commit or was climbing still relevant during life.

The goal of this study is to address this ongoing debate about the arboreal features of australopiths by taking on ontogenetic approach to create a comparative framework for understanding developmental plasticity in the distal humerus of extant hominoids. The distal humerus plays an important role as part of the elbow joint, a compound synovial joint that acts as the interface between the arm and forearm which is actively used during quadrupedal locomotion. Thus, studying the distal humerus may provide novel information on morphological changes related to locomotion and use during life in the elbow as has been observed by these methods for other morphological regions (Turley et al., 2018; Morimoto et al., 2018; Simons et al., 2019).

3.1.1 Objectives

The objectives of this ontogenetic study are first to determine if the distal humerus differs by developmental stage across genera. Second, is investigating if genera share similar allometric

patterns at different developmental stages. Lastly, I am comparing ontogenetic trajectories and evaluate the magnitude, amount of change, and direction, pattern of shape changes in the distal humerus.

3.2 Background

3.2.1 Ontogeny

Juvenile australopiths are rare in the fossil record but offer a unique opportunity to learn about the developmental history that led to the adult forms (Dart, 1925; Broom and Robinson, 1950; Johanson and Edey, 1981; Alemseged et al., 2006; Berger et al., 2010). Ontogeny is the study of growth (change in size) and development (change in shape) over time and has been employed to successfully detect skeletal modifications related to use during life (Inouye, 1994; Richmond, 2007; Jabbour, 2008; Zollikofer et al., 2010; Boren, 2014; Turley and Frost, 2014; Turley et al, 2015; 2018; Sarringhaus et al., 2016; Cowgill et al, 2018; Raichlen et al., 2017;; Tallman, 2016; Simons, 2019).

Ontogeny the study of growth (change in size) and development (change in shape) over the life of an organism is important to studies of evolutionary developmental biology and increasingly, paleoanthropology (Klingenberg, 2010). Ontogenetic research focuses on understanding factors that my influence the growth (change in size) and development (change in shape) of elements subject to frequent use (Inouye, 1994; Richmond, 2007; Zollikofer et al., 2010; Turley and Frost, 2014; Turley et al, 2015; 2018; Cowgill et al, 2018; Raichlen et al., 2017; Sarringhaus et al., 2016; Simons, 2019). Findings from previous studies have determined that taking an ontogenetic approach is useful for distinguishing skeletal modification related to use during life (Jabbour, 2008; Boren, 2014; Turley et al., 2015; 2018; Tallman, 2016; Simons et al., 2019). Regions of active use during life like the shoulder, talocrural joint, wrist and hands

have been studied using an ontogenetic approach (Inouye, 1994; Young, 2003; Richmond, 2007; Larson, 2007; Green and Alemseged, 2012; Turley and Frost 2014; Turley et al, 2015; 2018). These are important regions because depending on whether it is used by a biped or a quadruped use is inherently different, where quadrupedal hominoids will rely heavily on using the forelimb for locomotion, bipedal humans do not. Then there are bipedal australopiths like *Australopithecus afarensis* that show evidence having both ape-like and derived human-like skeletal features argued to either be primitive retentions (Lovejoy, 1988; Lovejoy and Latimer 1990; Lovejoy, 1990; Latimer, 1991) or evidence quadrupedalism remained important in their locomotor repertoire (Susman and Stern 1982; Susman, Stern and Jungers, 1983; Jungers et al., 1997; Ward, 2002). Therefore, taking an ontogenetic approach provides the opportunity to investigate factors that lead to the adult forms.

Taking an ontogenetic approach, this study aims to address the ongoing debate as to the importance of quadrupedalism like climbing in australopiths by focusing on the distal humerus.

3.3 Materials and Methods

3.3.1 Sample specimens

The sample included surface scans of 330 hominoid distal humeri representing three distinct developmental groups based on eruption of the molar teeth (Table 6). Previous ontogenetic studies have successfully used molar eruption stages as markers for development across diverse samples of primates, (e.g., McNulty et al., 2006; Singleton et al., 2010; 2016; Turley and Frost, 2014; Turley et al., 2018; Simons, 2019; Simons and Frost, 2021). The developmental stages used here are as follows: fully erupted M1 for juveniles, erupted M2 for adolescent/subadult and erupted M3 for adults (McNulty et al., 2006; Singleton et al., 2010; Simons and Frost, 2016; Turley et al., 2018; Simons, 2019; Figure 9). The sample includes six

genera: *Gorilla*, *Pongo*, *Homo*, *Hylobates*, *Symphalangus* and *Pan*. This is fewer than in chapter II due to the relative rarity of juvenile specimens for some genera. As in chapter II the species of *Pan* were treated separately because in Chapter II *Pan paniscus* appears to be functionally distinct from *Pan troglodytes*. Forty-five surface scans of adult specimens were generously shared by Dr. Joseph Plavcan, Dr. Carol Ward, Dr. Sergio Alméjica and Dr. Kelsey Pugh. Two-hundred-seventy-seven surface scans of specimens across five collections including: American Museum of Natural History (New York), Naturalis Biodiversity Center (Leiden, Netherlands) Royal Museum for Central Africa (Tervuren, Belgium), Universität Zürich (Zurich, Switzerland), Museu Nacional de História Natural e da Ciência (Lisbon, Portugal). Scans were collected using high resolution handheld structured light scanners, the Artec Space Spider (Artec 3D) and 3D Shining (Einstar). Details of included specimens are given in Appendix 2.

Skeletal collections of juvenile humans are very rare and are limited to a few repositories, including the Luis Lopes Cemetery collection housed in the Museu Nacional de História Natural e da Ciência in Lisbon, Portugal. M1 specimens from this collection lacked sufficient preservation and were unable to be included in this study. However, to circumvent this issue and increase the M1 sample eight CT scans of modern human juveniles were acquired with permission from the New Mexico Decedent Imaging Database (NMDID). The scans were acquired as CT DICOM stacks and converted using the open medical imaging software Slicer (Fedorov et al., 2012) to segment the humerus and generate polygon file format (ply) surface scans. For details of specimens from each collection, see Appendix 2.

Juvenile skeletal collections are even more rare due to their delicate nature and are limited to a few collections including the Luis Lopes Cemetery collection housed in Lisbon, Portugal. Many specimens from this collection lacked sufficient preservation at M1 and thus

scans were segmented from the New Mexico Decedent Imaging Database (NMDID) (Edgar et al., 2020).

Table 6: Chapter II specimens were sorted by developmental stages represented by complete eruption of molars at three distinct stages: M1 representing juveniles, M2 representing adolescent/intermediate, and M3 adults for a total of 330 specimens across 6 genera. Note the *Pan* genus was divided into species-level to account for an unbalanced amount of *Pan* specimens. Further details in Appendix 2.

Genus	**Males**			**Females**			**Unknown**			
	M1	**M2**	**M3**	**F1**	**F2**	**F3**	**U1**	**U2**	**U3**	**Total**
Gorilla	0	3	20	3	3	14	1	1	0	45
Homo	5	9	21	3	7	23	0	1	0	69
Hylobates	3	5	10	3	5	12	0	2	2	42
*Pan Paniscus**	2	6	12	2	4	9	1	0	1	37
*Pan troglodytes**	6	13	25	2	8	18	5	9	6	92
Pongo	3	2	6	0	4	12	4	4	0	33
Symphalangus	0	1	2	1	3	2	2	0	0	12
Total	**19**	**39**	**96**	**14**	**32**	**91**	**13**	**17**	**9**	**330**

Data collection

Due to the nature of immature specimens, a reduced landmarking protocol of 17 fixed single points on the distal humerus was modified from the 28 landmarks used in Chapter I and originally adapted from Tallman (2010) (but also see, McHenry, 1976; Bacon, 2000; Lague, 2014; Rosas et al., 2015; Zelazny, 2019). These are illustrated in Figure 8 and listed in Table 7. The reduced protocol considered the degree of maturation in the distal humerus at the M1

developmental stage as observed by the author. Although the degree of maturation in the distal humerus appears to vary across genera, the reduced protocol considers instances of an underdeveloped trochleae, trochlear groove and lack of ossifications for both lateral and medial epicondyles. Thus, the landmarks chosen for this study sufficiently capture overall distal humeral shape required to address the objectives.

Figure 8: Chapter III landmark protocol. Chapter III used a 17 single-point landmark protocol on a M1 male *Pongo* specimen demonstrated from Landmark Editor. A = anterior view, B = posterior view, C = medial view

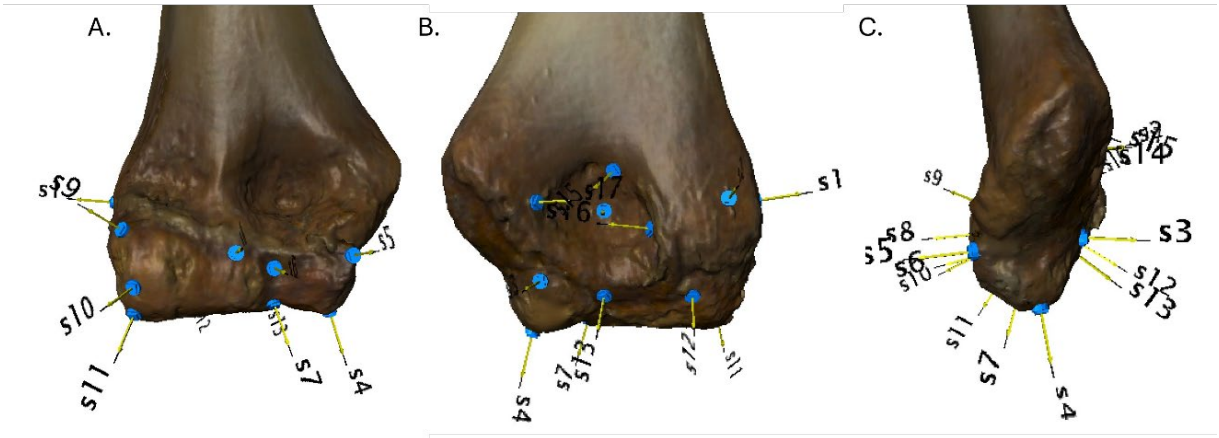

Figure 9: Chapter III Molar Eruption stages. Shows photographs of different mandibular molar eruption stages in occlusion. (A) M1 of *Gorilla* (B) M2 *Pan* (C) M3 of *Pongo*.

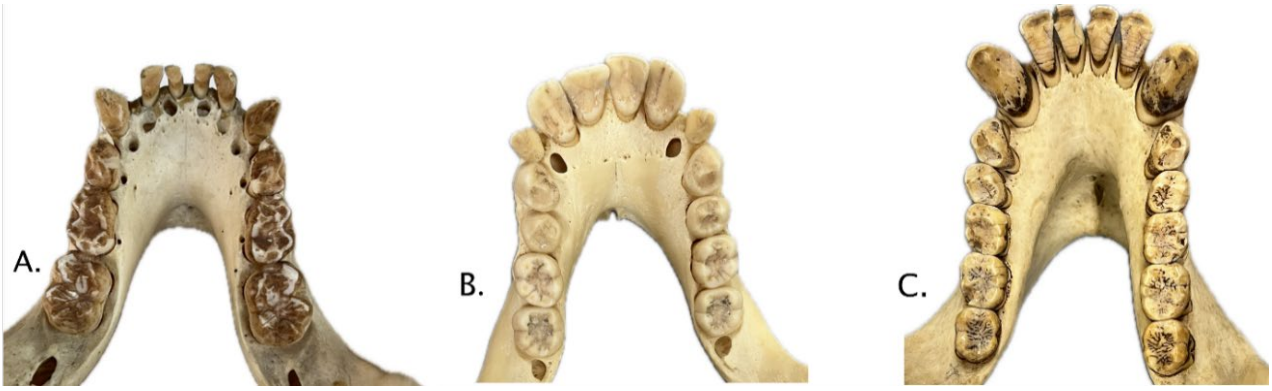

Table 7: Chapter III landmark description.

Landmarks	Description
Laterale Epicondyle	
1	most projecting point on the lateral epicondyle
2	posterior aspect of the lateral epicondyle
Trochlea	
3	most posterior medial corner of the trochlea
4	most inferior projecting point of along the trochlear border
5	most superior anterior projecting point of the trochlear border
Trochlear groove	
6	deepest superior point of the trochlear groove
7	deepest inferior point of the trochlear groove
Zona conoidea	
8	most superior point on the zona conoidea
Capitulum	
9	most superior lateral corner of the capitulum border
10	most anterior projecting point along on the capitulum border
11	most inferior projecting point along the capitulum border
12	most posterior projecting point along the capitulum border
Olecranon fossa	
13	most posterior point along the trochlear groove and inferior along the olecranon fossa
14	deepest point in the olecranon fossa
15	most medial point of the olecranon fossa border
16	most lateral point of the olecranon fossa border
17	most superior point of the olecranon fossa border

3.3.3 Analytical methods

The open-source scientific computing language software *R*, version 4.5.0. was used for all data analysis in this study (R Development Core Team, 2025). Geomorph version 4.0 (Adams and Otárola-Castillo, 2013; Adams and Collyer, 2018; Baken et al., 2021; Adams et al., 2025) was primarily used to run all major steps in 3D Geometric Morphometrics except for Stratovan Checkpoint which was used to collect the 3D Procrustes coordinate data. Additional packages like missMDA version 1.19 (Josse and Husson, 2016) were used for handling missing data using a PCA-based imputation method best applied to high dimensional data. PCA-based imputation is preferred because it treats missing data by replacing values by column means preserving the multivariate covariance in the landmarks, unlike univariate mean-substitution (Adams et al., 2004; Josse and Husson, 2016).

3.3.3.1 3D Geometric Morphometrics

As in Chapter II, 3D Geometric Morphometrics was used in this study to conduct all analyses to evaluate all aspects of shape at different stages of development across all genera (Bookstein, 1986, 1991; 1996; Goodall, 1991; Slice, 2007).

3.3.3.2 Generalized Procrustes analysis

The initial step after collecting the 3D coordinate data in 3D GM is superimposing the landmarks configurations (Bookstein, 1991; Slice, 2007). This is achieved by performing a Generalized Procrustes analysis (GPA), which removes all non-shape variables by translating and rotating each specimen to minimize the square Procrustes distances between landmarks on each configuration and the consensus (Bookstein, 1991; Slice, 2007). The specimens are then scaled to the same unit known as the centroid size (Bookstein, 1991; Slice, 2007).

3.3.3.3 Principal components analysis

A Principal Components analysis (PCA), also known as a relative warps analysis when performed on GM data, was conducted for data exploration (Rohlf, 1990; Bookstein, 1991; Slice, 2007; Klingenberg, 2020). It's important to note that a PCA holds no statistical power, it is an ordination and data reduction method (Rohlf, 1990; Bookstein, 1991; Slice, 2007; Klingenberg, 2020). Patterns of variance are extracted as eigenvalues and the amount is summarized as Principal Components (PC) that are subsequently orthogonal so the first few explain the most information (Slice, 2007; Klingenberg, 2020).

3.3.3.4 Phenotypic Trajectory Analysis

The crux of this study is the Phenotypic Trajectory Analysis (PTA) which maps out the direction and magnitude of shape change between developmental stages (Adams. And Collyer, 2009; Collyer and Adams 2013; Simons et al., 2019). Mapping the pattern (angle), and amount of shape change (magnitude) between developmental stages can provide insight when important changes occur over an individual's life and factors that may contribute to those changes can sometimes be identified. Previous studies have successfully conducted PTA analyses when looking at catarrhine cranial shape and the talocrural joint in hominoids (Turley et al., 2018; Simons, 2019; Simons and Frost, 2021).

Additional statistical analyses were conducted to quantify the angle (direction), magnitude (amount) and trajectory (paths) of pairs of genera (Collyer and Adams, 2018; Simons, 2019; Tables 9-12). The pairwise shape differences analysis quantifies the Procrustes distances between ontogenetic trajectories through shape space (Simons, 2019). The pairwise magnitudes test computes the trajectory path (length) in PC space by taking the sum of Procrustes distances between each developmental stage for each pair (Adams and Collyer, 2009). Lastly, the Pairwise

trajectory angles test for the direction of the shape change through multivariate space and the angle between the vectors that each genus trajectory summarizes (Adams and Collyer, 2009).

3.3.3.5 Procrustes ANOVA and ANCOVA

Procrustes ANOVA, analysis of variance and Procrustes ANCOVA, analysis of covariances are statistical analyses I used for testing my hypotheses about shape change in the distal humerus during ontogeny related to ontogenetic allometry, genus and their interaction. Procrustes ANOVA is a permutation-based analysis of variance that is applied to Procrustes-aligned coordinates testing for mean shape differences across the sample. After superimposition, Procrustes ANOVA then quantifies how much of the remaining shape variation is explained by other factors. Whereas Procrustes ANCOVA incorporates a continuous covariate like centroid size along with a categorical factor like genus, specifically testing if slopes of the size versus shape differ among genera.

3.4 Results

3.4.1 Principal Components Analysis

The first two principal components represent the most variance, where the first PC1 explains 15.1% and PC2 explains 10.3% (Table 8). Convex hulls were generated to separate each developmental stage color coded by genus. PC1 aligns with ontogeny across all genera, with M1 stages being positive and M3 negative. The M1 stage of *Homo* is the most positive and widely separated from all other genera (Figures 10-12). Along PC2 there is separation between *Homo*, *Hylobates*, and *Symphalangus* from *Gorilla*, *Pongo*, *Pan troglodytes* and *Pan paniscus* but mostly all genera overlap (Figure 10). The visualized shape deformation occurring along PC1 (Figure 14) demonstrates the olecranon fossa becoming wider superior-inferiorly and deeper along the negative end as well as the trochlear border becoming more anteriorly expanded. The

capitulum also appears rounder and larger along PC1. Whereas the visualized shape deformation occurring along PC2 (Figure 15) demonstrates elongation of the lateral epicondyle and minor retroflexion of the medial epicondyle. The trochlear groove also becomes increasingly spooled as you move to the negative end and the trochlear border more projecting.

Table 8: Proportion of the total variance by each PC The first five principal components and the variance explained, noting most of the variance is explained by the first two principal components

Principal Component	Variance Explained (%)
PC1	15.11
PC2	10.25
PC3	8.96
PC4	7.57
PC5	5.85

Figure 10: Ontogenetic PCA: by Genus and Stage. Principal components analysis genus with convex hulls by stage. PC1 represents 15.1% of the variance, while PC2 represents 10.3% of the variance. PC1 separates *Homo* at M1 from all other genera and stages, while PC2 somewhat separates *Homo*, *Hylobates* and *Symphalangus* from *Gorilla*, *Pongo*, *Pan troglodytes* and *Pan paniscus* but still shows overlap among genera.

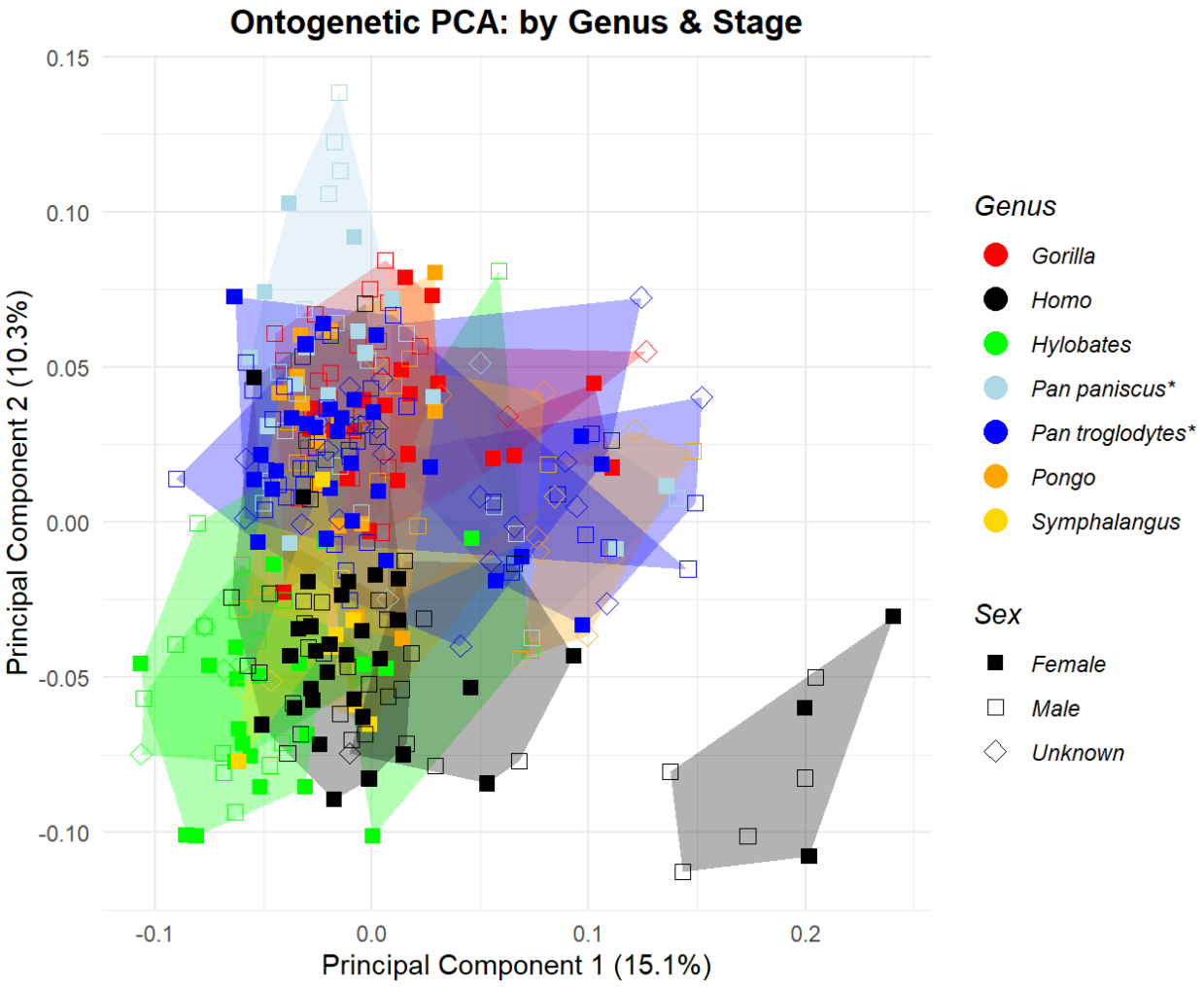

Figure 11: Chapter III Boxplot of PC1 by genus. This boxplot PC1 by genus shows overlapping across all genera with the exception being the M1 juvenile *Homo* that has a wider spread.

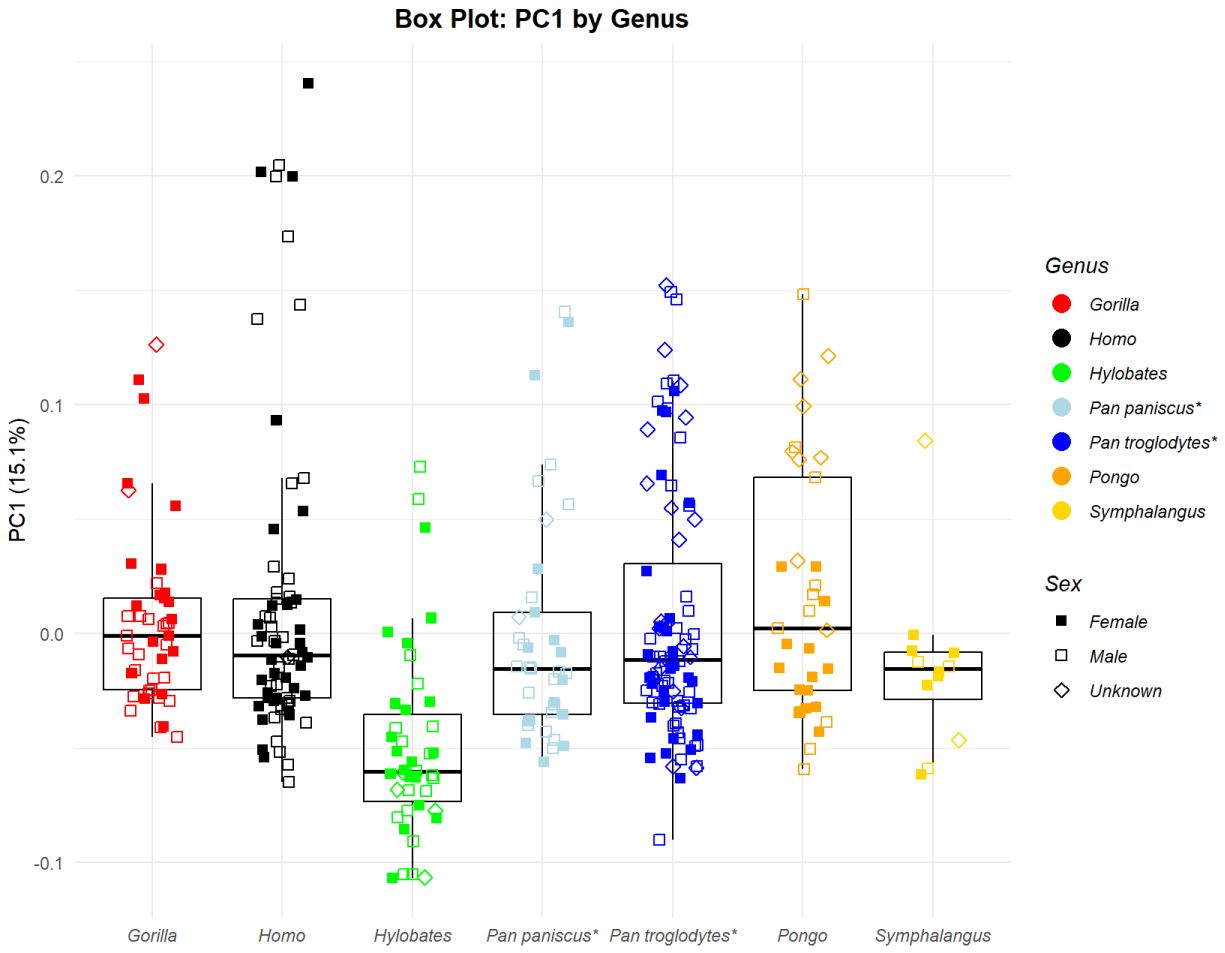

Figure 12: Chapter III Boxplot of PC2 by genus. showing PC2 versus genus. This plot highlights the overlap between all great apes but separation of *Homo*, *Hylobates*, and *Symphalangus*.

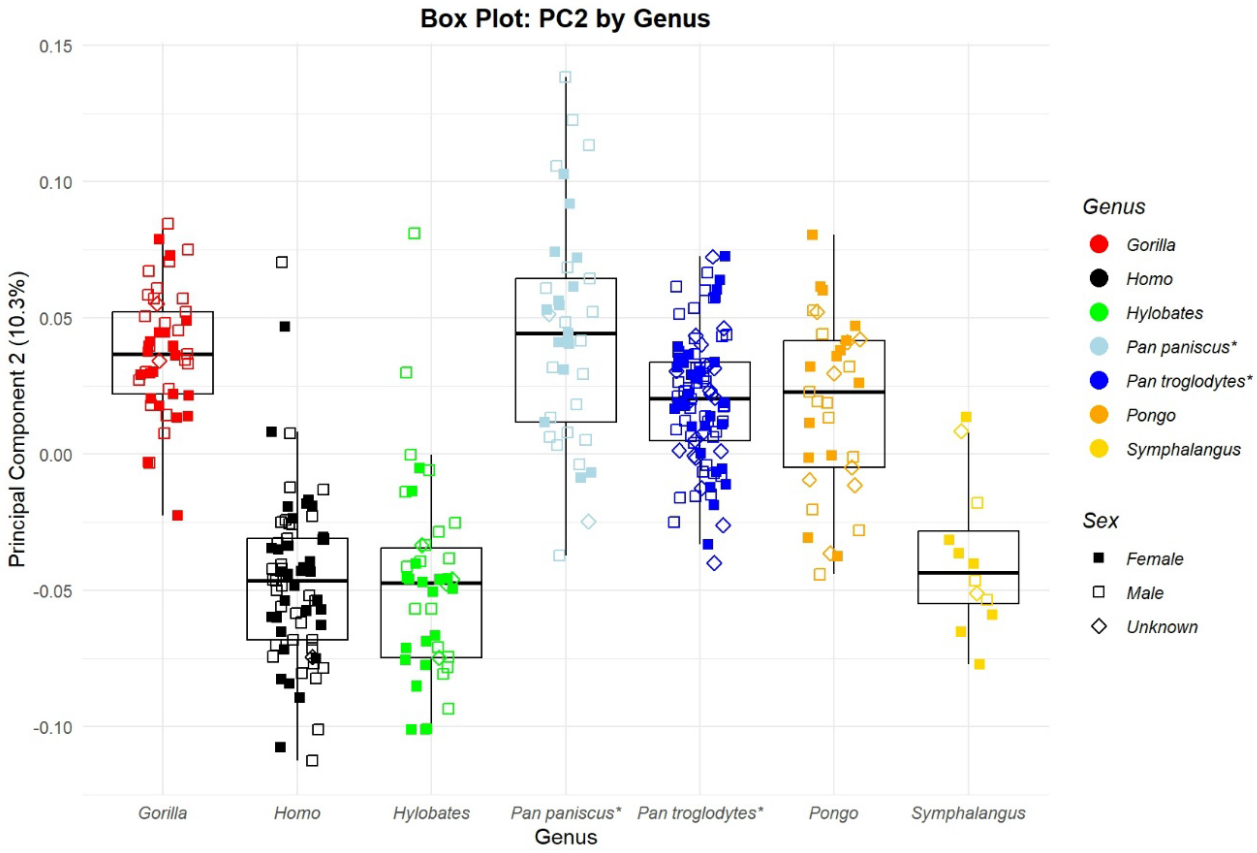

3.4.2 Phenotypic Trajectory Analysis

Results of the PTA show the shape of the trajectories differ mostly in *Homo*, *Pan paniscus*, *Hylobates* and *Symphalangus* (Figure 13, Tables 9-11). Between the stages of M1 and M2 *Homo* appears to have the greatest magnitude of change that aligns closer with *Hylobates* and *Symphalangus* than all other apes. The shape of the trajectory for *Hylobates* has a sharp almost 90-degree angle moving negatively and appears to have relatively large amount of change between M1 and M2 but minimal between M2 and M3. *Symphalangus* a unique pattern and very little magnitude change between stages. Additionally, the shape of the trajectory for

Symphalangus creates a sort of "v" or nearly 45-degree angle trending first negatively between M1 and M2 then positively between M2 and M3. Except for *Pan paniscus*, all the other apes including *Pongo* appear to share similar angles, or patterns, of shape change and lengths between stages of their trajectories with only *Gorilla* appearing to have an overall shorter path. All apes trend positively but *Pan pansicus* between M2 and M3 moves almost exponentially into the far positive end.

Figure 13: Chapter II Ontogenetic trajectories in PC space.. The PTA demonstrates the stages between M1 and M2 for *Homo* has the greatest magnitude compared to any other genus. *Hylobates* has their earliest stage aligning with all other M2 stages, same as *Symphalangus* suggesting they may mature much earlier due to the demands of being suspensory brachiators with little terrestrial locomotion in their repertoire. Great apes appear to all share similar trajectories except for *Pan paniscus* has a sharp trend positively between M2 and M3. This could be indicative of their exclusive arboreal quadrupedalism, which differs from the closely related *Pan troglodytes* which are terrestrial.

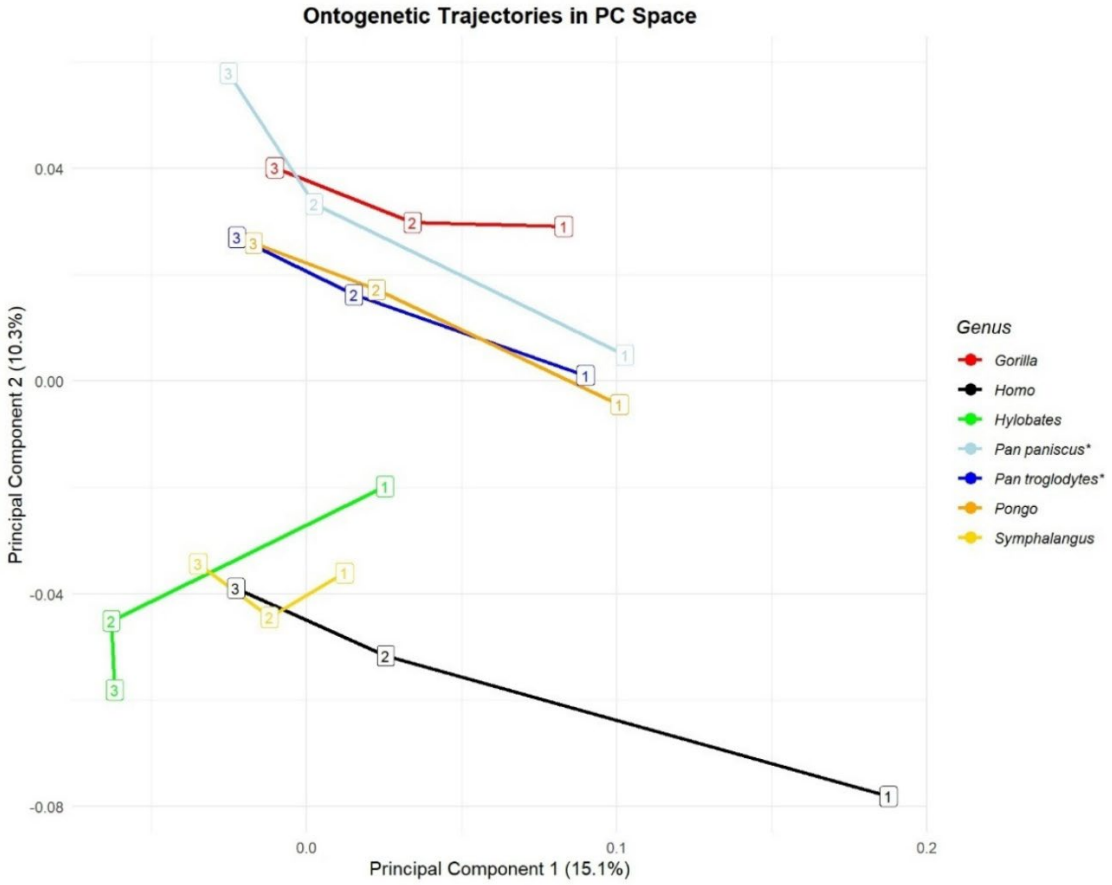

Table 9: Chapter III pairwise shape differences. The shape differences between pairs of genera. High values indicate the shape of the trajectory (how bent or straight it is) differs more between those two genera. Whereas lower values indicate they share about the same type of shape.

Pairwise Shape Differences (Procrustes distance)

	Go	Ho	Hy	Pan	Panp	Po	Sy
Go	NA	0.218	0.191	0.260	0.191	0.178	0.259
Ho	0.218	NA	0.055	0.234	0.139	0.132	0.433
Hy	0.191	0.055	NA	0.268	0.169	0.158	0.428
Pan	0.260	0.234	0.268	NA	0.100	0.113	0.308
Panp	0.191	0.139	0.169	0.100	NA	0.015	0.327
Po	0.178	0.132	0.158	0.113	0.015	NA	0.324
Sy	0.259	0.433	0.428	0.308	0.327	0.324	NA

Table 10: Chapter III pairwise magnitude differences. The magnitude of change between pairs of genera where high values indicate they amount of change between stages is greater between those two pairs, and lower values indicate they share about the same amount of change.

Pairwise Magnitude Differences ($|path_1 - path_2|$)

	Go	Ho	Hy	Pan	Panp	Po	Sy
Go	NA	0.137	0.037	0.047	0.002	0.028	0.047
Ho	0.137	NA	0.174	0.184	0.139	0.165	0.184
Hy	0.037	0.174	NA	0.009	0.035	0.010	0.010
Pan	0.047	0.184	0.009	NA	0.045	0.019	0.000
Panp	0.002	0.139	0.035	0.045	NA	0.026	0.045
Po	0.028	0.165	0.010	0.019	0.026	NA	0.019
Sy	0.047	0.184	0.010	0.000	0.045	0.019	NA

Table 11: Chapter III pairwise trajectory angle. This table summarizes the angle or direction of the shape change as it occurs, where the greater the angle the more different their patterns are when compared to lower values which indicate they share similar patterns of changes.

Pairwise Trajectory Angles (°)

	Go	Ho	Hy	Pan	Panp	Po	Sy
Go	NA	66.2	61.4	48.8	47.6	50.8	83.8
Ho	66.2	NA	63.3	60.7	59.3	51.9	80.3
Hy	61.4	63.3	NA	49.7	61.4	56.7	70.4
Pan	48.8	60.7	49.7	NA	36.4	49.2	66.3
Panp	47.6	59.3	61.4	36.4	NA	42.0	66.6
Po	50.8	51.9	56.7	49.2	42.0	NA	59.4
Sy	83.8	80.3	70.4	66.3	66.6	59.4	NA

3.4.3 Procrustes ANOVA and ANCOVA

Procrustes ANOVA and ANCOVA were used to assess the drivers of the variance seen in the PCA and in the PTA results. Procrustes ANOVA testing for size on shape resulted in a significant p-value but a small R^2 value suggesting that while size may influence shape, other factors, especially ontogenetic patterns and genus, play a larger role as noted by the high residual at 94% (Table 13). The genus on shape Procrustes ANOVA provided a slightly higher value for genus at 19.5% of the variance, suggesting genus plays a larger role, however, residual variance remained high at 80.5% (Table 14). Procrustes ANCOVA was used to test the interaction of both genus and size, which resulted in a low R^2 but a significant *p*-value indicating that while there is

an influence, genus alone is a larger driver and there is still 67.6% of the variance unexplained either size or genus (Table 15).

Table 12: Chapter III Procrustes ANOVA of Shape. against log10 transformed size indicates significant relationship with a high P-value but the R^2 is only 5.7% where the remainder of the variance not explained by size lies in the residuals at 94.3%.

Procrustes ANOVA: Shape ~ $\log_{10}$(Csize)

Term	Df	SS	MS	Rsq	F	Z	Pr(>F)
logCS	1	0.413	0.413	0.057	19.68	8.073	0.001
Residuals	328	6.878	0.021	0.943	NA	NA	NA
Total	329	7.291	NA	NA	NA	NA	NA

Table 13: Chapter III The Procrustes ANOVA of shape and genus suggests about 19.5% of the variance is explained by genus. However, 80.5% is not explained by genus and makes up the residual.

Procrustes ANOVA: Shape ~ Genus

Term	Df	SS	MS	Rsq	F	Z	Pr(>F)
genus	6	1.425	0.237	0.195	13.073	12.017	0.001
Residuals	323	5.866	0.018	0.805	NA	NA	NA
Total	329	7.291	NA	NA	NA	NA	NA

Table 14: Chapter III Procrustes ANCOVA. After considering shape and log 10 transformed size, size only accounts for 5.7%, genus about 21.9% and the interaction between size and genus about 4.9%. Most of the variance cannot be explained by size, genus or their interaction at 67.6% in the residual.

Procrustes ANCOVA: Shape ~ $\log_{10}$(Csize) * Genus

Term	Df	SS	MS	Rsq	F	Z	Pr(>F)
logCS	1	0.413	0.413	0.057	26.467	8.668	0.001
genus	6	1.597	0.266	0.219	17.070	13.785	0.001
logCS:genus	6	0.354	0.059	0.049	3.781	5.859	0.001
Residuals	316	4.928	0.016	0.676	NA	NA	NA
Total	329	7.291	NA	NA	NA	NA	NA

Figure 14: Chapter III PC1 deformation. Visualized deformation of *Pan paniscus* along PC1 demonstrates overall growth of the trochlea, the olecranon fossa expands superior-inferiorly becoming deeper and the trochlear border expands anteriorly creating more asymmetry.

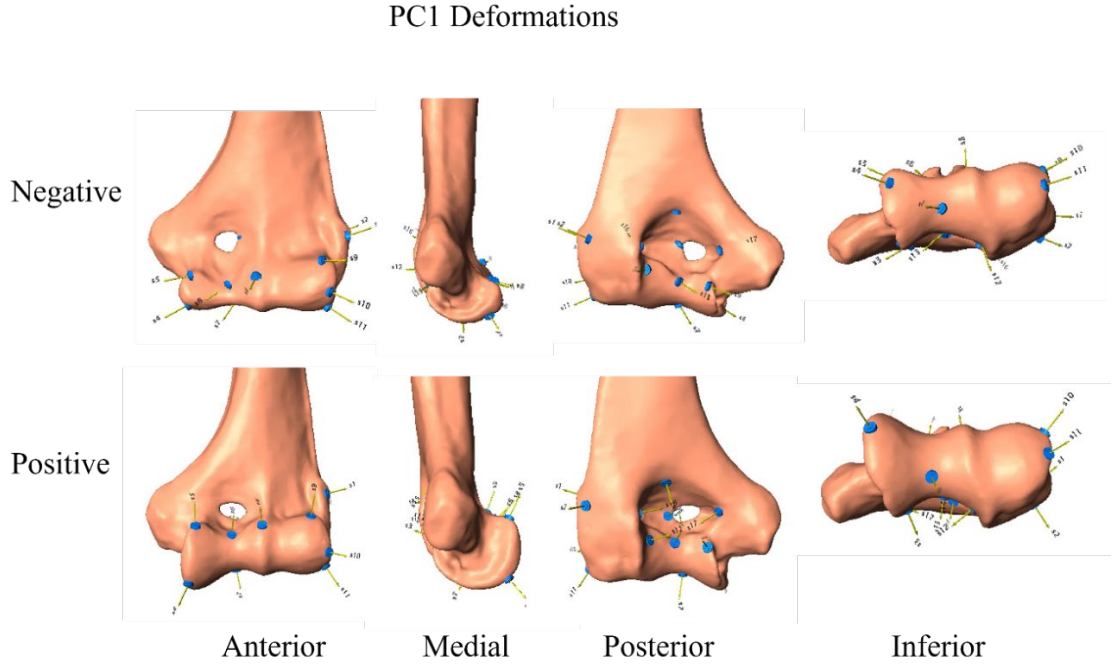

Figure 15: Chapter III PC2 deformation. Visualized deformation of *Pan paniscus* along PC2 shows elongation of the lateral epicondyle with some retroflexion of the medial epicondyle. The trochlear border becomes more anterior-inferiorly expanded while the capitulum also expands slightly.

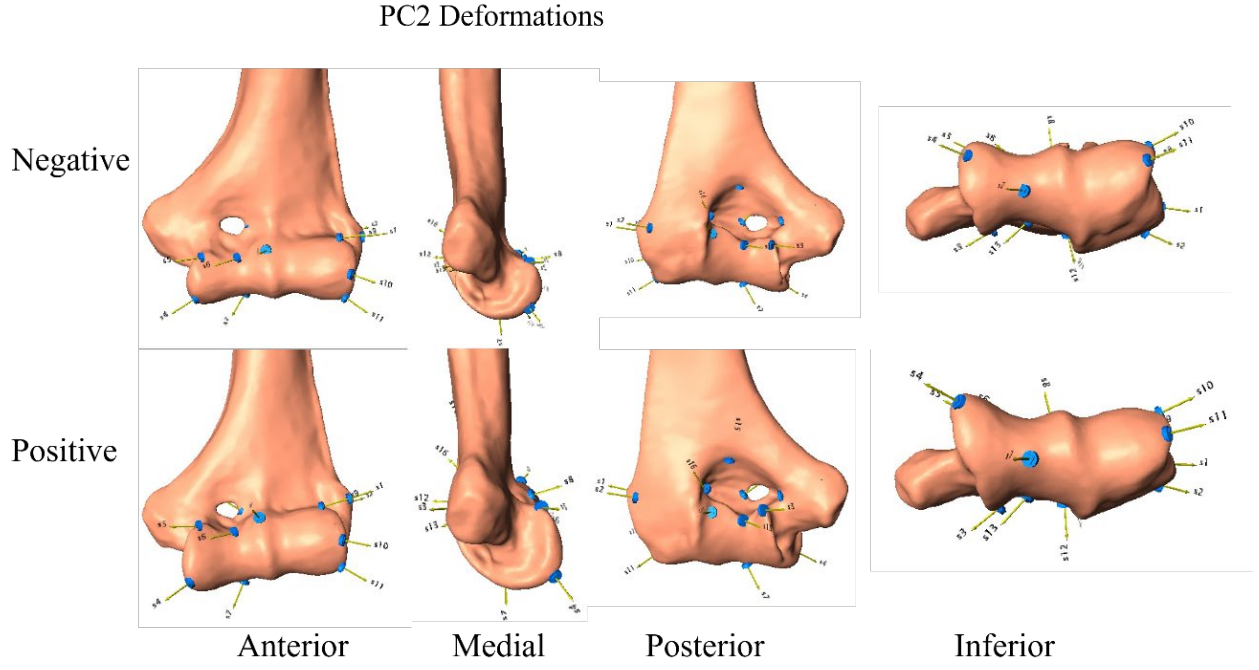

3.5 Discussion

The goal of this study was to analyze shape change in the distal humerus during ontogeny as a test for the effects of developmental plasticity. To evaluate shape change over development I performed a Phenotypic Trajectory Analysis to evaluate the overall shape of the trajectory (the specific path through shape change traversed over ontogeny), the total amount or magnitude of shape change (length or Procrustes' distance from start to end) and angle (pattern of shape change) of the trajectories (Figure 13). *Homo* appears to have the greatest magnitude of shape change overall, largely due to that between the stages of M1 and M2. The M1 individuals used in this study were all fully bipedal and between the ages of 9-11 from the United States. The amount of change the results demonstrate could suggest modern humans around 9-11 years old are using their elbow in a dynamic way (Ruff et al., 2006). I hypothesize this is likely due to children between those ages are typically very physically active and of school age meaning their curriculum is likely to include either some form of physical education or recess (Malina et al, 2004). The age range is also within a timeframe where they may experience more hormonal changes due to the onset of puberty (Rogol et al., 2000). These factors may differ by population and individual experiences during childhood. *Pan paniscus* and *Pongo* share virtually the same developmental pattern, possibly due to both being mainly arboreal, suggesting a selection for an elbow joint that develops rapidly to move through the canopy. Similarly, *Hylobates* shares a comparatively large amount of change between M1-M2 like *Homo*, however the shape of the trajectory differs as it is shorter and trends negatively along PC 2 between M2-M3. This may suggest that Hylobates experience heavy remodeling early on, also being strictly arboreal brachiators. The M1 stage for *Hylobates* and *Symphalangus*, when compared to all other hominoids appears to align with everyone else's M2 stage. This could mean that the degree of

development at M1 for suspensory brachiators comparatively mature to an M2 of all other genera. This further supports the possibility that the demands of high canopy brachiation must occur early on, possibly after individuals are no longer carried by the parents (Fleagle, 1974; Fleagle, 1976; Hunt, 1991; Malone, 2007; Alméjica et al., 2021). The shape of the distal humerus must then "lock in" into a more adult morphology to sustain the locomotor demands. It's possible that the change being dramatically shorter between M2 and M3 in *Hylobates* indicates they are no longer traveling long distances. Between the closely related *Pan paniscus* and *Pan troglodytes* we see *Pan paniscus* diverges positively away from all other apes possibly due to increased commitment to living in trees in their groups. Although it has been observed that *Pan pansicus* does occasionally descend and knuckle-walks terrestrially on the ground it does not appear to affect the shape of the distal humerus after M2 (White et al, 2020).

These findings give way to new insights on the possible demands of locomotion on distal humeral shape. Limitations that need to be acknowledged are due to the sample size of *Symphalangus* at all stages and *Homo* at M1. *Symphalangus* is not common in museum collections, like *Pongo* and *Pan paniscus* which are also rare and mostly found in collections were many species are mounted making them ineligible for scanning. Modern human osteological collections have been under scrutiny for the last several years due to numerous ethical considerations including lack of known provenance.

3.6 Conclusion

Ontogeny has great potential to fill in gaps in our knowledge about growth and development of extant hominoids. While this study demonstrates that ontogenetic allometry plays a role in differentiating the distal humerus between developmental stages, it also indicates genera do not all share the same amount of change between those stages. M1 modern humans

stood out a great deal and this could be due to epigenetic factors that influence how modern human juveniles use the forelimbs for activities outside of locomotion (Ruff et al., 2006; Sarringhaus et al., 2013; Turley and Frost, 2014; Turley et al., 2015, 2018; Deckers et al., 2021). Furthermore, it is worth considering the sample size for M1 modern humans was limited to eight individuals and the population of the M2 nearly all individuals from the Luis Lopes Cemetery Collection in Lisbon, Portugal dating back to the 1850-1940 (Cardoso, 2006). The M1 individuals in this study are from no later than 2010 (Edgar et al., 2020). Together the modern human sample consists of individuals belonging to different populations and different time periods.

Results of the extant non-human primates presented in this study show great apes (*Gorilla, Pan, Pongo*) differ from lesser apes (*Hylobates* and *Symphalangus*) during development in the morphology of the distal humerus. Previous studies looking at the talocrural joint found juvenile apes at M1 appear to have a more flexible ankle suggesting more time spent engaging in arboreal locomotor patterns, but diverge at M2-M3, specifically *Pan paniscus* from *Pan troglodytes*, the former of which becomes fully arboreal as adults (Turley and Frost, 2014; Turley et al, 2015; 2018). Other regions like the metacarpals of the hands have detected differences between knuckle-walking apes (Inouye, 1994). Inouye (1994) studied an ontogenetic sample of great ape metacarpals and noted chimpanzees engage the 2nd and 4th metacarpal more whereas gorillas almost always engage the 5th metacarpal during knuckle-walking mostly due to use rather than allometry.

This study is an important contribution to our understanding of growth and development in the distal humerus across extant hominoids to then assess juvenile australopiths which some do have a preserved distal humerus like DIK-1-1 and MH1 (Alemseged et al., 2006; Berger et

al., 2010). Building a comparative framework like this will allow for evaluation of shared patterns of growth in australopiths to extant hominoids. Additional factors to consider in the future are whether populations of extant hominoids are wild-caught or captive as this could potentially affect how they locomote and the different substrates they interact with and for how long (Turley and Frost, 2018).

CHAPTER IV

MORPHOLOGY OF THE DISTAL HUMERUS IN AUSTRLOPITHS

4.1 Introduction

Australopiths have been the center of a longstanding debate regarding the importance of quadrupedal locomotion to the origins of bipedalism in the *Homo* lineage. The reason being the overwhelming evidence of fossils recovered, like *Australopithecus afarensis* (A.L. 288-1) commonly known as "lucy" dated to nearly 3.2 Ma, that demonstrate a mosaic of both primitive ape-like and human-like derived features (Johanson et al., 1978; Johanson and Edey, 1981; Campisano and Feibel, 2007) . Researchers agree australopiths were bipedal due to skeletal evidence that show adaptations for upright walking. However, some see the primitive ape-like features to lack a functional purpose (Latimer, 1991; Lovejoy, 1988; Latimer and Lovejoy, 1990a,b), while others suggest quadrupedalism played an active role during life (Jungers, 1982; Susman and Stern, 1983; Susman, Stern and Jungers, 1984; Ward et al., 2001; Ward, 2002; Ruff et al., 2016).This ongoing debate has important implications for what we know about the selective pressure that led australopiths to walk upright, and is tied to larger evolutionary hypotheses regarding the *Homo* lineage (Washburn and Lancaster, 1968; Lovejoy, 1981; Hunt, et al, 1996; Wheeler, 1991; Aiello and Wheeler, 1995; Pontzer et al., 2009; Bramble and Lieberman, 2004; Bender et al., 2012; Marzke, 2013).

Therefore, this study focuses on assessing the morphology of the distal humerus, a major contributor of the elbow joint that is actively used during quadrupedalism to investigate possible morphological signatures indicative of use during life. This study includes a sample of australopiths spanning a long period of time (3.4 Ma – 1.5 Ma) across the genera *Australopithecus* and *Paranthropus*. For additional comparative purposes a single later *Homo*

neanderthalensis, Feldhofer 1, was included to compare an extinct bipedal individual from the same lineage.

4.1.1 Objectives

The objectives of this study are threefold: first to compare the morphology of the distal humerus of australopiths to extant hominoids. Second, if differences are detected, to then assess how different they are possibly contributing factors like static allometry or genus. Lastly, to determine if differences are detectable between fossil genera or species.

4.2 Background

Australopiths, like the famous *Australopithecus afarensis* skeleton commonly known as "Lucy" (AL288-1), are central to many studies focused on the origin of bipedalism due to strong skeletal postcranial evidence of upright walking including an anterior foramen magnum, valgus knee, elliptical-shape pelvis, presence of the Anterior Superior and Inferior Iliac spines and the Laetoli trace fossils (Latimer, 1991; Lovejoy, 1988; Latimer and Lovejoy, 1990a, b). AL288-1 is a remarkable partial skeleton recovered from the Afar region of Ethiopia and dating at 3.2 Ma (Johnson et al., 1978; Campisano and Feibel, 2007). However, Australopiths also have skeletal features often associated with quadrupedalism such as curved phalanges, ape-like limb proportions, robust upper extremity elements, and ape-like shoulder girdles which have been part of an ongoing debate as to the importance of arboreal locomotion during life (Jungers, 1982; Susman and Stern, 1983; Susman, Stern and Jungers, 1984; Ward et al., 2001; Ward, 2002; Ruff et al., 2016). While juvenile specimens are rare in the fossil record, the Dikika specimen, DIK-1-1 attributed *Australopithecus afarensis* and dated to 3.4 Ma was described as also having mosaic feature in the shoulder girdle suggesting climbing but also bipedalism (Alemseged et al., 2006). These mosaic-like features make the evolutionary history of bipedalism in the *Homo*

lineage unclear, thus making it a topic of interest for paleoanthropological studies using comparative extant hominoids. This study aims to address hypotheses related to early hominin locomotion with a focus on Australopiths and how their distal humeral morphology compares to that of extant hominoids. Chapter II and III have demonstrated there are morphological signals that support some degree of plasticity in the elbow and previously posited (Rose, 1988; Rose, 1993; Tallman, 2010), however not all features can solely be attributed to use as some may be associated with allometry (Zelazny, 2019). This study compares a small sample of 7 fossil hominins including specimens attributed to the genera *Australopithecus*, *Paranthropus* and early *Homo* to explore hypotheses on use of the forelimb for climbing or other arboreal quadrupedal postures.

4.2.2.1 Fossil Hominins

The distal humerus in fossil hominins is relatively well documented and numerous relative to other postcranial elements found in the fossil record across sites in eastern and southern Africa (Lague and Jungers, 2006; Tallman, 2010; Zelazny, 2019). While some have been fragmented, many have retained enough morphological integrity to make them good candidates for this research as described here (Table 17).

4.2.2.2 *Australopithecus afarensis*

A.L. 288-1

A.L. 288-1 a partial skeleton dating to 3.18 Ma from near the bottom of the Kada Hadar Member, Ethiopia attributed to *Australopithecus afarensis* (Campisano and Feibel, 2007). A.L. 288-1 was determined to be a small female individual with proportionally small limbs suggesting (Bacon, 2000; Lague, 2014). The specimen included in this study is a distal fragment of the left humerus with nearly intact articular surfaces. Some have argued the overall postcrania

morphology of A.L. 288-1 is selected for bipedalism (Latimer and Lovejoy, 1990a, b) while other suggest the primitive ancestral traits observed indicated quadrupedalism retained an important role in their locomotion (Stern and Susman, 1983; Susman et al, 1984). Lastly, previous studies have suggested there may be some evidence of handedness (laterality), along with increased humeral strength (Lague, 2015; Ruff et al., 2016).

AL 322-1

AL 322-1 dated to approximately 3.4 Ma was first described by Lovejoy et al (1982) from the lower Sidi Hakoma Member in Hadar (Lovejoy et al, 1982; Lague and Jungers, 1996). It is also attributed to *Australopithecus afarensis* and is older than the A.L. 288-1 specimen. It has been described as larger and more robust than A.L. 288-1 but still within range for the attributed genus and species and possibly representative of a male specimen (Lague and Jungers, 1996) The distal humerus has been described as having a deep olecranon with a human-like trochlea but a less pronounced medial epicondyle than see in knuckle-walking apes (Lague and Jungers, 1996).

4.2.2.3 *Australopithecus africanus*

StW 431c

StW 431 is a partial skeleton from Sterkfontein Member 4 (Kibii and Clark, 2003; Toussaint et al., 2003; Dobson, 2005; Lague and Menter, 2020). StW 431 attributed to *Australopithecus africanus* is dated around 2.6 Ma, however it is important to also note the age Member 4 has undergone recent debate with advancements in chronometric techniques, where studies using cosmogenic-nuclide burial data Al/Be suggest Member 4 closer to ~ 3.5Ma (Granger et al., 2015, 2022) but Uranium-Lead [U-Pb] flowstone chronology techniques and those including fossil cercopithecid monkeys like *Theropithecus oswaldi* dentition, which have a positive correlation between size and chronological age, suggest Member 4 to be between 2.6 ~ 2.0 Ma (Pickering et

al., 2019; Frost et al., 2022; but see Granger et al., 2022). The right distal humerus StW 431c has been suggested to look more ape-like, while other elements like the ilium have been argued to resemble *Paranthropus* (Lague and Junger, 1996; McHenry and Brown, 2008). Previous studies have suggested StW 431 looks similar to *Gorilla* in having a strong lateral trochlear crest, large lateral epicondyle and being relatively large compared to body size (Lague and Jungers, 1996; Toussaint et al., 2003 McHenry and Brown, 2008; McHenry and Berger, 1998b).

4.3.3.4 *Australopithecus sediba*

Uw88-57

Uw 88-57, commonly known as MH2, is a fossil specimen from the Malapa Caves site in southern Africa dated to 2.0 Ma attributed to *Australopithecus sediba* (Zipfel and Berger, 2010; Pickering et al., 2010; Berger, 2012; de Ruiter et al, 2013). It has been previously described in detail (see Churchill et al., 2018). However, some comparative observations include a strongly projecting medial epicondyle, a smaller distal articular breadth to biepicondylar breadth compared to australopiths and modern humans (Churchill et al., 2013). The medial epicondyle was noted to be less retroflexed and more distally oriented that A.L. 288-1suggesting reduced torque for pronation in the forearm (Ibáñez-Gimeno et al. 2017).

4.2.2.5 *Paranthropus boisei?*

KNM-ER-739

KNM-ER-739 is a left distal humerus from the Okote Member of the Koobi Fora Formation, Kenya dating at 1.5 Ma (Lague and Jungers, 1996). The taxonomy of KNM-ER-739 has been highly debated as it has temporally overlaps with early *Homo* like *H. erectus*, and morphologically appears robust when compared to *Australopithecus* but has no associated craniodental materials to confidently assign to *Paranthropus* which has very distinct large teeth

along with other cranial features like large flat zygomatics and a large sagittal crest as seen in TM1517 (*Paranthropus robustus*) (Feibel et al., 1989; Lague and Jungers, 1996; Lague, 2014). Previous studies, based on morphological features like a relatively large medial epicondyle, a relative shallow olecranon fossa, relatively narrower zona conoidea, a relatively smaller anteroposterior trochlear width and wider lateral and medial pillar suggest KNM-ER-739 is set apart from other Plio-Pleistocene hominid from Koobi Fora and place it closer to likely being *H. rudolfensis* (Lague and Jungers, 1996). However, earlier observations by Leakey (1971) and Senut (1981) tentatively assigned as a "robust" *Australopithecus* due to having large muscle attachment sites like the medial epicondyle the posited suggests some degree of knuckle-walking. This dissertation will follow previous studies that have assigned KNM-ER-739 to *Paranthropus boisei* to test how it morphologically compares to the other fossil genera when using 3D Geometric Morphometric methods

4.2.2.6 *Paranthropus robustus*

TM 1517

TM 1517 is from Kromdraai B ("Hominid") Member 3 dated between 1.9-1.6 Ma, and one of the first fossil humeri found with an associated skull and attributed *Paranthropus robustus* (Broom, 1938; Delson, 1988; Lague and Jungers, 1996). Broom found the overall morphology of the humerus was closer to that of modern humans than extant apes due to having less flared epicondyle when compared to apes and an overall gracile appearance suggesting it would be unlikely to engage in similar arboreality (Broom, 1938; Broom and Schepers, 1946). Large epicondyles as previously stated are associated with strong use of the extensor and flexor muscles often seen with extant great apes that actively engage their forelimbs when moving across the substrate (Lague and Jungers, 1996).

4.2.2.8 *Homo neanderthalensis*

HnP0208 (Feldhofer 1)

This specimen is commonly known as Feldhofer 1 or "Neanderthal" 1 and is the holotype specimen of *Homo neanderthalensis* recovered from the Feldhofer caves in the Neander Valley, Germany (Schmitz et al., 2002). It is dated to be approximately 40,000 years old, making it the youngest fossil in the dataset (Schmitz et al., 2002). I am including this specimen although it is not an australopith because it represents the later genus *Homo* of what would be anatomically the most similar to modern humans yet also a fossil of an extinct species.

4.3 Materials and Methods

4.3.1 Sample specimens

The sample consists of 171 surface scans of the distal humeri of extant hominoids and fossil hominins within the genus *Australopithecus* and *Paranthropus*. The extant genera includes *Gorilla*, *Homo*, *Pongo*, *Pan*, *Hylobates*, *Symphalangus* and *Nasalis* as the one large-bodied cercopithecid (Appendix 3). As in chapter II, I treated the two closely related species *Pan paniscus* and *Pan troglodytes* separately. *Nasalis* was included to represent an outlier group as a pronograde monkey that is strictly an arboreal quadruped inhabiting mangroves and lowland rain forests that mainly leaps but also clambers, is a proficient swimmer and has been observed to engage is some brachiation (Napier and Napier, 1967; Kawabe and Mano, 1972; Meijaard and Nijman, 2000, Su and Jablonski, 2009). Specimens were collected by the author across domestic and international museum collections using handle structured light scanners. Both scanners operate with high resolution up to 0.1mm and accuracy up to 0.5mm. 45 specimens surface scans were generously shared by Dr. Joseph Plavcan, Dr. Carol Ward, Dr. Sergio Alméjica and Dr. Kelsey Pugh. 5 of the 7 fossil specimens included in this study were generously shared by Dr.

William Harcourt-Smith from the American Museum of Natural History including, AL288-1, AL322-1, HnP0208, TM1517, KNMER739. Uw88-57 and StW 431c were downloaded from the online repository Morphosource. Details of the extant sample are provided in Appendix B.

Table 15: Chapter IV Fossil specimens were sorted by genus and the "+" indicates extinct.

Genus	Specimen	M	F	U	RowTotal
Australopithecus	AL288-1+	0	1	0	1
	AL322-1+	0	0	1	1
	StW431c+	0	0	1	1
	Uw8857b+	0	1	0	1
Paranthropus	KNM-ER-739+	0	0	1	1
	TM1517+	0	0	1	1
Homo	HnP0208+	0	0	1	1
Total		**0**	**2**	**5**	**7**

4.3.2 Data collection

Three-dimensional Procrustes coordinate data were collected using as the same 28-landmark configuration on the distal humerus of surface scans as Chapter II (Figure 16 and 17). Adapted from Tallman (2010), to fit the scope of this study, it captures all major articulations of the distal humerus (but also see, McHenry, 1976; Bacon, 2000; Lague, 2014; Rosas et al., 2015; Zelazny, 2019).

Figure 16: Chapter IV landmark protocol, the same 28 single-point landmark protocol as Chapter II

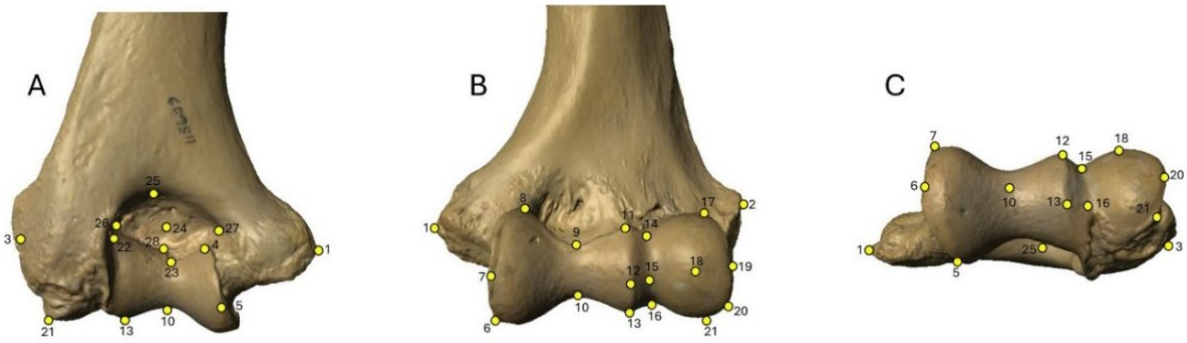

Figure 17: Chapter IV Fossil Surface scans. Scans of anterior view of fossil specimens included in this study, from left to right TM1517, AL, 288-1, AL 322-1, StW431c, Uw88-57, HnP0208, KNM-ER-739. Not that not all specimens are from the same side, some are from the right side of the body others are from the left. When running analyses code was included to reflect these specimens for proper alignment prior to running the GPA for superimposition.

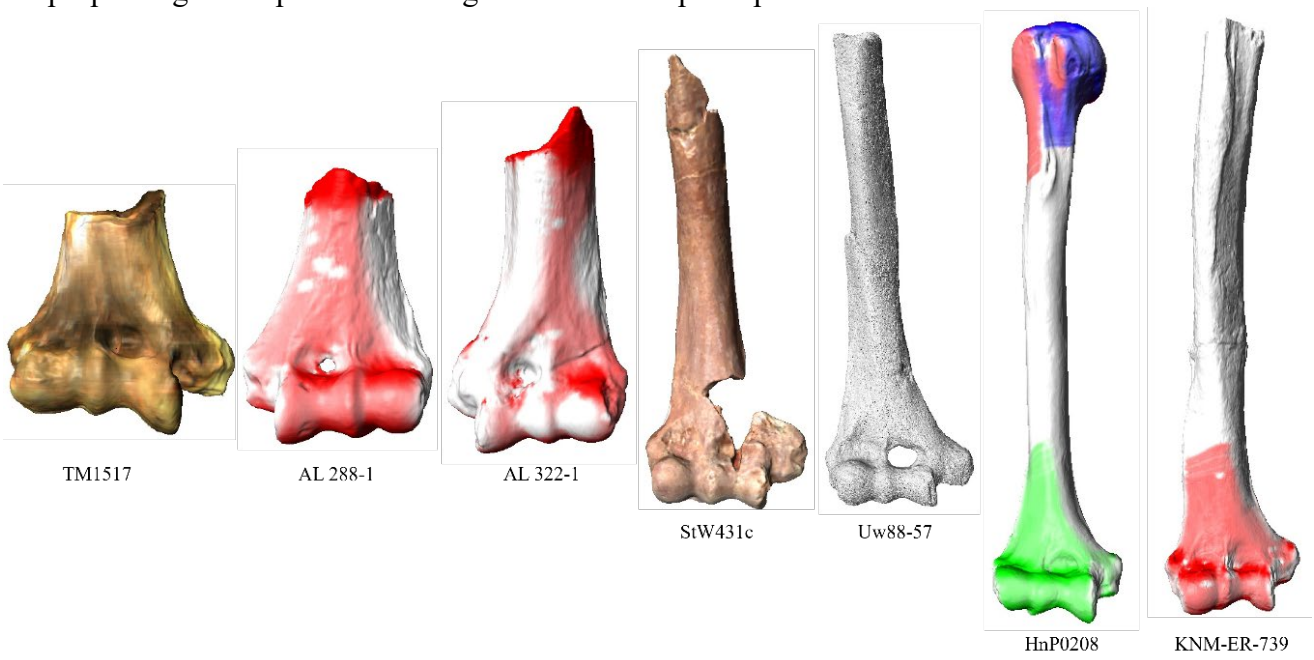

Table 16: Chapter IV Landmark descriptions same as Chapter II (Table 2).

Landmarks	Description
Medial Epicondyle	
1	most projecting point on the medial epicondyle
Laterale Epicondyle	
2	most projecting point on the lateral epicondyle
3	posterior aspect of the lateral epicondyle
Trochlea	
4	most posterior medial corner of the trochlea
5	most posterior projecting point of along the trochlear margin
6	most inferior projecting point of the trochlear margin
7	most anterior projecting point of the trochlear margin
8	most anterior midpoint projecting point of the trochlear margin
9	most superior anterior point of the trochlear margin
Trochlear groove	
9	deepest superior point of the trochlear groove
10	deepest inferior point of the trochlear groove
23	deepest point of the trochlear groove on the posterior aspect
Zona conoidea	
11	most superior point on the zona conoidea ridge
12	midpoint on the zona conoidea ridge
13	most inferior point on the zona conoidea ridge
14	deepest point parallel to lm 11
15	deepest point parallel to lm 12
16	deepest point parallel to lm 13

Table 16 (Continued)

Capitulum	
17	most superior lateral point of the capitulum margin
18	most projecting central point on the capitulum
19	point most in line with lm 18 along the capitulum margin
20	most inferior anterior point along the capitulum margin
21	most inferior point along the capitulum margin
22	most posterior point along the capitulum margin from the posterior aspect
Olecranon fossa	
24	deepest point in the olecranon fossa
25	most superior point along the olecranon fossa margin
26	most lateral point along the olecranon fossa margin
27	most medial point along the olecranon fossa margin
28	most inferior point along the midline of the olecranon fossa

4.3.3 Analytical methods

R, an open-source scientific computing language version 4.5.0 (R Core Team, 2025) was used for all analyses. Geomorph version 4.0, a package that allows for computing all steps of 3D Geometric Morphometrics was primarily used (Adams and Otárola-Castillo, 2013; Adams and Collyer, 2018; Baken et al., 2021; Adams et al., 2025). Missing data was handled using a PCA-based imputation method via the missMDA package in R (Josse and Husson, 2016).

4.3.3.1 3D Geometric Morphometrics

3D Geometric morphometrics (GM) is a tool that has proven useful for assessing shape variation in extant hominoids and fossil hominin (Bacon, 2000; Harcourt-Smith, 2002; Frost et

al., 2003; Tallman, 2010; Arias-Martorell et al., 2012; Lague, 2014; Turley and Frost, 2013; Turley and Frost, 2014; Turley et al, 2015; Di Vicenzo et al., 2015; Arias-Martorell, 2015; Simons, 2019; Zelazny, 2019). For the scope of this study, 3D GM is best applied for assessing the shape of the distal humeri which Chapter 1 previously found can separate specimens by both body size and genus. Chapter II also found genera varies by developmental stages, thus application to fossil hominins may help with future work investigating ontogeny of juvenile fossil remains.

4.3.3.2 Generalized Procrustes Analysis

To analyze shape from 3D Procrustes coordinates, the first step in 3D GM is to superimpose the data by translating, rotating, and scaling each specimen to remove all non-shape variables (Bookstein, 1991; Marcus and Corti, 1996; Slice, 2007). This allows for the data to retain all shape information for statistical comparison.

4.3.3.3 Principal Components Analysis

A Principal Components Analysis (PCA) was performed to explore the variance in the data. A PCA holds no statistical power, rather it is an exploratory tool that performs a singular value decomposition on the dimensionality of the data (Rohlf, 1990; Bookstein, 1991; Slice, 2007; Klingenberg, 2020). PCA is a common tool in 3D GM as it helps simplify and visualize patterns of shape variation guiding subsequent tests of the underlying drivers (Slice, 2007).

4.3.3.4 Procrustes ANOVA and ANCOVA

Procrustes ANOVA Procrustes ANOVA is an analysis of variance, a permutation-based method for testing hypotheses on shape that was used in this study to statistically assess differences due to static allometry, genus and their interactions (Adams and Collyer, 2018). I employ these to statistically test for differences between the extant genera and fossil hominins.

4.4 Results

4.4.1 Principal Components Analysis

The first principal component (PC1) explains 21.6% of the variance in the data, while the second principal component (PC2) represents 8.8% of the variance in the data (Figure 18). PC1 appears to separate genera by size suggesting an allometric effect where *Gorilla* separates from other great apes and *Hylobatids*. PC1 also separates Australopiths from extant apes placing them intermediate between *Homo* and Hylobatids, which is expected due to their comparatively smaller size. However, the *Australopithecus africanus* specimen StW 431c appears different from all other australopiths fall between *Homo* and *Gorilla* along the negative end of PCAPC2 appears to separate specimens based on possible locomotor differences. PC2 separates *Pan paniscus* from *Pan troglodytes*, and *Nasalis* from apes as the only cercopithecid (Figure 19-20). Australopiths fall low along PC2, but within range of *Homo*. While *Paranthropus* is close to *Homo* it mostly falls within *Australopithecus* except for KNM-ER-739 tentatively assigned to *Paranthropus* which falls between *Homo* and *Australopithecus*. HnP0802, the Feldhofer 1 specimen appears to fall within the range of modern humans which is expected given it is within the same genus and temporally closer to modern humans as an obligatory biped (Figure 18).

Figure 18: Chapter IV PCA of fossil distal humeri. PC1 represents 21.6% of the variance while PC2 represents 8.8% of the variance. Convex hulls were included to highlight the different genera.

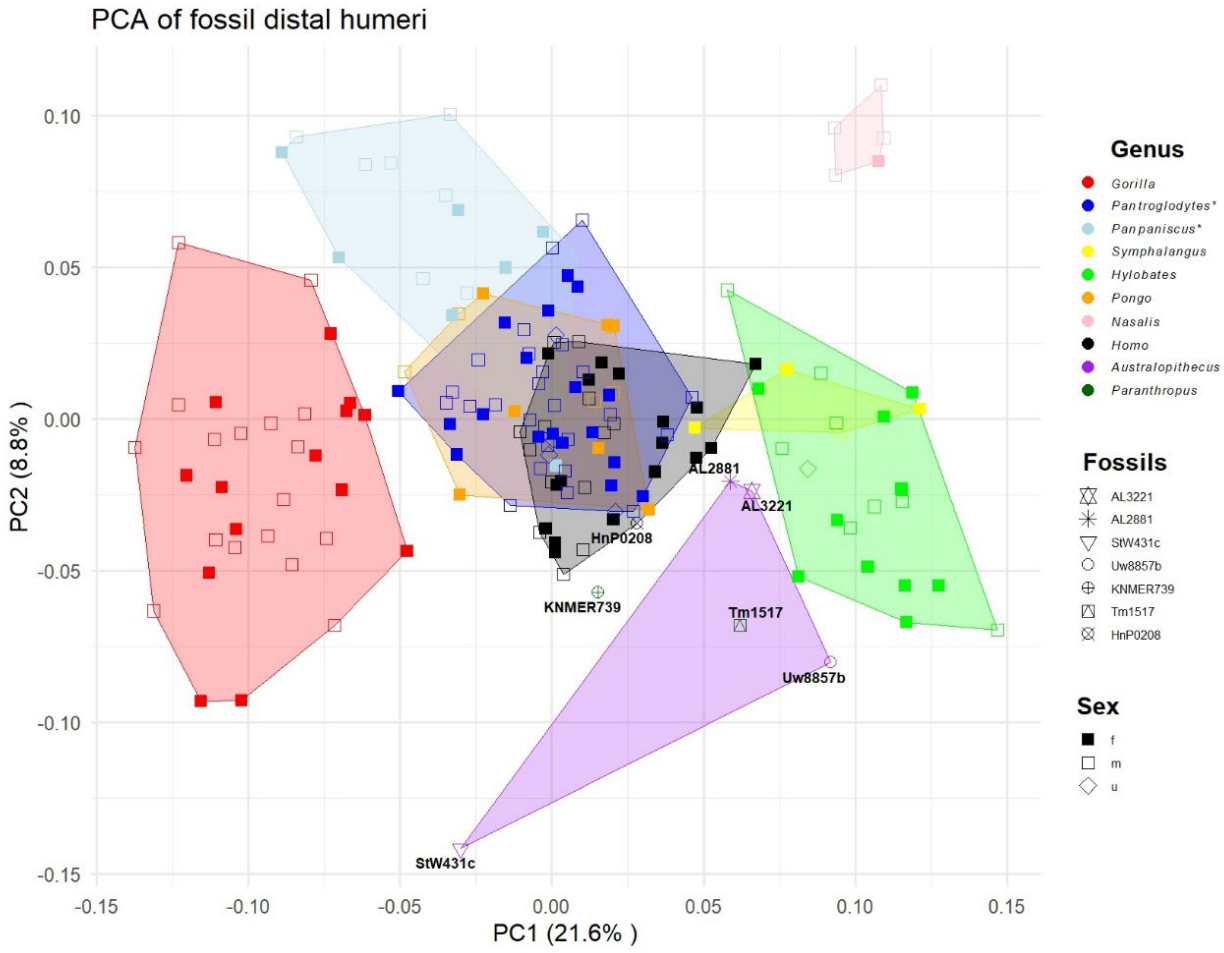

Figure 19: Chapter IV Boxplot of PC1 by genus. The boxplot shows an overlap between *Pan troglodytes*, *Pongo* and *Homo* with less overlap between *Pan troglodytes* and *Pan paniscus*. The fossil *Australopithecus* and *Paranthropus* overlap but do not overlap with the extant sample except for HnP0208 which falls within *Homo*.

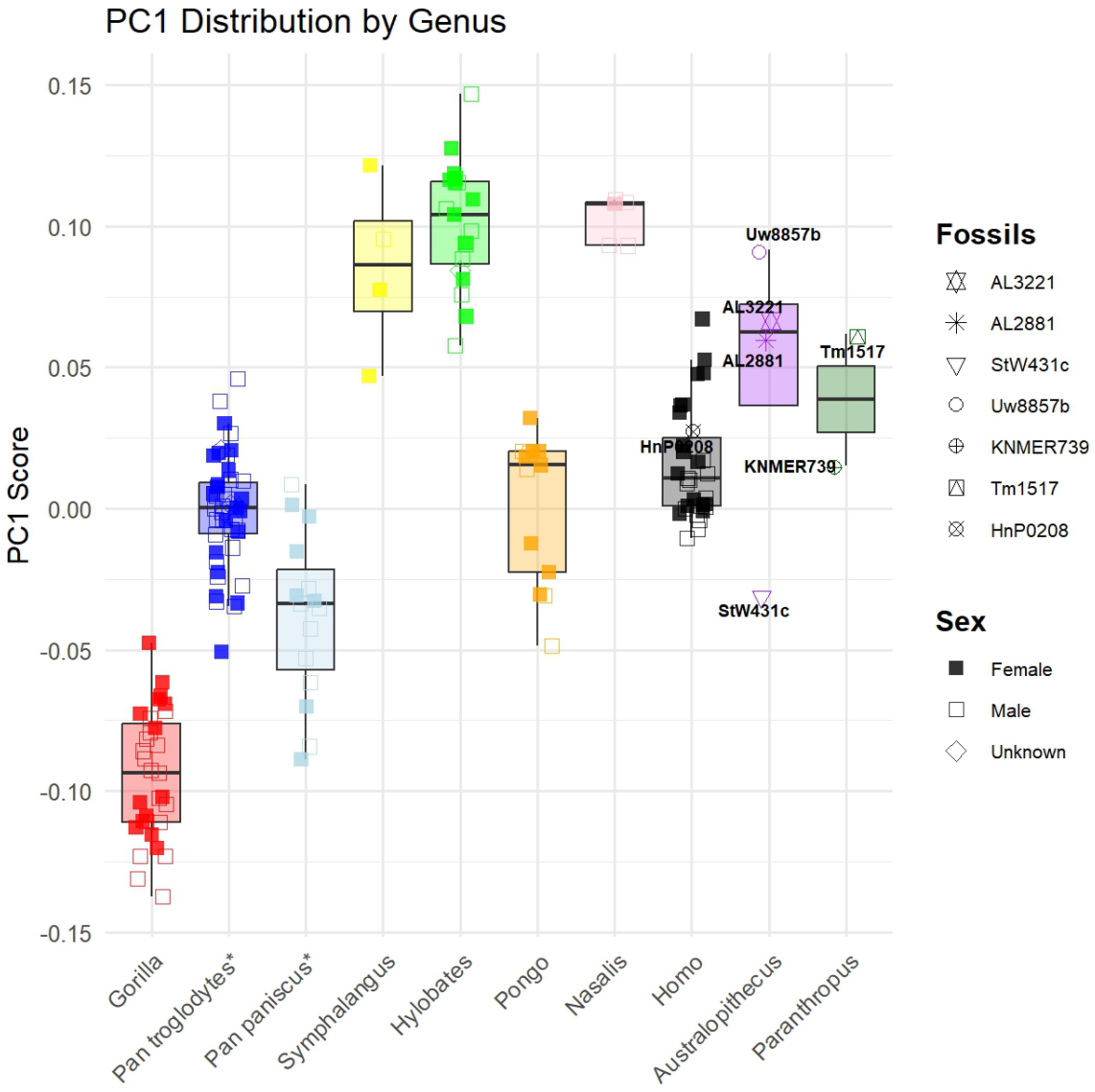

Figure 20: PC2 versus genus box plot where you can see how within *Australopithecus* A.L. 288-1 and A.L. 322-1 falls within range of *Homo* more than the other Australopiths.

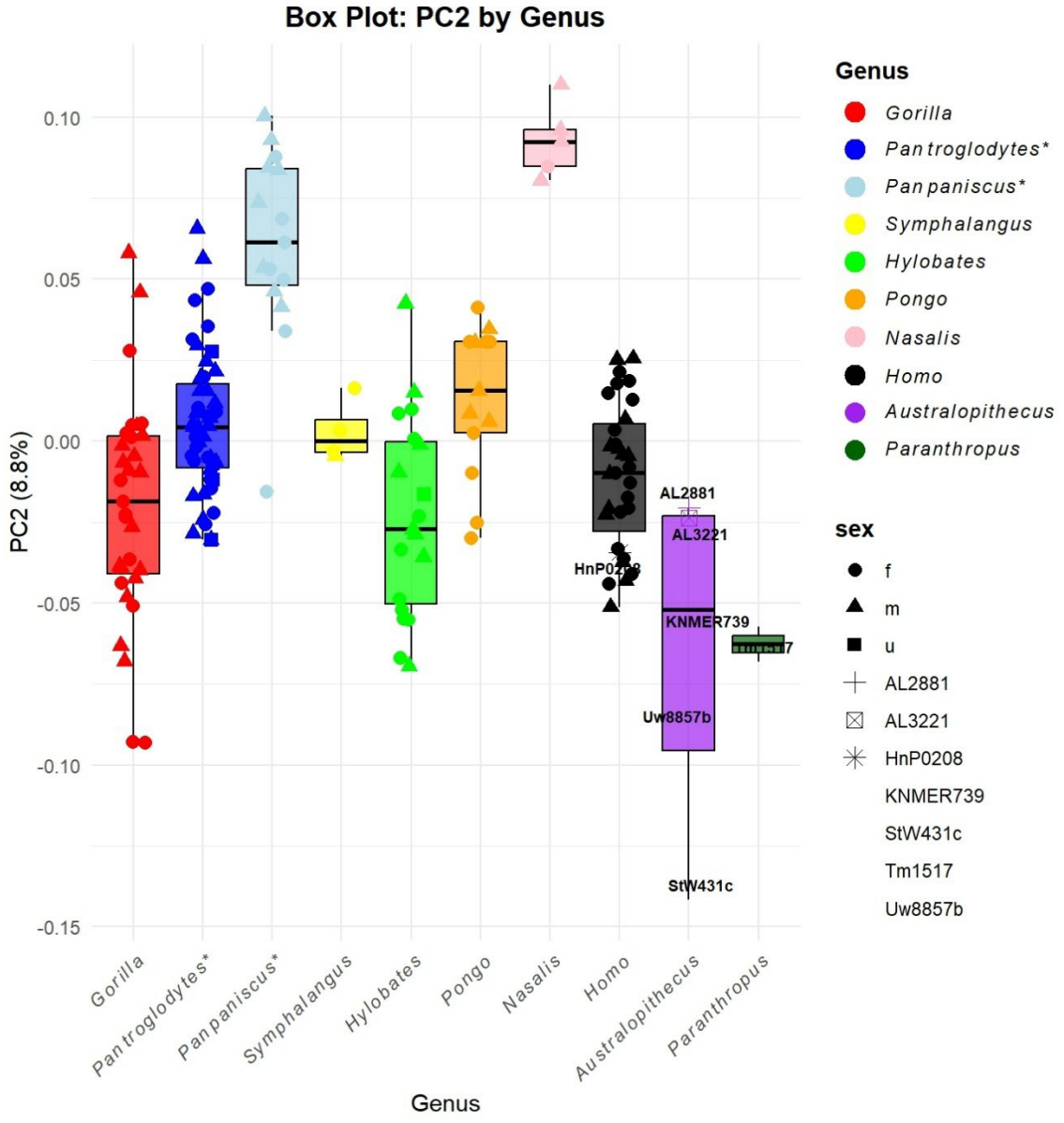

4.4.2 Procrustes ANOVA and ANCOVA

Results from the Procrustes ANOVA indicate that size drives 5% of the variance explained while the other 95% is unexplained and within the residual (Table 17). Genus however appears to drive 40% of the variance while nearly 60% is unexplained in the residual (Table 18). The interaction between size and genus only accounts for 5% of the variance explained, while

size along also accounts for another 5%, genus accounts for 36% and the residual, variance unexplained by genus or size is 54% (Table 19).

Table 17: Procrustes ANOVA: Shape against log 10 transformed size yielded a very low but significant correlation at a P-value of 0.001 but a Rsq of 5% where the residuals make up 95% of the variance.

Procrustes ANOVA: Shape ~ $\log_{10}$(Csize)

	Term	Df	SS	MS	Rsq	F	Z	Pr(>F)
logCS	logCS	1	0.158	0.158	0.05	8.926	5.152	0.001
Residuals	Residuals	169	2.990	0.018	0.95	NA	NA	NA
Total	Total	170	3.148	NA	NA	NA	NA	NA

Table 18: Shape against genus yields a larger effect from genu at a R^2 of 40.5% and residuals of 59.5%. This suggests genus is a larger driver of the variance but a little over half of the variance is still not explained by it.

Procrustes ANOVA: Shape ~ Genus

	Term	Df	SS	MS	Rsq	F	Z	Pr(>F)
genus	genus	9	1.274	0.142	0.405	12.164	8.912	0.001
Residuals	Residuals	161	1.874	0.012	0.595	NA	NA	NA
Total	Total	170	3.148	NA	NA	NA	NA	NA

Table 19: Looking at the interaction with genus yielded only 49% of the variance while the majority still lies in genus alone at 36.2% followed by the residuals at 53.9%.

Procrustes ANOVA: Shape ~ $\log_{10}$(Csize) * Genus

	Term	Df	SS	MS	Rsq	F	Z	Pr(>F)
logCS	logCS	1	0.158	0.158	0.050	14.044	5.876	0.001
genus	genus	9	1.139	0.127	0.362	11.251	9.586	0.001
logCS:genus	logCS:genus	9	0.153	0.017	0.049	1.515	3.026	0.001
Residuals	Residuals	151	1.698	0.011	0.539	NA	NA	NA
Total	Total	170	3.148	NA	NA	NA	NA	NA

4.5 Discussion

Australopiths are a diverse group of early hominins that, for decades, have led researchers to differing interpretations as to the importance of climbing in their daily repertoire (Susman and Stern, 1982, 1991; Stern and Susman, 1983; Latimer, 1987; White and Suwa, 1987; Latimer and Lovejoy, 1990a, b). This study aimed to contribute to ongoing debate by looking at the distal humerus as it is actively engaged during quadrupedal locomotion in extant hominoids. Modern humans use their upper extremity in a very different way, focused on a wider range of motions with little need for stability over flexibility to the degree seen among hominoids

Results from this study suggest A.L.288-1 is closest to modern humans when compared to other Australopiths along with A.L. 322-1. This is interesting because these are the oldest fossils ranging from 3.4-3.2 Ma included in this study (Lague and Jungers, 1996; Campisano and Feibel, 2007). This suggests that morphologically, these two specimens of *Australopithecus afarensis* appear closer to modern humans than to apes possibly due to maintaining an extended

posture in the elbow when walking bipedally (Rose, 1988, 1993; Harcourt-Smith and Aiello, 2004). Within the genus *Australopithecus* StW431c attributed to *Australopithecus africanus* appears to be the most distinct aligning between *Homo* and *Gorilla*. This is interesting because previous studies have posited StW431 to appear more gorilla-like in the distal humerus having a strong lateral trochlear crest and a large lateral epicondyle (Lague and Jungers, 1996; Toussaint et al., 2003; McHenry and Brown, 2008). Others have suggested the distal humerus is large relative to its body size which could explain why it separates as almost an outlier within *Australopithecus* and between the *Gorilla* and *Homo* range (McHenry and Berger, 1998b). TM1517*, Paranthropus robustus*, falls within range of *Australopithecus* and slightly closer Uw 88-57, *Australopithecus sediba*, also from southern Africa relative to the eastern African *Australopithecus* and tentative *Paranthropus boisei* KNM-ER-739. Uw 88-57 differs from the other *Australopithecus* species aligning closer to Hylobatids suggesting it was likely within the same size range since PC1 appears to be driven by size but only accounts for about 21% of the variance, whereas PC2 by locomotion which may also suggest a more flexible elbow than other australopiths or modern humans but only accounts for 8% of the variance. KNM-ER-739 interestingly falls outside of the range of Australopithecus and closer to modern humans which can be seen as somewhat supporting that it may be different from "robust" Australopithecus and still tentative taxonomically as to whether is closer to early Homo or Paranthropus (Leakey, 1971; Lague and Jungers, 1996).

Further investigation is needed to look at differences among Australopiths as StW431c (*A. africanus*) appears to be the most different from both *A. afarensis* and *A. sediba*. This may suggest different growth patterns between the Australopiths found in South Africa than in East or Central Africa. Factors that are worth looking into could be related to palaeoecological

differences at critical points during their development. It would be worth also including later hominins from the same region such as *Homo naledi* for a comparison over time, especially since the Rising Star Caves have yielded an abundance of fossils from a wide age range important for taking an ontogenetic approach.

4.6 Conclusion

Modern humans are unique in their way of bipedal walking by placing one foot in front of the other with a clear biomechanical pattern from heel-strike to toe-off with only the sole of the foot interacting with the substrate (Harcourt-smith, 2002; Harcourt-Smith and Aiello, 2004). Fossil evidence supports that australopiths like *Australopithecus afarensis* was bipedal but also had features that are primitive and ape-like when compared to extant hominoids (Susman and Stern, 1982, 1991; Stern and Susman, 1983; Latimer, 1987; White and Suwa, 1987; Latimer and Lovejoy, 1990a, b). The degree as to which they may have engaged in quadrupedal locomotion during life remains uncertain, however, the morphology of the distal humerus as summarized in this study suggests differences are likely driven by factors other that size and genus. The shape of the distal humerus of australopiths when compared to extant hominoids lies outside of the range of great apes with the exception of StW 431 that has been described to appear more gorilla-like based on strong features of the medial and lateral epicondyle, possibly pointing to strong forearm muscles as seen in quadrupedal apes (Lague and Jungers, 1996; Toussaint et al., 2003; McHenry and Brown, 2008). Furthermore, this study found that the KNM-ER-739 distal humerus with tentative taxonomic affinity to *Paranthropus boisei* suggests it is different from *Australopithecus* and *Paranthropus robustus* of the same genus and more closely aligned with modern humans although not fully within their range. This further complicates the possible affinity with early Homo as opposed to *Paranthropus*, both which have been found from the

Okote Member of the Koobi Fora Formation (Lague and Jungers, 1996). Unsurprisingly, the later *Homo neanderthalensis* falls within the range of modern humans as it is known to be a fully bipedal individual from within the same genus.

This study aimed to shed new light on the morphology of the distal humerus in fossil australopiths when compared to a large and diverse sample of extant hominoids. Limitations met by this study included having small sample of fossil readily available to include in this study. Future work will aim to increase the sample of fossils and to incorporate juvenile fossil specimens to follow up with an ontogenetic study on the distal humerus from Chapter III.

V. CONCLUSION

This dissertation has furthered my understanding of the functional morphology of the distal humerus in both adult and juvenile extant hominoids, and fossil hominins. While acting as an important interface between the arm and forearm, the distal humerus appears to show little remodeling once reaching the ossified adult form. Rather, morphology is more driven by static allometry and genus. Taking an ontogenetic approach proved useful for learning more about how the distal humerus changes shape over development. Using molar eruption stages was a more reliable marker than using age since most great ape specimens are often wild-caught or from zoos so age based on birth is unknown. However, similar to previous studies (Turley and Frost, 2015; Turley et al., 2018), important changes were noted when assessing the trajectories between different developmental stages where the greatest amount of change was within *Homo* at M1-M2. Surprisingly, hylobatids share a similar shape pattern to modern humans rather than other apes, possibly suggesting a similarity in extended postures that should be investigated further.

A.L. 288-1 and A.L. 322-1, the two oldest specimens included in this study appeared to be closest to modern humans than apes suggesting possible similar extended posture during bipedalism. It is worth exploring the variation within fossil hominins by including juvenile hominin specimens as well. Ultimately the australopiths fell within their own range appearing to be unlike modern humans but also outside of extant great apes. The only fossil exception was *Homo neanderthalensis* that fell directly within the range of modern humans as was expected due to being a later species within the same genus. The distribution of australopiths when comparing across genera australopiths suggests that within these extinct genera there is more diversity than expected. In future it is worth considering possible pressures related to the

paleoecology or other epigenetic factors that may have influenced their locomotor patterns during life.

Future work will address the limitations of this study by first increasing the sample size of the extant juvenile specimens and including fossil juvenile australopiths. This will provide a more thorough analysis of the distal humerus and possible differences in growth and development of fossil hominins when compared to extant hominoids. I will also perform similar analyses for the proximal radius and ulna of these specimens for which I also collected surface scans. This will give me the opportunity to perform a large scale ontogenetic study on the entire elbow joint complex in extant hominoids and fossil hominins.

APPENDIX A

CHAPTER II SPECIMENS

Specimen	Genus	Species	Catalog Number	Institution	Sex	Side
Gobemm3hamnh54089	*Gorilla*	*beringei*	54089	amnh	m	L
Gobemm3hamnh54090	*Gorilla*	*beringei*	54090	amnh	m	L
Gobefm3hamnh54091	*Gorilla*	*beringei*	54091	amnh	f	L
Gobefm3hamnh54092	*Gorilla*	*beringei*	54092	amnh	f	L
Gobemm3hamnh115609	*Gorilla*	*beringei*	115609	amnh	m	L
Gobemm3hamnh202932	*Gorilla*	*beringei*	202932	amnh	m	L
Gobefm3hrmca2263	*Gorilla*	*beringei*	2263	rmca	f	L
Gobemm3hrmca8187	*Gorilla*	*beringei*	8187	rmca	m	L
Gobemm3hnmnh395636	*Gorilla*	*beringei*	395636	nmnh	m	L
Gogofm3hamnh167339	*Gorilla*	*gorilla*	167339	amnh	f	L
Gogomm3hamnh239597	*Gorilla*	*gorilla*	239597	amnh	m	L
Gogofm3hamnh54327	*Gorilla*	*gorilla*	h54327	amnh	f	L
Gogomm3hamnh54355	*Gorilla*	*gorilla*	54355	amnh	m	L
Gogofm3hamnh54356	*Gorilla*	*gorilla*	54356	amnh	f	L
Gogofm3hamnh81652	*Gorilla*	*gorilla*	81652	amnh	f	L
Gogomm3hamnh90194	*Gorilla*	*gorilla*	90194	amnh	m	L
Gogomm3hamnh90289	*Gorilla*	*gorilla*	90289	amnh	m	L
Gogomm3hamnh90290	*Gorilla*	*gorilla*	90290	amnh	m	L
Gogomm3hcmnh2767	*Gorilla*	*gorilla*	2767	cmnh	m	L
Gogomm3hcmnhb1407	*Gorilla*	*gorilla*	b1407	cmnh	m	R

Specimen	Genus	Species	Catalog Number	Institution	Sex	Side
Gogomm3hcmnhb1409	*Gorilla*	*gorilla*	b1409	cmnh	m	L
Gogofm3hcmnhb1423	*Gorilla*	*gorilla*	b1423	cmnh	f	R
Gogofm3hcmnhb1710	*Gorilla*	*gorilla*	b1710	cmnh	f	R
Gogomm3hcmnhb1733	*Gorilla*	*gorilla*	b1733	cmnh	m	L
Gogofm3hcmnhb1756	*Gorilla*	*gorilla*	b1756	cmnh	f	L
Gogofm3hcmnhb1765	*Gorilla*	*gorilla*	b1765	cmnh	f	R
Gogofm3hcmnhb1798	*Gorilla*	*gorilla*	b1798	cmnh	f	L
Gogofm3hcmnhb1806	*Gorilla*	*gorilla*	b1806	cmnh	f	R
Gogofm3hcmnhb1856	*Gorilla*	*gorilla*	b1856	cmnh	f	R
Gogomm3hnbcl16865	*Gorilla*	*gorilla*	16865	nbcl	m	L
Gogomm3hnmnh174722	*Gorilla*	*gorilla*	174722	nmnh	m	L
Hosamm3hamnh203501	*Homo*	*sapiens*	203501	amnh	m	L
Hosafm3hcmnh1032	*Homo*	*sapiens*	1032	cmnh	f	R
Hosafm3hcmnh1065rr	*Homo*	*sapiens*	1065rr	cmnh	f	L
Hosafm3hcmnh1102rr	*Homo*	*sapiens*	1102rr	cmnh	f	R
Hosafm3hcmnh1109r	*Homo*	*sapiens*	1109r	cmnh	f	R
Hosafm3hcmnh1123r	*Homo*	*sapiens*	1123r	cmnh	f	L
Hosamm3hcmnh1158rr	*Homo*	*sapiens*	1158rr	cmnh	m	R
Hosamm3hcmnh1331	*Homo*	*sapiens*	1331	cmnh	m	L
Hosamm3hcmnh1360	*Homo*	*sapiens*	1360	cmnh	m	R
Hosafm3hcmnh1396	*Homo*	*sapiens*	1396	cmnh	f	R
Hosamm3hcmnh1533	*Homo*	*sapiens*	1533	cmnh	m	L

Specimen	Genus	Species	Catalog Number	Institution	Sex	Side
Hosafm3hcmnh1604	*Homo*	*sapiens*	1604	cmnh	f	L
Hosamm3hcmnh1618	*Homo*	*sapiens*	1618	cmnh	m	R
Hosamm3hcmnh496	*Homo*	*sapiens*	496	cmnh	m	R
Hosafm3hcmnh512	*Homo*	*sapiens*	512	cmnh	f	R
Hosamm3hcmnh729r	*Homo*	*sapiens*	729r	cmnh	m	L
Hosamm3hcmnh928r	*Homo*	*sapiens*	928r	cmnh	m	L
Hosafm3hcmnh934	*Homo*	*sapiens*	934	cmnh	f	R
Hosafm3hcmnhhth1562	*Homo*	*sapiens*	1562	cmnh	f	L
Hosamm3hcmnhhth1769	*Homo*	*sapiens*	1769	cmnh	m	L
Hosamm3hcmnhhth1926	*Homo*	*sapiens*	1926	cmnh	m	L
Hosafm3hcmnhhth2056	*Homo*	*sapiens*	2056	cmnh	f	L
Hosafm3hcmnhhth2057	*Homo*	*sapiens*	2057	cmnh	f	L
Hosafm3hcmnhhth2105	*Homo*	*sapiens*	2105	cmnh	f	R
Hosamm3hcmnhhth2268	*Homo*	*sapiens*	2268	cmnh	m	L
Hosafm3hcmnhhth2303	*Homo*	*sapiens*	2303	cmnh	f	L
Hosafm3hcmnhhth2511	*Homo*	*sapiens*	2511	cmnh	f	R
Hosamm3hcmnhhth2525	*Homo*	*sapiens*	2525	cmnh	m	L
Hosafm3hcmnhhth2857	*Homo*	*sapiens*	2857	cmnh	f	R
Hosafm3hcmnhhth3123	*Homo*	*sapiens*	3123	cmnh	f	R
Hyagmm3hnbcl4607	*Hylobates*	*agilis*	4607	nbcl	m	L
Hyagfm3hanmh106575	*Hylobates*	*agilis*	106575	anmh	f	L
Hyalfm3hamnh103665	*Hylobates*	*albibarbis*	103665	amnh	f	L

Specimen	Genus	Species	Catalog Number	Institution	Sex	Side
Hyalmm3hamnh103667	*Hylobates*	*albibarbis*	103667	amnh	m	L
Hyklmm3hamnh103344	*Hylobates*	*klossii*	103344	amnh	m	L
Hyklmm3hamnh103347	*Hylobates*	*klossii*	103347	amnh	m	L
Hylaum3hamnh119601	*Hylobates*	*lar*	119601	amnh	u	L
Hylafm3hamnh200752	*Hylobates*	*lar*	200752	amnh	f	L
Hylafm3hmocz41419	*Hylobates*	*lar*	41419	mocz	f	L
Hylafm3hmocz41421	*Hylobates*	*lar*	41421	mocz	f	L
Hylafm3hmocz41424	*Hylobates*	*lar*	41424	mocz	f	L
Hylamm3hmocz41427	*Hylobates*	*lar*	41427	mocz	m	L
Hylamm3hmocz41431	*Hylobates*	*lar*	41431	mocz	m	L
Hylafm3hmocz41440	*Hylobates*	*lar*	41440	mocz	f	L
Hylafm3hmocz41442	*Hylobates*	*lar*	41442	mocz	f	L
Hylamm3hmocz41464	*Hylobates*	*lar*	41464	mocz	m	L
Hylafm3hmocz41494	*Hylobates*	*lar*	41494	mocz	f	L
Hylamm3hmocz41505	*Hylobates*	*lar*	41505	mocz	m	R
Hylafm3hnmnh271047	*Hylobates*	*lar*	271047	nmnh	f	L
Nalafm3hamnh103669	*Nasalis*	*lar*	103669	amnh	f	L
Nalamm3hamnh106272	*Nasalis*	*lar*	106272	amnh	m	L
Nalamm3hamnh106273	*Nasalis*	*lar*	106273	amnh	m	R
Nalamm3hamnh106274	*Nasalis*	*lar*	106274	amnh	m	L
Nalamm3hamnh106275	*Nasalis*	*lar*	106275	amnh	m	L
Popymm3hamnh140426	*Pongo*	*pygmaeus*	140426	amnh	m	R

Specimen	Genus	Species	Catalog Number	Institution	Sex	Side
Popyfm3hamnh200563	*Pongo*	*pygmaeus*	200563	amnh	f	L
Popyfm3hcmnhb1055	*Pongo*	*pygmaeus*	b1055	cmnh	f	L
Popyfm3hcmnhb1167	*Pongo*	*pygmaeus*	b1167	cmnh	f	L
Popyfm3hnmnh145300	*Pongo*	*pygmaeus*	145300	nmnh	f	L
Popyfm3hnmnh145302	*Pongo*	*pygmaeus*	145302	nmnh	f	L
Popymm3hnmnh145304	*Pongo*	*pygmaeus*	145304	nmnh	m	L
Popyfm3hnmnh142169	*Pongo*	*pygmaeus*	142169	nmnh	f	L
Popyfm3hnmnh145309	*Pongo*	*pygmaeus*	145309	nmnh	f	L
Popyfm3hnmnh142169	*Pongo*	*pygmaeus*	142169	nmnh	f	L
Popymm3hnmnh145301	*Pongo*	*pygmaeus*	145301	nmnh	m	L
Popymm3hnmnh145305	*Pongo*	*pygmaeus*	145305	nmnh	m	L
Popymm3hnmnh153823	*Pongo*	*pygmaeus*	153823	nmnh	m	L
Ppanfm3hamnh86857	*Pan*	*paniscus*	86857	amnh	f	L
Ppanfm3hrmca13201	*Pan*	*paniscus*	13201	rmca	f	L
Ppanmm3hrmca13202	*Pan*	*paniscus*	13202	rmca	m	L
Ppanfm3hrmca15293	*Pan*	*paniscus*	15293	rmca	f	L
Ppanmm3hrmca15294	*Pan*	*paniscus*	15294	rmca	m	L
Ppanmm3hrmca15295	*Pan*	*paniscus*	15295	rmca	m	L
Ppanmm3hrmca15296	*Pan*	*paniscus*	15296	rmca	m	L
Ppanmm3hrmca23509	*Pan*	*paniscus*	23509	rmca	m	L
Ppanmm3hrmca27696	*Pan*	*paniscus*	27696	rmca	m	L
Ppanfm3hrmca27698	*Pan*	*paniscus*	27698	rmca	f	L

Specimen	Genus	Species	Catalog Number	Institution	Sex	Side
Ppanmm3hrmca27699	*Pan*	*paniscus*	27699	rmca	m	L
Ppanfm3hrmca29035	*Pan*	*paniscus*	29035	rmca	f	R
Ppanfm3hrmca29042	*Pan*	*paniscus*	29042	rmca	f	L
Ppanmm3hrmca29044	*Pan*	*paniscus*	29044	rmca	m	L
Ppanfm3hrmca29045	*Pan*	*paniscus*	29045	rmca	f	R
Ppanmm3hrmca29047	*Pan*	*paniscus*	29047	rmca	m	R
Ppanmm3hrmca29052	*Pan*	*paniscus*	29052	rmca	m	R
Ppanmm3hsbuc871	*Pan*	*paniscus*	uc871	hsb	m	L
Ptromm3hrmca23511m5	*Pan*	*troglodytes*	23511m5	rmca	m	L
Ptromm3hscrmca1048	*Pan*	*troglodytes*	1048	rmca	m	L
Ptroum3hscrmca14579	*Pan*	*troglodytes*	14579	rmca	u	L
Ptromm3hsrmca179	*Pan*	*troglodytes*	179	rmca	m	L
Ptroum3hsrmca3466	*Pan*	*troglodytes*	3466	rmca	u	L
Ptromm3hamnh10276	*Pan*	*troglodytes*	10276	amnh	m	L
Ptromm3hamnh165763	*Pan*	*troglodytes*	165763	amnh	m	L
Ptromm3hamnh167341	*Pan*	*troglodytes*	167341	amnh	m	L
Ptrofm3hamnh167343	*Pan*	*troglodytes*	167343	amnh	f	L
Ptromm3hamnh167344	*Pan*	*troglodytes*	167344	amnh	m	L
Ptromm3hamnh167346	*Pan*	*troglodytes*	167346	amnh	m	R
Ptrofm3hamnh174860	*Pan*	*troglodytes*	174860	amnh	f	L
Ptrofm3hamnh90292	*Pan*	*troglodytes*	90292	amnh	f	L
Ptrofm3hcmnhb1707	*Pan*	*troglodytes*	b1707	cmnh	f	L

Specimen	Genus	Species	Catalog Number	Institution	Sex	Side
Ptromm3hcmnhb1708	*Pan*	*troglodytes*	b1708	cmnh	m	R
Ptrofm3hcmnhb1713	*Pan*	*troglodytes*	b1713	cmnh	f	L
Ptrofm3hcmnhb1719	*Pan*	*troglodytes*	b1719	cmnh	f	R
Ptrofm3hcmnhb1720	*Pan*	*troglodytes*	b1720	cmnh	f	L
Ptrofm3hcmnhb1721	*Pan*	*troglodytes*	b1721	cmnh	f	L
Ptrofm3hcmnhb1723	*Pan*	*troglodytes*	b1723	cmnh	f	L
Ptromm3hcmnhb1738	*Pan*	*troglodytes*	b1738	cmnh	m	L
Ptromm3hcmnhb1739	*Pan*	*troglodytes*	b1739	cmnh	m	L
Ptromm3hcmnhb1745	*Pan*	*troglodytes*	b1745	cmnh	m	R
Ptrofm3hcmnhb1748	*Pan*	*troglodytes*	b1748	cmnh	f	L
Ptromm3hcmnhb1758	*Pan*	*troglodytes*	b1758	cmnh	m	L
Ptrofm3hcmnhb1766	*Pan*	*troglodytes*	b1766	cmnh	f	R
Ptrofm3hcmnhb1843	*Pan*	*troglodytes*	b1843	cmnh	f	R
Ptromm3hcmnhb1882	*Pan*	*troglodytes*	b1882	cmnh	m	L
Ptromm3hcmnhb2072	*Pan*	*troglodytes*	b2072	cmnh	m	L
Ptromm3hcmnhb2746	*Pan*	*troglodytes*	b2746	cmnh	m	L
Ptrofm3hcmnhb3539	*Pan*	*troglodytes*	b3539	cmnh	f	R
Ptrofm3hcmnhb3551	*Pan*	*troglodytes*	b3551	cmnh	f	R
Ptromm3hcmnhb3552	*Pan*	*troglodytes*	b3552	cmnh	m	L
Ptroum3hrmca30660	*Pan*	*troglodytes*	30660	rmca	u	L
Ptrofm3hnmnh176226	*Pan*	*troglodytes*	176226	nmnh	f	L
Ptrofm3hnmnh220064	*Pan*	*troglodytes*	220064	nmnh	f	L

Specimen	Genus	Species	Catalog Number	Institution	Sex	Side
Ptromm3hnmnh220327	*Pan*	*troglodytes*	220327	nmnh	m	L
Ptromm3hnmnh395820	*Pan*	*troglodytes*	395820	nmnh	m	L
Ptromm3hnmnh48104	*Pan*	*troglodytes*	48104	nmnh	m	L
Ptrofm3hvamnh89351	*Pan*	*troglodytes*	89351	amnh	f	L
Ptrofm3hvamnh89354	*Pan*	*troglodytes*	89354	amnh	f	L
Ptromm3hvamnh89355	*Pan*	*troglodytes*	89355	amnh	m	L
Ptromm3hvamnh89407	*Pan*	*troglodytes*	89407	amnh	m	L
Ptroum3hrmca30847	*Pan*	*troglodytes*	30847	rmca	u	L
Sysymm3hamnh106581	*Symphalangus*	*symphalangus*	106581	amnh	m	L
Sysyfm3hamnh106583	*Symphalangus*	*symphalangus*	106583	amnh	f	L
Sysyfm3hamnh106584	*Symphalangus*	*symphalangus*	106584	amnh	f	L
Sysyfm3hnmnh271048	*Symphalangus*	*symphalangus*	271048	nmnh	f	L

APPENDIX B

CHAPTER III SPECIMENS

specimen	Genus	Species	Catalog Number	Institution	Sex	Side	Stage
Gobemm3hamnh54089	*Gorilla*	*beringei*	54089	amnh	m	L	M3
Gobemm3hamnh54090	*Gorilla*	*beringei*	54090	amnh	m	L	M3
Gobefm3hamnh54091	*Gorilla*	*beringei*	54091	amnh	f	L	M3
Gobefm3hamnh54092	*Gorilla*	*beringei*	54092	amnh	f	L	M3
Gobemm3hamnh115609	*Gorilla*	*beringei*	115609	amnh	m	L	M3
Gobemm3hamnh202932	*Gorilla*	*beringei*	202932	amnh	m	L	M3
Gobefm3hrmca2263	*Gorilla*	*beringei*	2263	rmca	f	L	M3
Gobemm3hrmca8187	*Gorilla*	*beringei*	8187	rmca	m	L	M3
Gobemm3hnmnh395636	*Gorilla*	*beringei*	395636	nmnh	m	L	M3
Gogofm3hamnh167339	*Gorilla*	*gorilla*	167339	amnh	f	L	M3
Gogomm3hamnh239597	*Gorilla*	*gorilla*	239597	amnh	m	L	M3
Gogofm3hamnh54327	*Gorilla*	*gorilla*	54327	amnh	f	L	M3
Gogomm3hamnh54355	*Gorilla*	*gorilla*	54355	amnh	m	L	M3
Gogofm3hamnh54356	*Gorilla*	*gorilla*	54356	amnh	f	L	M3
Gogofm3hamnh81652	*Gorilla*	*gorilla*	81652	amnh	f	L	M3
Gogomm3hamnh90194	*Gorilla*	*gorilla*	90194	amnh	m	L	M3
Gogomm3hamnh90289	*Gorilla*	*gorilla*	90289	amnh	m	L	M3
Gogomm3hamnh90290	*Gorilla*	*gorilla*	90290	amnh	m	L	M3
Gogomm3hcmnh2767	*Gorilla*	*gorilla*	2767	cmnh	m	L	M3
Gogomm3hcmnhb1407	*Gorilla*	*gorilla*	b1407	cmnh	m	R	M3

specimen	Genus	Species	Catalog Number	Institution	Sex	Side	Stage
Gogomm3hcmnhb1409	*Gorilla*	*gorilla*	b1409	cmnh	m	L	M3
Gogofm3hcmnhb1423	*Gorilla*	*gorilla*	b1423	cmnh	f	R	M3
Gogofm3hcmnhb1710	*Gorilla*	*gorilla*	b1710	cmnh	f	R	M3
Gogomm3hcmnhb1728	*Gorilla*	*gorilla*	b1728	cmnh	m	L	M3
Gogomm3hcmnhb1731	*Gorilla*	*gorilla*	b1731	cmnh	m	L	M3
Gogomm3hcmnhb1733	*Gorilla*	*gorilla*	b1733	cmnh	m	L	M3
Gogofm3hcmnhb1756	*Gorilla*	*gorilla*	b1756	cmnh	m	L	M3
Gogofm3hcmnhb1765	*Gorilla*	*gorilla*	b1765	cmnh	m	R	M3
Gogofm3hcmnhb1798	*Gorilla*	*gorilla*	b1798	cmnh	f	L	M3
Gogofm3hcmnhb1806	*Gorilla*	*gorilla*	b1806	cmnh	f	R	M3
Gogofm3hcmnhb1856	*Gorilla*	*gorilla*	b1856	cmnh	f	R	M3
Gogomm3hnbcl16865	*Gorilla*	*gorilla*	16865	cmnh	f	L	M3
Gogomm3hnmnh174722	*Gorilla*	*gorilla*	174722	cmnh	f	L	M3
Gospmm3hamnh235603	*Gorilla*	*sp.*	235603	amnh	m	L	M3
Gogoum2hamnh170362	*Gorilla*	*gorilla*	170362	amnh	u	L	M2
Gogomm2hnbcl23880	*Gorilla*	*gorilla*	23880	nbcl	m	L	M2
Gogomm2hnbcl2720	*Gorilla*	*gorilla*	2720	nbcl	m	L	M2
Gogofm2huzhc6787	*Gorilla*	*gorilla*	6787	uzhc	f	L	M2
Gogofm2huzhc6788	*Gorilla*	*gorilla*	6788	uzhc	f	L	M2
Gogofm2huzhc6842	*Gorilla*	*gorilla*	6842	uzhc	f	L	M2
Gogomm2hamnh145600	*Gorilla*	*gorilla*	145600	amnh	m	L	M2
Gogoum1hamnh150285	*Gorilla*	*gorilla*	150285	amnh	u	L	M1

specimen	Genus	Species	Catalog Number	Institution	Sex	Side	Stage
Gogofm1hamnh200056	*Gorilla*	*gorilla*	200056	amnh	f	R	M1
Gogofm1hamnh22832	*Gorilla*	*gorilla*	22832	amnh	f	L	M1
Gogofm1huzhc6994	*Gorilla*	*gorilla*	6994	uzhc	f	L	M1
Hyagmm3hnbcl4607	*Hylobates*	*agilis*	4607	nbcl	m	L	M3
Hyagfm3hanmh106575	*Hylobates*	*agilis*	106575	anmh	f	L	M3
Hyagum2hamnh119602	*Hylobates*	*agilis*	119602	amnh	u	L	M2
Hyagmm2hamnh106576	*Hylobates*	*agilis*	106576	amnh	m	L	M2
Hyagfm2hamnh106580	*Hylobates*	*agilis*	106580	amnh	f	L	M2
Hyalfm3hamnh103664	*Hylobates*	*albibarbis*	103664	amnh	f	L	M3
Hyalfm3hamnh103665	*Hylobates*	*albibarbis*	103665	amnh	f	L	M3
Hyalmm3hamnh103667	*Hylobates*	*albibarbis*	103667	amnh	m	L	M3
Hyalmm2hamnh103345	*Hylobates*	*albibarbis*	103345	amnh	m	L	M2
Hyalmm2hamnh103346	*Hylobates*	*albibarbis*	103346	amnh	m	L	M2
Hyklmm3hamnh103344	*Hylobates*	*klossii*	103344	amnh	m	L	M3
Hyklmm3hamnh103347	*Hylobates*	*klossii*	103347	amnh	m	L	M3
Hylaum3hamnh119601	*Hylobates*	*lar*	119601	amnh	u	L	M3
Hylafm3hamnh200752	*Hylobates*	*lar*	200752	amnh	f	L	M3
Hylamm3hamnh202384	*Hylobates*	*lar*	202384	amnh	m	L	M3
Hylafm3hmocz41419	*Hylobates*	*lar*	41419	mocz	f	L	M3
Hylafm3hmocz41421	*Hylobates*	*lar*	41421	mocz	f	L	M3
Hylafm3hmocz41424	*Hylobates*	*lar*	41424	mocz	f	L	M3
Hylamm3hmocz41427	*Hylobates*	*lar*	41427	mocz	m	L	M3

specimen	Genus	Species	Catalog Number	Institution	Sex	Side	Stage
Hylamm3hmocz41431	*Hylobates*	*lar*	41431	mocz	m	L	M3
Hylafm3hmocz41440	*Hylobates*	*lar*	41440	mocz	f	L	M3
Hylafm3hmocz41442	*Hylobates*	*lar*	41442	mocz	f	L	M3
Hylamm3hmocz41464	*Hylobates*	*lar*	41464	mocz	m	L	M3
Hylafm3hmocz41494	*Hylobates*	*lar*	41494	mocz	f	L	M3
Hylamm3hmocz41505	*Hylobates*	*lar*	41505	mocz	m	R	M3
Hylafm3hnmnh271047	*Hylobates*	*lar*	271047	nmnh	f	L	M3
Hylamm2hamnh146725	*Hylobates*	*lar*	146725	amnh	m	R	M2
Hylafm2hamnh43064	*Hylobates*	*lar*	43064	amnh	f	L	M2
Hylafm2hamnh43063	*Hylobates*	*lar*	43063	amnh	f	L	M2
Hymofm2hamnh200853	*Hylobates*	*moloch*	200853	amnh	f	L	M2
Hymofm2hnbcl2686	*Hylobates*	*moloch*	2686	nbcl	f	L	M2
Hymomm2hnbcl4610	*Hylobates*	*moloch*	4610	nbcl	m	L	M2
Hylofm1huzhc1628	*Hylobates*	*moloch*	1628	uzhc	f	L	M1
Hylofm1huzhc1644	*Hylobates*	*moloch*	1644	uzhc	f	L	M1
Hylomm1huzhc1645	*Hylobates*	*moloch*	1645	uzhc	m	L	M1
Hylomm1huzhc1655	*Hylobates*	*moloch*	1655	uzhc	m	R	M1
Hyspum3hamnh202513	*Hylobates*	*sp.*	202513	amnh	u	L	M3
Hyspfm3hamnh208985	*Hylobates*	*sp.*	208985	amnh	f	L	M3
Hyspmm3hamnh238068	*Hylobates*	*sp.*	238068	amnh	m	L	M3
Hyspum2hamnh15971	*Hylobates*	*sp.*	15971	amnh	u	R	M2
Hyspfm1hamnh148202	*Hylobates*	*sp.*	148202	amnh	f	R	M1

specimen	Genus	Species	Catalog Number	Institution	Sex	Side	Stage
Hyspmm1hamnh19013	*Hylobates*	*sp.*	19013	amnh	m	R	M1
Popymm3hamnh140426	*Pongo*	*pygmaeus*	140426	amnh	m	R	M3
Popyfm3hamnh200563	*Pongo*	*pygmaeus*	200563	amnh	f	L	M3
Popyfm3hamnh200898	*Pongo*	*pygmaeus*	200898	amnh	f	L	M3
Popyfm3hamnh200900	*Pongo*	*pygmaeus*	200900	amnh	f	L	M3
Popyfm3hcmnhb1030	*Pongo*	*pygmaeus*	b1030	cmnh	f	L	M3
Popyfm3hcmnhb1055	*Pongo*	*pygmaeus*	b1055	amnh	f	L	M3
Popyfm3hcmnhb1167	*Pongo*	*pygmaeus*	b1167	amnh	f	L	M3
Popyfm3hcmnhb1443	*Pongo*	*pygmaeus*	142169	cmnh	f	L	M3
Popymm3hcmnhb1444	*Pongo*	*pygmaeus*	b1444	cmnh	m	L	M3
Popyfm3hnmnh145300	*Pongo*	*pygmaeus*	145300	cmnh	f	L	M3
Popymm3hnmnh145304	*Pongo*	*pygmaeus*	145304	cmnh	f	L	M3
Popyfm3hnmnh142169	*Pongo*	*pygmaeus*	142169	nmnh	f	L	M3
Popyfm3hnmnh145309	*Pongo*	*pygmaeus*	145309	cmnh	m	L	M3
Popymm3hnmnh145301	*Pongo*	*pygmaeus*	145301	nmnh	m	L	M3
Popyfm3hnmnh145302	*Pongo*	*pygmaeus*	145302	cmnh	f	L	M3
Popymm3hnmnh145305	*Pongo*	*pygmaeus*	145305	nmnh	m	L	M3
Popyfm3hnmnh153805	*Pongo*	*pygmaeus*	145305	nmnh	f	L	M3
Popymm3hnmnh153823	*Pongo*	*pygmaeus*	153823	nmnh	f	L	M3
Popyum2hamnh28252	*Pongo*	*pygmaeus*	28252	amnh	u	R	M2
Popymm2hamnh28253	*Pongo*	*pygmaeus*	28253	amnh	m	R	M2
Popyfm2hamnh35549	*Pongo*	*pygmaeus*	35549	amnh	f	L	M2

specimen	Genus	Species	Catalog Number	Institution	Sex	Side	Stage
Popymm2hamnh80008	*Pongo*	*pygmaeus*	80008	amnh	m	R	M2
Popyum2hamnh90395	*Pongo*	*pygmaeus*	90395	amnh	u	R	M2
Popyum2huzhc1767	*Pongo*	*pygmaeus*	1767	uzhc	u	L	M2
Popyum2huzhc15451	*Pongo*	*pygmaeus*	15451	uzhc	u	L	M2
Pospfm2hamnh239847	*Pongo*	*pygmaeus*	239847	amnh	f	L	M2
Popymm1hamnh146612	*Pongo*	*pygmaeus*	146612	amnh	m	L	M1
Popyum1hamnh150227	*Pongo*	*pygmaeus*	150227	amnh	u	L	M1
Popymm1hamnh16593	*Pongo*	*pygmaeus*	16593	amnh	m	R	M1
Popymm1hamnh17339	*Pongo*	*pygmaeus*	17339	amnh	m	L	M1
Popyum1hamnh19180	*Pongo*	*pygmaeus*	19180	amnh	u	L	M1
Popyum1hamnh284	*Pongo*	*pygmaeus*	284	amnh	u	L	M1
Popyum1huzhc10141	*Pongo*	*pygmaeus*	10141	uzhc	u	L	M1
Ppanfm3hamnh86857	*Pan*	*paniscus*	86857	amnh	f	L	M3
Ppanfm3hrmca13201	*Pan*	*paniscus*	13201	rmca	f	L	M3
Ppanmm3hrmca13202	*Pan*	*paniscus*	13202	rmca	m	L	M3
Ppanfm3hrmca15293	*Pan*	*paniscus*	15293	rmca	f	L	M3
Ppanmm3hrmca15294	*Pan*	*paniscus*	15294	rmca	m	L	M3
Ppanmm3hrmca15295	*Pan*	*paniscus*	15295	rmca	m	L	M3
Ppanmm3hrmca15296	*Pan*	*paniscus*	15296	rmca	m	L	M3
Ppanmm3hrmca23509	*Pan*	*paniscus*	23509	rmca	m	L	M3
Ppanmm3hrmca27696	*Pan*	*paniscus*	27696	rmca	m	L	M3
Ppanfm3hrmca27698	*Pan*	*paniscus*	27698	rmca	f	L	M3

specimen	Genus	Species	Catalog Number	Institution	Sex	Side	Stage
Ppanmm3hrmca27699	*Pan*	*paniscus*	27699	rmca	m	L	M3
Ppanfm3hrmca29035	*Pan*	*paniscus*	29035	rmca	f	R	M3
Ppanfm3hrmca29040	*Pan*	*paniscus*	29040	rmca	f	L	M3
Ppanfm3hrmca29042	*Pan*	*paniscus*	29042	rmca	f	L	M3
Ppanmm3hrmca29044	*Pan*	*paniscus*	29044	rmca	f	L	M3
Ppanfm3hrmca29045	*Pan*	*paniscus*	29045	rmca	m	R	M3
Ppanmm3hrmca29047	*Pan*	*paniscus*	29047	rmca	f	R	M3
Ppanmm3hrmca29052	*Pan*	*paniscus*	29052	rmca	m	R	M3
Ppanfm3hrmca29060	*Pan*	*paniscus*	29060	rmca	f	L	M3
Ppanmm3hrmca29063	*Pan*	*paniscus*	29063	rmca	m	L	M3
Ppanum3hrmca5374	*Pan*	*paniscus*	5374	rmca	u	L	M3
Ppanmm3hsbuc871	*Pan*	*paniscus*	uc871	hsb	m	L	M3
Ppanmm2hrmca29036	*Pan*	*paniscus*	29036	rmca	m	R	M2
Ppanmm2hrmca29051	*Pan*	*paniscus*	29051	rmca	m	R	M2
Ppanmm2hrmca29053	*Pan*	*paniscus*	29053	rmca	m	R	M2
Ppanfm2hrmca29055	*Pan*	*paniscus*	29055	rmca	f	L	M2
Ppanfm2hrmca29057	*Pan*	*paniscus*	29057	rmca	f	R	M2
Ppanfm2hrmca20529	*Pan*	*paniscus*	20529	rmca	f	L	M2
Ppanmm2hrmca29028	*Pan*	*paniscus*	29028	rmca	m	L	M2
Ppanfm2hrmca29032	*Pan*	*paniscus*	29032	rmca	f	L	M2
Ppanmm2hrmca29054	*Pan*	*paniscus*	29054	rmca	m	L	M2
Ppanmm2hrmca29056	*Pan*	*paniscus*	29056	rmca	m	R	M2

specimen	Genus	Species	Catalog Number	Institution	Sex	Side	Stage
Ppanfm1hrmca11528	*Pan*	*paniscus*	11528	rmca	f	L	M1
Ppanmm1hrmca12087	*Pan*	*paniscus*	12087	rmca	m	L	M1
Ppanum1hrmca23464	*Pan*	*paniscus*	23464	rmca	u	R	M1
Ppanfm1hrmca29048	*Pan*	*paniscus*	29048	rmca	f	L	M1
Ppanmm1hrmca84036	*Pan*	*paniscus*	84036	rmca	m	L	M1
Ptromm3hrmca23511m5	*Pan*	*troglodytes*	23511m5	rmca	m	L	M3
Ptromm3hscrmca1048	*Pan*	*troglodytes*	1048	rmca	m	L	M3
Ptroum3hscrmca14579	*Pan*	*troglodytes*	14579	rmca	u	L	M3
Ptromm3hsrmca179	*Pan*	*troglodytes*	179	rmca	m	L	M3
Ptroum3hsrmca3466	*Pan*	*troglodytes*	3466	rmca	u	L	M3
Ptromm3hamnh10276	*Pan*	*troglodytes*	10276	amnh	m	L	M3
Ptromm3hamnh165763	*Pan*	*troglodytes*	165763	amnh	m	L	M3
Ptromm3hamnh167341	*Pan*	*troglodytes*	167341	amnh	m	L	M3
Ptrofm3hamnh167343	*Pan*	*troglodytes*	167343	amnh	f	L	M3
Ptromm3hamnh167344	*Pan*	*troglodytes*	167344	amnh	m	L	M3
Ptromm3hamnh167346	*Pan*	*troglodytes*	167346	amnh	m	R	M3
Ptrofm3hamnh174860	*Pan*	*troglodytes*	174860	amnh	f	L	M3
Ptromm3hamnh174861	*Pan*	*troglodytes*	174861	amnh	m	L	M3
Ptrofm3hamnh90292	*Pan*	*troglodytes*	90292	amnh	m	L	M3
Ptrofm3hcmnhb1707	*Pan*	*troglodytes*	b1707	amnh	f	L	M3
Ptromm3hcmnhb1708	*Pan*	*troglodytes*	b1708	cmnh	f	R	M3
Ptrofm3hcmnhb1713	*Pan*	*troglodytes*	b1713	cmnh	m	L	M3

specimen	Genus	Species	Catalog Number	Institution	Sex	Side	Stage
Ptrofm3hcmnhb1719	*Pan*	*troglodytes*	b1719	cmnh	f	R	M3
Ptrofm3hcmnhb1720	*Pan*	*troglodytes*	b1720	cmnh	f	L	M3
Ptrofm3hcmnhb1721	*Pan*	*troglodytes*	b1721	cmnh	f	L	M3
Ptrofm3hcmnhb1723	*Pan*	*troglodytes*	b1723	cmnh	f	L	M3
Ptromm3hcmnhb1738	*Pan*	*troglodytes*	b1738	cmnh	f	L	M3
Ptromm3hcmnhb1739	*Pan*	*troglodytes*	b1739	cmnh	m	L	M3
Ptromm3hcmnhb1745	*Pan*	*troglodytes*	b1745	cmnh	m	R	M3
Ptrofm3hcmnhb1748	*Pan*	*troglodytes*	b1748	cmnh	m	L	M3
Ptromm3hcmnhb1758	*Pan*	*troglodytes*	b1758	cmnh	f	L	M3
Ptrofm3hcmnhb1766	*Pan*	*troglodytes*	b1766	cmnh	m	R	M3
Ptrofm3hcmnhb1843	*Pan*	*troglodytes*	b1843	cmnh	f	R	M3
Ptromm3hcmnhb1882	*Pan*	*troglodytes*	b1882	cmnh	f	L	M3
Ptromm3hcmnhb2072	*Pan*	*troglodytes*	b2072	cmnh	m	L	M3
Ptromm3hcmnhb2746	*Pan*	*troglodytes*	b2746	cmnh	m	L	M3
Ptromm3hcmnhb2747	*Pan*	*troglodytes*	2747	cmnh	m	L	M3
Ptrofm3hcmnhb3539	*Pan*	*troglodytes*	b3539	cmnh	m	R	M3
Ptrofm3hcmnhb3551	*Pan*	*troglodytes*	b3551	cmnh	m	R	M3
Ptromm3hcmnhb3552	*Pan*	*troglodytes*	b3552	cmnh	f	L	M3
Ptroum3hrmca30660	*Pan*	*troglodytes*	30660	cmnh	f	L	M3
Ptrofm3hnmnh176226	*Pan*	*troglodytes*	176226	cmnh	m	L	M3
Ptrofm3hnmnh220064	*Pan*	*troglodytes*	220064	rmca	u	L	M3
Ptromm3hnmnh220327	*Pan*	*troglodytes*	220327	nmnh	f	L	M3

specimen	Genus	Species	Catalog Number	Institution	Sex	Side	Stage
Ptromm3hnmnh395820	*Pan*	*troglodytes*	395820	nmnh	f	L	M3
Ptromm3hnmnh48104	*Pan*	*troglodytes*	48104	nmnh	m	L	M3
Ptrofm3hvamnh89351	*Pan*	*troglodytes*	89351	amnh	m	L	M3
Ptrofm3hvamnh89354	*Pan*	*troglodytes*	89354	amnh	m	L	M3
Ptromm3hvamnh89355	*Pan*	*troglodytes*	89355	amnh	f	L	M3
Ptromm3hvamnh89406	*Pan*	*troglodytes*	89406	amnh	m	L	M3
Ptromm3hvamnh89407	*Pan*	*troglodytes*	89407	amnh	f	L	M3
Ptroum3hrmca30847	*Pan*	*troglodytes*	30847	rmca	m	L	M3
Ptromm2hamnh35199	*Pan*	*troglodytes*	35199	amnh	m	R	M2
Ptrofm2hamnh35550	*Pan*	*troglodytes*	35550	amnh	f	L	M2
Ptroum2hamnh90201	*Pan*	*troglodytes*	90201	amnh	u	L	M2
Ptromm2hamnh89352	*Pan*	*troglodytes*	89352	amnh	m	L	M2
Ptromm2hamnh89353	*Pan*	*troglodytes*	89353	amnh	m	L	M2
Ptromm2hamnh167342	*Pan*	*troglodytes*	167342	amnh	m	L	M2
Ptroum2hamnh167345	*Pan*	*troglodytes*	167345	amnh	u	L	M2
Ptrofm2hamnh201469	*Pan*	*troglodytes*	201469	amnh	f	L	M2
Ptromm2hamnh54330	*Pan*	*troglodytes*	54330	amnh	m	L	M2
Ptromm2hamnh90291	*Pan*	*troglodytes*	90291	amnh	m	L	M2
Ptromm2hamnh90293	*Pan*	*troglodytes*	90293	amnh	m	L	M2
Ptroum2hrmca23508	*Pan*	*troglodytes*	23508	rmca	u	L	M2
Ptromm2huzhcpal175	*Pan*	*troglodytes*	pal175	uzhc	m	L	M2
Ptrofm2hrmca89326	*Pan*	*troglodytes*	89326	rmca	f	L	M2

specimen	Genus	Species	Catalog Number	Institution	Sex	Side	Stage
Ptromm1hamnh201192	*Pan*	*troglodytes*	201192	amnh	m	L	M1
Ptrofm1hamnh35121	*Pan*	*troglodytes*	35121	amnh	f	L	M1
Ptromm1hamnh89425	*Pan*	*troglodytes*	89425	amnh	m	R	M1
Paspum3hamnh201239	*Pan*	*troglodytes*	201239	amnh	u	R	M3
Paspum3hamnh202874	*Pan*	*troglodytes*	202874	amnh	u	L	M3
Pannfm2hrmca16380	*Pan*	*troglodytes*	16316	rmca	f	L	M2
Psatmm2hrmca13716	*Pan*	*troglodytes*	13716	rmca	m	R	M2
Psatmm2hrmca29072	*Pan*	*troglodytes*	29072	rmca	m	L	M2
Psatfm2hrmca458	*Pan*	*troglodytes*	458	rmca	f	L	M2
Psatum2hrmca5378	*Pan*	*troglodytes*	5378	rmca	u	L	M2
Psatmm2hrmca5893	*Pan*	*troglodytes*	5893	rmca	m	L	M2
Ptscum2hrmca26494	*Pan*	*troglodytes*	26494	rmca	u	R	M2
Paspum2hamnh201242	*Pan*	*troglodytes*	201242	amnh	u	L	M2
Psatfm2hrmca11527	*Pan*	*troglodytes*	11527	rmca	f	L	M2
Psatfm2hrmca2487	*Pan*	*troglodytes*	2487	rmca	f	L	M2
Psatum2hrmca3430	*Pan*	*troglodytes*	3430	rmca	u	L	M2
Psatum2hrmca3472	*Pan*	*troglodytes*	3472	rmca	u	L	M2
Psatfm2hrmca5301	*Pan*	*troglodytes*	5301	rmca	f	L	M2
Psatfm2hrmca8257	*Pan*	*troglodytes*	8257	rmca	f	L	M2
Ptscum2hrmca23505	*Pan*	*troglodytes*	23505	rmca	u	L	M2
Ptscmm2hrmca30676	*Pan*	*troglodytes*	30676	rmca	m	L	M2
Pannum1hrmca26495	*Pan*	*troglodytes*	26495	rmca	u	L	M1

specimen	Genus	Species	Catalog Number	Institution	Sex	Side	Stage
Psatmm1hrmca12185	*Pan*	*troglodytes*	12185	rmca	m	R	M1
Psatmm1hrmca13094	*Pan*	*troglodytes*	13094	rmca	m	L	M1
Psatfm1hrmca13717	*Pan*	*troglodytes*	13717	rmca	f	L	M1
Psatum1hrmca15235	*Pan*	*troglodytes*	15235	rmca	u	L	M1
Psatum1hrmca21700	*Pan*	*troglodytes*	21700	rmca	u	L	M1
Psatum1hrmca25491	*Pan*	*troglodytes*	25491	rmca	u	L	M1
Psatmm1hrmca29076	*Pan*	*troglodytes*	29076	rmca	m	R	M1
Psatmm1hrmca5894	*Pan*	*troglodytes*	5894	rmca	m	R	M1
Ptscum1hrmca23504	*Pan*	*troglodytes*	23504	rmca	u	L	M1
Sysymm3hamnh106581	*Symphalangus*	*syndactylus*	106581	amnh	m	L	M3
Sysyfm3hamnh106583	*Symphalangus*	*syndactylus*	106583	amnh	f	L	M3
Sysyfm3hamnh106584	*Symphalangus*	*syndactylus*	106584	amnh	f	L	M3
Sysymm3hamnh140230	*Symphalangus*	*syndactylus*	140230	amnh	m	L	M3
Sysyfm3hnmnh271048	*Symphalangus*	*syndactylus*	271048	amnh	m	L	M3
Sysyfm2hamnh102463	*Symphalangus*	*syndactylus*	102463	amnh	f	L	M2
Sysyfm2hamnh106582	*Symphalangus*	*syndactylus*	106582	amnh	f	L	M2
Sysyfm2hamnh90337	*Symphalangus*	*syndactylus*	90337	amnh	f	L	M2
Sysymm2hamnh35613	*Symphalangus*	*syndactylus*	35613	amnh	m	L	M2
Sysyum1hamnh201316	*Symphalangus*	*syndactylus*	201316	amnh	u	L	M1
Sysyum1hamnh237504	*Symphalangus*	*syndactylus*	237504	amnh	u	L	M1
Sysyfm1hamnh90268	*Symphalangus*	*syndactylus*	90268	amnh	f	L	M1
Hosamm3hamnh203501	*Homo*	*sapiens*	203501	amnh	m	L	M3

specimen	Genus	Species	Catalog Number	Institution	Sex	Side	Stage
Hosamm3hamnh204072	*Homo*	*sapiens*	204072	amnh	m	L	M3
Hosafm3hamnh998376	*Homo*	*sapiens*	998376	amnh	f	L	M3
Hosafm3hcmnh1032	*Homo*	*sapiens*	1032	amnh	m	R	M3
Hosafm3hcmnh1065rr	*Homo*	*sapiens*	1065rr	amnh	f	L	M3
Hosafm3hcmnh1102rr	*Homo*	*sapiens*	1102rr	cmnh	f	R	M3
Hosafm3hcmnh1109r	*Homo*	*sapiens*	1109r	cmnh	f	R	M3
Hosafm3hcmnh1123r	*Homo*	*sapiens*	1123r	cmnh	f	L	M3
Hosamm3hcmnh1158rr	*Homo*	*sapiens*	1158rr	cmnh	f	R	M3
Hosamm3hcmnh1221	*Homo*	*sapiens*	1221	cmnh	m	R	M3
Hosamm3hcmnh1256	*Homo*	*sapiens*	1256	cmnh	m	R	M3
Hosamm3hcmnh1322	*Homo*	*sapiens*	1322	cmnh	m	L	M3
Hosamm3hcmnh1331	*Homo*	*sapiens*	1331	cmnh	f	L	M3
Hosafm3hcmnh1344r	*Homo*	*sapiens*	1344r	cmnh	f	R	M3
Hosamm3hcmnh1360	*Homo*	*sapiens*	1360	cmnh	m	R	M3
Hosafm3hcmnh1396	*Homo*	*sapiens*	1396	cmnh	m	R	M3
Hosamm3hcmnh1533	*Homo*	*sapiens*	1533	cmnh	m	L	M3
Hosafm3hcmnh1604	*Homo*	*sapiens*	1604	cmnh	m	L	M3
Hosafm3hcmnh1605	*Homo*	*sapiens*	1605	cmnh	f	R	M3
Hosamm3hcmnh1618	*Homo*	*sapiens*	1618	cmnh	m	R	M3
Hosamm3hcmnh496	*Homo*	*sapiens*	496	cmnh	f	R	M3
Hosafm3hcmnh512	*Homo*	*sapiens*	512	cmnh	m	R	M3
Hosamm3hcmnh729r	*Homo*	*sapiens*	729r	cmnh	f	L	M3

specimen	Genus	Species	Catalog Number	Institution	Sex	Side	Stage
Hosamm3hcmnh928r	*Homo*	*sapiens*	928r	cmnh	m	L	M3
Hosafm3hcmnh934	*Homo*	*sapiens*	934	cmnh	f	R	M3
Hosafm3hcmnhhth1562	*Homo*	*sapiens*	1562	cmnh	f	L	M3
Hosamm3hcmnhhth1769	*Homo*	*sapiens*	1769	cmnh	m	L	M3
Hosamm3hcmnhhth1926	*Homo*	*sapiens*	1926	cmnh	m	L	M3
Hosafm3hcmnhhth2056	*Homo*	*sapiens*	2056	cmnh	f	L	M3
Hosafm3hcmnhhth2057	*Homo*	*sapiens*	2057	cmnh	m	L	M3
Hosafm3hcmnhhth2105	*Homo*	*sapiens*	2105	cmnh	m	R	M3
Hosamm3hcmnhhth2268	*Homo*	*sapiens*	2268	cmnh	f	L	M3
Hosafm3hcmnhhth2303	*Homo*	*sapiens*	2303	cmnh	f	L	M3
Hosafm3hcmnhhth2511	*Homo*	*sapiens*	2511	cmnh	m	R	M3
Hosamm3hcmnhhth2525	*Homo*	*sapiens*	2525	cmnh	m	L	M3
Hosafm3hcmnhhth2857	*Homo*	*sapiens*	2857	cmnh	f	R	M3
Hosafm3hcmnhhth3123	*Homo*	*sapiens*	3123	cmnh	f	R	M3
Hosafm3hnmnh1512	*Homo*	*sapiens*	1512	nmnh	f	L	M3
Hosamm3hnmnh942	*Homo*	*sapiens*	942	nmnh	m	L	M3
Hosamm3hmuhac1415	*Homo*	*sapiens*	1415	muhnac	m	L	M3
Hosafm3hmuhac1418	*Homo*	*sapiens*	1418	muhnac	f	L	M3
Hosamm3hmuhac1569	*Homo*	*sapiens*	1569	muhnac	m	R	M3
Hosamm3hmuhac1593	*Homo*	*sapiens*	1593	muhnac	m	L	M3
Hosafm3hmuhac1672	*Homo*	*sapiens*	1672	muhnac	f	L	M3
Hosaum2hamnh90288	*Homo*	*sapiens*	90288	amnh	u	L	M2

specimen	Genus	Species	Catalog Number	Institution	Sex	Side	Stage
Hosafm2hmuhac83	*Homo*	*sapiens*	83	muhnac	f	L	M2
Hosafm2hmuhac175	*Homo*	*sapiens*	175	muhnac	f	L	M2
Hosamm2hmuhac258	*Homo*	*sapiens*	258	muhnac	m	L	M2
Hosamm2hmuhac336	*Homo*	*sapiens*	336	muhnac	m	R	M2
Hosamm2hmuhac379	*Homo*	*sapiens*	379	muhnac	m	L	M2
Hosamm2hmuhac380	*Homo*	*sapiens*	380	muhnac	m	L	M2
Hosamm2hmuhac684	*Homo*	*sapiens*	684	muhnac	m	L	M2
Hosafm2hmuhac759	*Homo*	*sapiens*	759	muhnac	f	R	M2
Hosamm2hmuhac1127	*Homo*	*sapiens*	1127	muhnac	m	L	M2
Hosamm2hmuhac1448	*Homo*	*sapiens*	1448	muhnac	m	R	M2
Hosamm2hmuhac1562	*Homo*	*sapiens*	1562	muhnac	m	R	M2
Hosafm2hmuhac1565	*Homo*	*sapiens*	1565	muhnac	f	L	M2
Hosamm2hmuhac1587	*Homo*	*sapiens*	1587	muhnac	m	L	M2
Hosafm2hmuhac1588	*Homo*	*sapiens*	1588	muhnac	f	L	M2
Hosafm2hmuhac1669	*Homo*	*sapiens*	1669	muhnac	f	L	M2
Hosafm2hmuhac1673	*Homo*	*sapiens*	1673	muhnac	f	L	M2
Hosafm1hnmdid127657	*Homo*	*sapiens*	127657	NMDID	f	L	M1
Hosafm1hnmdid159187	*Homo*	*sapiens*	159187	NMDID	f	R	M1
Hosafm1hnmdid177365	*Homo*	*sapiens*	177365	NMDID	f	L	M1
Hosamm1hnmdid169985	*Homo*	*sapiens*	169985	NMDID	m	L	M1
Hosamm1hnmdid181341	*Homo*	*sapiens*	181341	NMDID	m	L	M1
Hosamm1hnmdid183689	*Homo*	*sapiens*	183689	NMDID	m	L	M1

specimen	Genus	Species	Catalog Number	Institution	Sex	Side	Stage
Hosamm1hnmdid191031	*Homo*	*sapiens*	191031	NMDID	m	L	M1
Hosamm1hnmdid193039	*Homo*	*sapiens*	193039	NMDID	m	L	M1

APPENDIX C

CHAPTER IV SPECIMENS

Specimen	Genus	Species	Catalog Number	Institution	Sex	Side
Gobemm3hamnh54089	*Gorilla*	*beringei*	54089	amnh	m	L
Gobemm3hamnh54090	*Gorilla*	*beringei*	54090	amnh	m	L
Gobefm3hamnh54091	*Gorilla*	*beringei*	54091	amnh	f	L
Gobefm3hamnh54092	*Gorilla*	*beringei*	54092	amnh	f	L
Gobemm3hamnh115609	*Gorilla*	*beringei*	115609	amnh	m	L
Gobemm3hamnh202932	*Gorilla*	*beringei*	202932	amnh	m	L
Gobefm3hrmca2263	*Gorilla*	*beringei*	2263	rmca	f	L
Gobemm3hrmca8187	*Gorilla*	*beringei*	8187	rmca	m	L
Gobemm3hnmnh395636	*Gorilla*	*beringei*	395636	nmnh	m	L
Gogofm3hamnh167339	*Gorilla*	*gorilla*	167339	amnh	f	L
Gogomm3hamnh239597	*Gorilla*	*gorilla*	239597	amnh	m	L
Gogofm3hamnh54327	*Gorilla*	*gorilla*	54327	amnh	f	L
Gogomm3hamnh54355	*Gorilla*	*gorilla*	54355	amnh	m	L
Gogofm3hamnh54356	*Gorilla*	*gorilla*	54356	amnh	f	L
Gogofm3hamnh81652	*Gorilla*	*gorilla*	81652	amnh	f	L
Gogomm3hamnh90194	*Gorilla*	*gorilla*	90194	amnh	m	L
Gogomm3hamnh90289	*Gorilla*	*gorilla*	90289	amnh	m	L
Gogomm3hamnh90290	*Gorilla*	*gorilla*	90290	amnh	m	L
Gogomm3hcmnh2767	*Gorilla*	*gorilla*	2767	cmnh	m	L
Gogomm3hcmnhb1407	*Gorilla*	*gorilla*	b1407	cmnh	m	R

Specimen	Genus	Species	Catalog Number	Institution	Sex	Side
Gogomm3hcmnhb1409	*Gorilla*	*gorilla*	b1409	cmnh	m	L
Gogofm3hcmnhb1423	*Gorilla*	*gorilla*	b1423	cmnh	f	R
Gogofm3hcmnhb1710	*Gorilla*	*gorilla*	b1710	cmnh	f	R
Gogomm3hcmnhb1733	*Gorilla*	*gorilla*	b1733	cmnh	m	L
Gogofm3hcmnhb1756	*Gorilla*	*gorilla*	b1756	cmnh	f	L
Gogofm3hcmnhb1765	*Gorilla*	*gorilla*	b1765	cmnh	f	R
Gogofm3hcmnhb1798	*Gorilla*	*gorilla*	b1798	cmnh	f	L
Gogofm3hcmnhb1806	*Gorilla*	*gorilla*	b1806	cmnh	f	R
Gogofm3hcmnhb1856	*Gorilla*	*gorilla*	b1856	cmnh	f	R
Gogomm3hnbcl16865	*Gorilla*	*gorilla*	16865	nbcl	m	L
Gogomm3hnmnh174722	*Gorilla*	*gorilla*	174722	nmnh	m	L
Hosamm3hamnh203501	*Homo*	*sapiens*	203501	amnh	m	L
Hosafm3hcmnh1032	*Homo*	*sapiens*	1032	cmnh	f	R
Hosafm3hcmnh1065rr	*Homo*	*sapiens*	1065rr	cmnh	f	L
Hosafm3hcmnh1102rr	*Homo*	*sapiens*	1102rr	cmnh	f	R
Hosafm3hcmnh1109r	*Homo*	*sapiens*	1109r	cmnh	f	R
Hosafm3hcmnh1123r	*Homo*	*sapiens*	1123r	cmnh	f	L
Hosamm3hcmnh1158rr	*Homo*	*sapiens*	1158rr	cmnh	m	R
Hosamm3hcmnh1331	*Homo*	*sapiens*	1331	cmnh	m	L
Hosamm3hcmnh1360	*Homo*	*sapiens*	1360	cmnh	m	R
Hosafm3hcmnh1396	*Homo*	*sapiens*	1396	cmnh	f	R
Hosamm3hcmnh1533	*Homo*	*sapiens*	1533	cmnh	m	L

Specimen	Genus	Species	Catalog Number	Institution	Sex	Side
Hosafm3hcmnh1604	*Homo*	*sapiens*	1604	cmnh	f	L
Hosamm3hcmnh1618	*Homo*	*sapiens*	1618	cmnh	m	R
Hosamm3hcmnh496	*Homo*	*sapiens*	496	cmnh	m	R
Hosafm3hcmnh512	*Homo*	*sapiens*	512	cmnh	f	R
Hosamm3hcmnh729r	*Homo*	*sapiens*	729r	cmnh	m	L
Hosamm3hcmnh928r	*Homo*	*sapiens*	928r	cmnh	m	L
Hosafm3hcmnh934	*Homo*	*sapiens*	934	cmnh	f	R
Hosafm3hcmnhhth1562	*Homo*	*sapiens*	1562	cmnh	f	L
Hosamm3hcmnhhth1769	*Homo*	*sapiens*	1769	cmnh	m	L
Hosamm3hcmnhhth1926	*Homo*	*sapiens*	1926	cmnh	m	L
Hosafm3hcmnhhth2056	*Homo*	*sapiens*	2056	cmnh	f	L
Hosafm3hcmnhhth2057	*Homo*	*sapiens*	2057	cmnh	f	L
Hosafm3hcmnhhth2105	*Homo*	*sapiens*	2105	cmnh	f	R
Hosamm3hcmnhhth2268	*Homo*	*sapiens*	2268	cmnh	m	L
Hosafm3hcmnhhth2303	*Homo*	*sapiens*	2303	cmnh	f	L
Hosafm3hcmnhhth2511	*Homo*	*sapiens*	2511	cmnh	f	R
Hosamm3hcmnhhth2525	*Homo*	*sapiens*	2525	cmnh	m	L
Hosafm3hcmnhhth2857	*Homo*	*sapiens*	2857	cmnh	f	R
Hosafm3hcmnhhth3123	*Homo*	*sapiens*	3123	cmnh	f	R
Hyagmm3hnbcl4607	*Hylobates*	*agilis*	4607	nbcl	m	L
Hyagfm3hanmh106575	*Hylobates*	*agilis*	106575	anmh	f	L
Hyalfm3hamnh103665	*Hylobates*	*albibarbis*	103665	amnh	f	L

Specimen	Genus	Species	Catalog Number	Institution	Sex	Side
Hyalmm3hamnh103667	*Hylobates*	*albibarbis*	103667	amnh	m	L
Hyklmm3hamnh103344	*Hylobates*	*klossii*	103344	amnh	m	L
Hyklmm3hamnh103347	*Hylobates*	*klossii*	103347	amnh	m	L
Hylaum3hamnh119601	*Hylobates*	*lar*	119601	amnh	u	L
Hylafm3hamnh200752	*Hylobates*	*lar*	200752	amnh	f	L
Hylafm3hmocz41419	*Hylobates*	*lar*	41419	mocz	f	L
Hylafm3hmocz41421	*Hylobates*	*lar*	41421	mocz	f	L
Hylafm3hmocz41424	*Hylobates*	*lar*	41424	mocz	f	L
Hylamm3hmocz41427	*Hylobates*	*lar*	41427	mocz	m	L
Hylamm3hmocz41431	*Hylobates*	*lar*	41431	mocz	m	L
Hylafm3hmocz41440	*Hylobates*	*lar*	41440	mocz	f	L
Hylafm3hmocz41442	*Hylobates*	*lar*	41442	mocz	f	L
Hylamm3hmocz41464	*Hylobates*	*lar*	41464	mocz	m	L
Hylafm3hmocz41494	*Hylobates*	*lar*	41494	mocz	f	L
Hylamm3hmocz41505	*Hylobates*	*lar*	41505	mocz	m	R
Hylafm3hnmnh271047	*Hylobates*	*lar*	271047	nmnh	f	L
Nalafm3hamnh103669	*Nasalis*	*lar*	103669	amnh	f	L
Nalamm3hamnh106272	*Nasalis*	*lar*	106272	amnh	m	L
Nalamm3hamnh106273	*Nasalis*	*lar*	106273	amnh	m	R
Nalamm3hamnh106274	*Nasalis*	*lar*	106274	amnh	m	L
Nalamm3hamnh106275	*Nasalis*	*lar*	106275	amnh	m	L
Popymm3hamnh140426	*Pongo*	*pygmaeus*	140426	amnh	m	R

Specimen	Genus	Species	Catalog Number	Institution	Sex	Side
Popyfm3hamnh200563	*Pongo*	*pygmaeus*	200563	amnh	f	L
Popyfm3hcmnhb1055	*Pongo*	*pygmaeus*	b1055	cmnh	f	L
Popyfm3hcmnhb1167	*Pongo*	*pygmaeus*	b1167	cmnh	f	L
Popyfm3hnmnh145300	*Pongo*	*pygmaeus*	145300	nmnh	f	L
Popyfm3hnmnh145302	*Pongo*	*pygmaeus*	145302	nmnh	f	L
Popymm3hnmnh145304	*Pongo*	*pygmaeus*	145304	nmnh	m	L
Popyfm3hnmnh142169	*Pongo*	*pygmaeus*	142169	nmnh	f	L
Popyfm3hnmnh145309	*Pongo*	*pygmaeus*	145309	nmnh	f	L
Popyfm3hnmnh142169	*Pongo*	*pygmaeus*	142169	nmnh	f	L
Popymm3hnmnh145301	*Pongo*	*pygmaeus*	145301	nmnh	m	L
Popymm3hnmnh145305	*Pongo*	*pygmaeus*	145305	nmnh	m	L
Popymm3hnmnh153823	*Pongo*	*pygmaeus*	153823	nmnh	m	L
Ppanfm3hamnh86857	*Pan*	*paniscus*	86857	amnh	f	L
Ppanfm3hrmca13201	*Pan*	*paniscus*	13201	rmca	f	L
Ppanmm3hrmca13202	*Pan*	*paniscus*	13202	rmca	m	L
Ppanfm3hrmca15293	*Pan*	*paniscus*	15293	rmca	f	L
Ppanmm3hrmca15294	*Pan*	*paniscus*	15294	rmca	m	L
Ppanmm3hrmca15295	*Pan*	*paniscus*	15295	rmca	m	L
Ppanmm3hrmca15296	*Pan*	*paniscus*	15296	rmca	m	L
Ppanmm3hrmca23509	*Pan*	*paniscus*	23509	rmca	m	L
Ppanmm3hrmca27696	*Pan*	*paniscus*	27696	rmca	m	L
Ppanfm3hrmca27698	*Pan*	*paniscus*	27698	rmca	f	L

Specimen	Genus	Species	Catalog Number	Institution	Sex	Side
Ppanmm3hrmca27699	*Pan*	*paniscus*	27699	rmca	m	L
Ppanfm3hrmca29035	*Pan*	*paniscus*	29035	rmca	f	R
Ppanfm3hrmca29042	*Pan*	*paniscus*	29042	rmca	f	L
Ppanmm3hrmca29044	*Pan*	*paniscus*	29044	rmca	m	L
Ppanfm3hrmca29045	*Pan*	*paniscus*	29045	rmca	f	R
Ppanmm3hrmca29047	*Pan*	*paniscus*	29047	rmca	m	R
Ppanmm3hrmca29052	*Pan*	*paniscus*	29052	rmca	m	R
Ppanmm3hsbuc871	*Pan*	*paniscus*	uc871	hsb	m	L
Ptromm3hrmca23511m5	*Pan*	*troglodytes*	23511m5	rmca	m	L
Ptromm3hscrmca1048	*Pan*	*troglodytes*	1048	rmca	m	L
Ptroum3hscrmca14579	*Pan*	*troglodytes*	14579	rmca	u	L
Ptromm3hsrmca179	*Pan*	*troglodytes*	179	rmca	m	L
Ptroum3hsrmca3466	*Pan*	*troglodytes*	3466	rmca	u	L
Ptromm3hamnh10276	*Pan*	*troglodytes*	10276	amnh	m	L
Ptromm3hamnh165763	*Pan*	*troglodytes*	165763	amnh	m	L
Ptromm3hamnh167341	*Pan*	*troglodytes*	167341	amnh	m	L
Ptrofm3hamnh167343	*Pan*	*troglodytes*	167343	amnh	f	L
Ptromm3hamnh167344	*Pan*	*troglodytes*	167344	amnh	m	L
Ptromm3hamnh167346	*Pan*	*troglodytes*	167346	amnh	m	R
Ptrofm3hamnh174860	*Pan*	*troglodytes*	174860	amnh	f	L
Ptrofm3hamnh90292	*Pan*	*troglodytes*	90292	amnh	f	L
Ptrofm3hcmnhb1707	*Pan*	*troglodytes*	b1707	cmnh	f	L

Specimen	Genus	Species	Catalog Number	Institution	Sex	Side
Ptromm3hcmnhb1708	*Pan*	*troglodytes*	b1708	cmnh	m	R
Ptrofm3hcmnhb1713	*Pan*	*troglodytes*	b1713	cmnh	f	L
Ptrofm3hcmnhb1719	*Pan*	*troglodytes*	b1719	cmnh	f	R
Ptrofm3hcmnhb1720	*Pan*	*troglodytes*	b1720	cmnh	f	L
Ptrofm3hcmnhb1721	*Pan*	*troglodytes*	b1721	cmnh	f	L
Ptrofm3hcmnhb1723	*Pan*	*troglodytes*	b1723	cmnh	f	L
Ptromm3hcmnhb1738	*Pan*	*troglodytes*	b1738	cmnh	m	L
Ptromm3hcmnhb1739	*Pan*	*troglodytes*	b1739	cmnh	m	L
Ptromm3hcmnhb1745	*Pan*	*troglodytes*	b1745	cmnh	m	R
Ptrofm3hcmnhb1748	*Pan*	*troglodytes*	b1748	cmnh	f	L
Ptromm3hcmnhb1758	*Pan*	*troglodytes*	b1758	cmnh	m	L
Ptrofm3hcmnhb1766	*Pan*	*troglodytes*	b1766	cmnh	f	R
Ptrofm3hcmnhb1843	*Pan*	*troglodytes*	b1843	cmnh	f	R
Ptromm3hcmnhb1882	*Pan*	*troglodytes*	b1882	cmnh	m	L
Ptromm3hcmnhb2072	*Pan*	*troglodytes*	b2072	cmnh	m	L
Ptromm3hcmnhb2746	*Pan*	*troglodytes*	b2746	cmnh	m	L
Ptrofm3hcmnhb3539	*Pan*	*troglodytes*	b3539	cmnh	f	R
Ptrofm3hcmnhb3551	*Pan*	*troglodytes*	b3551	cmnh	f	R
Ptromm3hcmnhb3552	*Pan*	*troglodytes*	b3552	cmnh	m	L
Ptroum3hrmca30660	*Pan*	*troglodytes*	30660	rmca	u	L
Ptrofm3hnmnh176226	*Pan*	*troglodytes*	176226	nmnh	f	L
Ptrofm3hnmnh220064	*Pan*	*troglodytes*	220064	nmnh	f	L

Specimen	Genus	Species	Catalog Number	Institution	Sex	Side
Ptromm3hnmnh220327	*Pan*	*troglodytes*	220327	nmnh	m	L
Ptromm3hnmnh395820	*Pan*	*troglodytes*	395820	nmnh	m	L
Ptromm3hnmnh48104	*Pan*	*troglodytes*	48104	nmnh	m	L
Ptrofm3hvamnh89351	*Pan*	*troglodytes*	89351	amnh	f	L
Ptrofm3hvamnh89354	*Pan*	*troglodytes*	89354	amnh	f	L
Ptromm3hvamnh89355	*Pan*	*troglodytes*	89355	amnh	m	L
Ptromm3hvamnh89407	*Pan*	*troglodytes*	89407	amnh	m	L
Ptroum3hrmca30847	*Pan*	*troglodytes*	30847	rmca	u	L
Sysymm3hamnh106581	*Symphalangus*	*syndactylus*	106581	amnh	m	L
Sysyfm3hamnh106583	*Symphalangus*	*syndactylus*	106583	amnh	f	L
Sysyfm3hamnh106584	*Symphalangus*	*syndactylus*	106584	amnh	f	L
Sysyfm3hnmnh271048	*Symphalangus*	*syndactylus*	271048	nmnh	f	L
AL3221	*Aus*	*afarensis*	AL3221	NME	u	L
HnP0208	*Ho*	*neanderthalensis*	HnP0208	RLM	u	R
KNMER739	*Par*	*boisei*	KNMER739	NMK	u	R
AL2881	*Aus*	*afarensis*	AL2881	NME	f	R
StW431c	*Aus*	*africanus*	StW431c	DNM	u	R
Tm1517	*Par*	*robustus*	Tm1517	DNM	u	R
Uw8857b	*Aus*	*sediba*	Uw8857b	UWJ	f	R

REFERENCE CITED

Adams, D.C., Rohlf, FJ, Slice, D.E. 2004. Geometric morphometrics: ten years of progress following the 'revolution'. Italian Journal of Zoology. 71.1, 5-16.

Adams, D.C., Collyer, M.L. 2009. A general framework for the analysis of phenotypic trajectories in evolutionary studies. Evolution. 63(5):1143–1154.

Adams, D.C., Collyer, M.L., Kaliontzopoulou, A., & Baken, E. 2025. Geomorph: Software for geometric morphometric analyses. R package version 4.0.10. *https://cran.r-project.org/package=geomorph*.

Adams, D.C., Otárola-Castillo, E. 2013. geomorph: an R package for the collection and analysis of geometric morphometric shape data. *Methods in Ecology and Evolution*. 4(4):393–399.

Adolf, K.E., Franchak, J.M. 2017. The Development of Motor Behavior. WIREs Cognitive Science. 8, no. 1-2: 33-47.

Aiello, L., Dean, C. 1990. *An Introduction to Human Evolutionary Anatomy*. Academic Press, London.

Alméjica, S, Hammond, A.S., Thompson, N.E., Pugh, K.D., Moyà-Solà, S. and Alba, D.M. 2021. Fossil apes and human evolution. *Science*. 372(587) 1–12.

Alemseged, Z., Spoor, F., Kimbel, W.H., Bobe, R., Geraads, D., Reed, D. and Wynn, J.G. 2006. A juvenile early hominin skeleton from Dikika, Ethiopia. Nature. 443(7109). 296-301.

Arias-Martorell J., Potau, J.M., Bello-Hellegouarch, G., Pastor, J.F. and Pérez-Pérez, A. 2012. 3D geometric morphometric analysis of the proximal epiphysis of the hominoid humerus. Journal of Anatomy. 221.5, 394-405.

Arias-Martorell, J., Tallman, M., Potau, J.M., Bello-Hellegouarch, G. and Pérez-Pérez, A. 2015. Shape analysis of the proximal humerus in orthograde and semi-orthograde primates: Correlates of suspensory behavior. American Journal of Primatology. 77(1):1–19.

Arias-Martorell, J. 2018. The morphology and evolutionary history of the glenohumeral joint of hominoids: A review. Ecology and Evolution. 9, 703-722.

Bacon, A.M. 2000. Principal components analysis of distal humeral shape in Pliocene to recent African hominids: the contribution of geometric morphometrics. American Journal of Physical Anthropology. 111(4):479–487.

Baken, E., Collyer, M.L., Kaliontzopoulou, A., & Adams, D.C. 2021. geomorph v4.0 and gmShiny: enhanced analytics and a new graphical interface for a comprehensive morphometric experience. Methods in Ecology and Evolution. 12:12. 2355-2363.

Bender, R., Tobias, P.V. and Bender, N. 2012. The Savannah Hypothesis: Origin, Reception and Impact on Paleoanthropology. Hist. Phil. Life. Sci. 34, 147-184.

Berger, L.R. 2012. *Australopithecus sediba* and the earliest origins of the genus *Homo*. *JASs.* 90. 117-131.

Berger, L.R., De Ruiter, D.J., Churchill, S.E., Schmid, P., Carlson, K.J., Dirks, P.H. and Kibii, J.M. 2010. *Australopithecus sediba*: A New Species of *Homo*-Like Australopith from South Africa. Science. 328, 195-204.

Breuer, T., Hockemba, M.B.N., Olejniczak, C., Parnell, R.J. and Stokes, E.J. 2009. Physical maturation, life-history classes and age estimates of free-ranging western gorillas —insights from Mbeli Bai, Republic of Congo. American Journal of Primatology. 71(2) 106-119.

Bookstein, F.L. 1986. Size and shape spaces for landmark data in two dimensions. Statistical Science. 1(2):181–242.

Bookstein, F.L. 1991. Morphometric Tools for Landmark Data: Geometry and Biology. Springer-Verlag, New York.

Bookstein, F.L. 1996. Combining the tools of geometric morphometrics. In L.F. Marcus, M. Corti, A. Loy, G.J.P. Naylor & D.E. Slice (Eds.), Advances in Morphometrics (pp. 131–151). Springer, Boston.

Boren, S. 2014. 3-D Morphometric Analysis of the Primate Elbow Joint. University of Arkansas. Masters Thesis.

Bramble, D.M., Lieberman, D.E. 2004. Endurance running and the evolution of *Homo.* Nature. 432(7015), 345-352.

Broom, R. 1938. *Plesianthropus transvaalensis.* Transvaal Museum Memoirs. 2(1), 43-83.

Broom, R, Robinson, J.T. 1950. Man contemporaneous with the Swartkrans ape-man. *American Journal of Physical Anthropology*. 8(2), 151-156.

Broom, R, Schepers, G.W.H. 1946. *Paranthropus robustus* Paranthropus robustus Broom. Transvaal Museum Memoirs, *2*(1), 84-122.

Brunet, M. Pilbeam, D., Mackaye, H.T., Likius, A., Ahounta, D., Beauvilain, A., Blondel, C., Bocherens, H., Boisserie, J.R. and De Bonis, L. 2002. A new hominid from Upper Miocene of Chad, Central Africa. Nature, 418 (6894); 145-151.

Cant, J.G.H. 1987. Positional behavior of female Bornean orangutans (*Pongo pygmaeus*). American Journal of Primatology. 12(1):71–90.

Campisano, CJ., Feibel, C.S. 2007. Connecting local environmental sequences to global climate patterns: evidence from the hominin-bearing Hadar Formation, Ethiopia. Journal of Human Evolution. 53.5, 515-527.

Cardini, A. 2025. Allometry and phylogenetic divergence: Correspondence or incongruence?. The Anatomical Record. 308(3), 868-891.

Carlson, K.J, Green, D.J., Jashashvili, T., Pickering, T.R., Heaton, J.L., Beaudet, A., Stratford, D., Crompton, R., Kuman, K., Bruxelles, L. and Clarke, R.J. 2021. The pectoral girdle of StW 573 ('Little Foot') and its implications for shoulder evolution in the Hominina. Journal of Human Evolution. 158, 102983.

Churchill, S.E., Holliday, T.W., Carlson, K.J., Jashashvili, T., Macias, M.E., Mathews, S., Sparling, T.L., Schmid, P., de Ruiter, D.J. and Berger, L.R. 2013. The Upper limb of *Australopithecus sediba.* Science. 340.6219, 1233477.

Churchill, S.E., Green, D.J., Feuerriegel, E.M., Macias, M.E., Matthews, S., Carlson, K.J., Schmid, P. and Berger, L.R. 2018. Special Issue: *Australopithecus sediba,* The Shoulder, Arm, and Forearm, of *Australopithecus sediba*. PaleoAnthropology Society. 234-281.

Clarke, R.J. 1998. First ever discovery of a well-preserved skull and associated skeleton of *Australopithecus*. South African Journal of Science. 94, pp. 460-463.

Clarke, R.J. 2008. Latest information on Sterkfontein's *Australopithecus* skeleton and a new look at *Australopithecus:* research in action. South African Journal of Science. 104.11, 443-449.

Clarke, R. J., Tobias, P.V. 1995. Sterkfontein Member 2 foot bones of the oldest South African hominid. Science. 269, pp. 521-524.

Cazenave, M, Dean, C., Zanolli, C., Oettlé, A.C., Hoffman, J., Tawane, M., Thackeray, F. and Macchiarelli, R. 2020. Reassessment of the TMI1517 odonto-postcranial assemblage from Kromdraai B, South Africa and the maturational pattern of *Paranthropus robustus*. American Journal of Physical Anthropology. 172, 714-722.

Cazenave, M M., Pina, M., Hammond, A., Böhme, M., Begun, D., Spassov, N., Gazabón, A.V., Zanolli, C., Bergeret-Medina, A., Marchi, D. and Macchiarelli, R. 2024. Postcranial evidence does not support habitual bipedalism in *Sahelanthropus tchadensis*: A reply to Daver et al. (2022). Journal of Human Evolution. 103557.

Collyer, M.L., Adams, D.C. 2018. RRPP: an R package for fitting linear models to high-dimensional data using residual randomization. Methods in Ecology and Evolution. 9(10):1772–1780.

Collyer, M.L., Adams, D.C. 2024. RRPP: Linear model evaluation with randomized residuals in a permutation procedure. R package version 2.0.4. *https://cran.r-project.org/package=RRPP*.

Cooke, S.B., Terhune, C.E. 2015. Form, function, and geometric morphometrics. *The* Anatomical Record. 298(1):5–28.

Cowgill, L.W., Johnston, R.A. 2018. Biomechanical implications of the onset of walking. Journal of Human Evolution. 122:133–145.

Dart, R.A. 1925. *Australopithecus africanus*: The man-ape of South Africa. *Nature* 115.

Davers, G., Guy, F., Mackaye, H.T., Likius, A., Boisserie, J.R., Moussa, A., Pallas, L., Vignaud, P. and Clarisse, N.D. 2022. Postcranial evidence of late Miocene hominin bipedalism in Chad. Nature. 609, 94-100.

Deckers, K., segai, Z.J., Skinner, M.M., Zeininger, A. and Kivell, T.L. 2022. Ontogenetic changes to metacarpal trabecular bone structure in mountain and western lowland gorillas. Journal of Anatomy. 241: 82-100.

Delson, E. Chronology of South African australopith site units. Evolutionary history of the "robust" australopithecines. 317-324.

Demes, B., Tsegai, Z.J., Skinner, M.M., Zeininger, A. and Kivell, T.L.1991. Mechanical analysis of quadrupedal walking in primates: experiments with chimpanzees. Journal of Experimental Biology. 154:113–129.

Di Vincenzo, F., Rodriguez, L., Carretero, J.M., Collina, C., Geraads, D., Piperno, M. and Manzi, G. 2015. The massive fossil humerus from the Oldowan horizon of Gombore I, Melka Kunture (Ethiopia, >1.39 Ma). Quaternary Science Reviews. 122, 207-221.

Dobson, SD. 2005. Are the differences between StW 431 (*Australopithecus africanus*) and A.L. 288-1 (*A. afarensis*) significant?. Journal of Human Evolution. 49 (1). 143-514.

Doran, D.M. 1992. The ontogeny of chimpanzee and pygmy chimpanzee locomotor behavior: a case study of pedomorphism and its behavioral correlates. Journal of Human Evolution. 23(2):139–157.

Doran, D.M. 1997. Ontogeny of locomotion in mountain gorillas and chimpanzees. Journal of Human Evolution. 32.4, 323-344.

Doran, D.M. 1996. Comparative positional behavior of the African apes. In M. McGrew, L. Marchant & T. Nishida (Eds.), *Great Ape Societies* (pp. 213–224). Cambridge University Press.

Edgar, H.J.H, Daneshvari Berry, S., Moes, E., Adolphi, N.L., Bridges, P. and Nolte, K.B. 2020. New Mexico Decedent Image Database. Office of the Medical Investigator, University of New Mexico. doi.org/10.25827/5s8c-n515.

Fedorov, A., Beichel, R., Kalpathy-Cramer, J., Finet, J., Fillion-Robin, J.C., Pujol, S., Bauer, C., Jennings, D., Fennessy, F., Sonka, M. and Buatti, J. 2012. 3D Slicer as an Image Computing Platform for Quantitative Imaging Network. Magnetic Resonance Imaging. Nov; 3(9):1323=41. PMID: 22770690. PMCID: PMC3466397.

Feldesman, M.R. Morphometric analysis of the distal humerus of some Cenozoic Catarrhines: the Late Divergence Hypothesis revisited. American Journal of Physical Anthropology. 59,73-95.

Feibel, C.S, Brown, F.H. and McDougall, I. et al.1989. Stratigraphic context of fossil hominids from the Omo Group deposits: northern Turkana Basin, Kenya and Ethiopia. American Journal of Physical Anthropology. 78.4, 595-622.

Figus, C., Carlson, K.J., Bortolini, E., Saers, J., Seghi, F., Sorrentino, R., Bernardini, F., Vazzana, A., Erjavec, I., Novak, M. and Tuniz, C. 2025. The Ontogeny of the human calcaneus: insights from morphological and trabecular changes during postnatal growth. American Journal of Biological Anthropology. 186:e70007, 1-24.

Fleagle, J. Dynamic of a brachiating siamang [*Hylobates* (*Symphalangus*) *syndactylus*] Nature. 248, 5445.

Fleagle, J.G. 1976. Locomotion and posture of the Malayan siamang and implications for hominoid evolution. Folia primatological. 26(4), 245-269.

Fornai, C., Krenn, V.A., Mitteroecker, P., Webb, N.M. and Haeusler, M. 2021. Sacrum morphology supports taxonomic heterogeneity of "*Australopithecus africanus*" at Sterkfontein Member 4. Communications Biology. 4, 347. https://doi.org/10.1038/s42003-021-01850-7.

Frost, S.R., White, F.J., Reda, H.G. and Gilbert, C.C. 2022. Biochronology of South African hominin-bearing sites: A reassessment using cercopithecid primates. *PNAS*. 119 (45), pp. 1-9, e2210627119.

Gebo, D.L. 1996. Climbing, brachiation and terrestrial quadrupedalism: historical precursors of hominid bipedalism. American Journal of Physical Anthropology. 101(1):55–92.

Goodall, J. 1986. Social rejection, exclusion and shunning among the Gombe chimpanzees. Ethology and Sociobiology. 7.3-1, 227-236.

Goodall, C.R. 1991. Procrustes methods in the statistical analysis of shape. Journal of the Royal Statistical Society, Series B (Methodological). 53(2):285–321.

Granger D.E., Gibbon, R.J., Kuman, K., Clarke, R.J., Bruxelles, L. and Caffee, M.W. 2015. New cosmogenic burial ages for Sterkfontein Member 2 *Australopithecus* and Member 5 Oldowan. *Nature*. 85-88.

Granger, D.E., Stratford, D., Bruxelles, L., Gibbon, R.J., Clarke, R.J. and Kuman, K. et al. 2022. Cosmogenic nuclide dating of *Australopithecus* at Sterkfontein, South Africa. Proc. Natl. Acad. Sci. U.S.A. 119, e2123516119.

Green, D.J., Alemseged, Z. 2012. *Australopithecus afarensis* scapular ontogeny, function, and the role of climbing in human evolution. Science. 338.6106, 514-517.

Hatala, K.G., Demes, B. and Richmond, B.G. 2016. Laetoli footprints reveal bipedal gait biomechanics different from those of modern humans and Chimpanzees. Proceedings of the Royal Society B. 283, 20160235.

Haile-Selassie, Y., Latimer, B.M., Alene, M., Deino, A.L., Gibert, L., Melillo, S.M., Saylor, B.Z., Scott, G.R. and Lovejoy, C.O. 2010. An early *Australopithecus afarensis* postcranium from Woranso-Mille, Ethiopia. Proceedings of the National Academy of Sciences. 107.27, 12121-12126.

Harcourt-Smith, W.H.S. 2002. Form and function in the hominoid tarsal skeleton. Ph.D. Dissertation. University College London.

Harcourt-Smith, W.H.S, Aiello, L.C. 2004. Fossils, feet and the evolution of human bipedal locomotion. Journal of Anatomy. 204 (5), 403-416.

Hunt, K.D. 1991. Mechanical implications of chimpanzee positional behavior. American Journal of Physical Anthropology. 86:521–536.

Hunt, K.D. 1992. Positional behavior of *Pan troglodytes* in the Mahale Mountains and Gombe Stream National Parks, Tanzania. American Journal of Physical Anthropology. 87(1):83–105.

Hunt, K.D., Cant, J.G., Gebo, D.L., Rose, M.D., Walker, S.E. and Youlatos, D. 1996. Standardized description of primate locomotor and postural modes. *Primates*. 37, 363-387.

Huxley, J.S. 1932. *Problems of Relative Growth*. Methuen, London.

Ibáñez-Gimeno, P., P., Galtes, I., Manyosa, J., Malgosa, A. and Jordana, X. 2014. Analysis of the forearm rotational efficiency in extant hominoids: New insights into the functional implications of upper limb skeletal structure. Journal of Human Evolution. 76: 165-176.

Ibáñez-Gimeno, P., Manyosa, J., Galtes, I., Jordana, X., Moyà-Solà, S. and Malgosa, A. 2017. Forearm pronation efficienty in AL 288-1 (*Australopithecus afarensis*) and MH2 (*Australopithecus sediba*): Inisghts into their locomotor and manipulative habits. American Journal of Physical Anthropology. 164.4, 788-800.

Inouye, S.E. 1994. Ontogeny of knuckle-walking hand postures in African apes. Journal of Human Evolution. 26(5):459–485.

Jabbour, R.S. 2008. *Geographic variation in the forelimb and hindlimb skeletons of African apes*. Ph.D. diss., The City University of New York.

Johanson, D.C., White, T.D., & Coppens, Y. 1978. A new species of the genus *Australopithecus* (Primates: Hominidae) from the Pliocene of eastern Africa. *Kirtlandia*. 28:1–14.

Johanson, D.C., Edey, 1981. Lucy: The Beginnings of Humankind. Simon & Schuster, New York.

Josse, J, Husson, F. 2016. missMDA: A Package for Handling Missing Values in Multivariate Data Analysis. Journal of Statistical Software. 70.1, 1-31.

Karasik, L.B., Adolph, K.E., Tamis-LeMonda, C.S. and Zuckerman, A.L. 2012. Carry on: Spontaneous Object Carrying in 13-Month-Old Crawling and Walking Infants. Developmental psychology. 48.2, 389.

Karasik, L.B., Tamis-LeMonda, C.S., Adolph, K.E. and Bornstein, M.H. 2015. Places and Postures: A Cross-Cultural Comparison of Sitting in 5-Month-Olds. Journal of Cross-Cultural Psychology. 46, no. 8: 1023-1038.

Kawabe, M., Mano, T. 1972. Ecology and behavior of the wild proboscis monkey, *Nasalis larvatus*, in Sabah, Malaysia. *Primates*. 13(3):213–228.

Kibii, J.M., Clarke, R.J. 2003. A reconstruction of the StW 431 *Australopithecus* pelvis based on newly discovered fragments. South African Journal of Science, 99, 225-226.

Kimbel, W.H., Delezene, L.K. 2009. "Lucy" redux: A review of research on *Australopithecus afarensis*. American Journal of Physical Anthropology. 140(S49), 2-48.

Kimbel, W.H, White, T.D. 1988. Variation, sexual dimorphism and the taxonomy of *Australopithecus*. Evolutionary history of the "robust" australopithecines. Aldine de Gruyter, New York, 175-192.

Kimbel, W.H., Johanson, D.C. and Rak, Y. 1994. The first skull and other new discoveries of *Australopithecus afarensis* at Hadar, Ethiopia. Nature. 368.6470, 449-451.

Klingenberg, C.P. 2020. Walking on Kendall's shape space: understanding shape and its coordinate systems. Evolutionary Biology. 47(4):334–352.

Klingenberg, C.P., McIntyre, G.S. 1998. Geometric morphometrics of developmental instability: analyzing patterns of fluctuating asymmetry with Procrustes methods. *Evolution*. 52(5):1363–1375.

Kramers, J.D and Dirks, P.H.G.M. 2017a. The age of fossil StW573 ('Little Foot'): an alternative interpretation of 26A1/10Be burial data. South African Journal of Science. 113 p. #2016-0085.

Kramers, J.D and Dirks, P.H.G.M. 2017b. The age of fossil StW573 ('Little Foot"): reply to comments by Stratford et al., 2017. South African Journal of Science. 113, p. #a0222.

Knussman, R. 1967. Humerus, ulna und radius der simia. Bibliotheca Primatologica. 5: 1-399.

Köhler, M., Alba, D.M., Solà, S.M. and MacLatchy, L. 2002. Taxonomic affinities of the Eppelsheim femur. American Journal of Physical Anthropology. 119, 297-304.

Lague, M.R. 2014. The pattern of hominin postcranial evolution reconsidered in the light of size-related shape variation of the distal humerus. Journal of Human Evolution. 75:90–109.

Lague, M.R., Jungers, W.L. 1996. Morphometric variation in Plio-Pleistocene hominid distal humeri. American Journal of Physical Anthropology. 101, 401-427.

Lague, M.R., Menter, C.G. 2020. Distal Humerus: Hominin Postcranial Remains from Sterkfontein, South Africa 1936-1995, 49.

Larson, S.G .1998. Parallel evolution in the hominoid trunk and forelimb. Evolutionary. Anthropology. 6:87-99.

Larson, S.G. 2007. Evolutionary transformation of the hominin shoulder. Evolutionary Anthropology. 16(5), 172-187.

Latimer B. 1991. Locomotor adaptations in *Australopithecus afarensis*: the issue of arboreality. In: Senut B, Coppens Y, editors. Origine(s) de la bipe´die chez les Hominide´s. Paris: CNRS. p 169–176.

Latimer, B., Lovejoy, C.O. 1990a. Hallucal tarsometatarsal joint in *Australopithecus afarensis*. American Journal of Phyiscal Anthropology. 82.2. 125-133.

Latimer, B., Lovejoy, C.O. 1990b. Metatarsophalangeal joints of *Australopithecus afarensis*. American Journal of Physical Anthropology. 83.13-23.

Leakey, R. 1971. Further evidence of Lower Pleistocene hominids from East Rudolf, North Kenya. Nature. 231:241-245.

Leakey, M.D., Hay, R.L. 1979. Pliocene footprints in the Laetolil Beds at Laetoli, northern Tanzania. Nature. 278.5702, 317-323.

Le Gros Clark, W.E. 1947. Observation on the anatomy of the fossil Australopithecinae. Journal of Anatomy. 81, 300-333.

Lovejoy, C.O. 1981. The origin of Man. *Science*. 211(4480). 341-250.

Lovejoy, C. O. 1988. Evolution of human walking. Scientific American. 259:5, 118-125.

Luis Lopes Cemetery Collection. 2023. Museu Nacional de História Natural e da Ciência. University of Lisbon, Portugal.

Macchiarelli, R., Bergeret-Medina, A., Marchi, D. and Wood, B. 2020. Nature and relationships of *Sahelanthropus tchadensis*. Journal of Human Evolution. 149, 102898.

Malone, N.M. 2007. The Socioecology of the critically endangered Javan Gibbon (*Jylobates Moloch*): Assessing the Impact of Anthropogenic disturbance on Primate Social Systems. Ph.D. Dissertation. University of Oregon.

Malina, R.M, et al. 2004. Growth, maturation, and physical activity. Human kinetics.

Marzke, M.W. 1997. Precision grips, hand morphology, and tools. American Journal of Physical Anthropology. 102 (1). 91-110.

Marzke, M.W. 2013. Tool making, hand morphology and fossil hominins. Philosophical Transactions of the Royla Society B: Biological Sciences. 368.1630, 20120414.

Marcus, L.F., Corti, M. 1996. Overview of the new, or geometric, morphometrics. In L.F. Marcus et al. (Eds.), Advances in Morphometrics. 1–13. Springer, Boston.

McHenry, H.M. 1976. Multivariate analysis of early hominid humeri. *Measures and Man: Theory, Method & Case Studies in Anthropometry*. 338-371.

McHenry, H.M., Berger, L.R. 1998. Body proportions in *Australopithecus afarensis* and *A. africanus* and the origin of the genus *Homo*. Journal of Human Evolution. 35:1-22.

McHenry, H.M and Brown, C.C. 2008. Side step: the erratic pattern of hominin postcranial change through time. Journal of Human Evolution. 35: 1-22.

McHenry, H.M., Corruccini, R.S. Distal humerus in hominoid evolution. Folia Primatologica. 23.3, 227-244.

McNulty, K.P., Frost, S.R. and Strait, D.S. 2006. Examining affinities of the Taung child by developmental simulation. Journal of Human Evolution. 51.3, 274-296.

Meijaard, E., Nijman, V. 2000. Distribution and conservation of the proboscis monkey (*Nasalis larvatus*) in Kalimantan, Indonesia. Biological Conservation. 92(1):15–24.

Mitteroecker, P., Gunz, P. 2009. Advances in geometric morphometrics. Evolutionary Biology. 36(2):235–247.

Morimoto, N. 2018. Femoral ontogeny in humans and great apes and its implications for their last common ancestor. *Scientific reports*. 81 (2018): 1930.

Napier, J.R. 1967. The evolution of the hand and forearm in the anthropoid primates. *Philosophical Transactions of the Royal Society B*. 255(778):125–139.

Napier, J.R., Napier, P.H. 1967. *A Handbook of Living Primates*. Academic Press, London.

Oishi, M., Ogihara, N., Endo, H. and Asari, M. 2008. Muscle architecture of the upper limb in the orangutan. Primates. 49, 204-209.

Orr, C.M. 2018. Kinematics of the anthropoid os centrale and the functional consequences of scaphoid-centrale fusion in African apes and hominins. Journal of Human Evolution. 114, 102-117.

Pickering, R., Dirks, P.H., Jinnah, Z., De Ruiter, D.J., Churchill, S.E., Herries, A.I., Woodhead, J.D., Hellstrom, J.C. and Berger, L.R. 2011. *Australopithecus sediba* at 1.977 Ma and implications for the origin of the genus *Homo*. Science. 333, 1421-1423.

Pickering, R., Herries, A.I., Woodhead, J.D., Hellstrom, J.C., Green, H.E., Paul, B., Ritzman, T., Strait, D.S., Schoville, B.J. and Hancox, P.J. 2019. U-Pb-dated flowstones restrict South African early hominin record to dry climate phases. Nature. 565, 226-229.

Pina, M. 2016. Unraveling the positional behaviour of fossil hominoids: Morpho-functional and structural analysis of the primate hindlimb. Ph.D. Dissertation. Universitat Autònoma de Barcelona.

Pina M., Kikuchi, Y., Nakatsukasa, M., Nakano, Y., Kunimatsu, Y., Ogihara, N., Shimizu, D., Takano, T., Tsujikawa, H. and Ishida, H. 2021. New femoral remains of *Nacholapithecus kerioi*: Implications of intraspecific variation & Miocene hominoid evolution. Journal of Human Evolution. 155, 102982.

Pontzer, H., Raichlen, D.A. and Sockol, M.D. 2009. The metabolic cost of walking in humans, chimpanzees, and early hominins. Journal of Human Evolution. 56.1, 43-54.

Pusey, A.E. 1983. Mother-offspring relationships in chimpanzees after weaning. Animal Behaviour. 31,2, 363-377.

R Core Team, 2025. R: A language and environment for statistical computing Version 4.5.0. R Foundation for Statistical Computing. Vienna, Austria. https://www.R-project.org.

Randall, R.H. 1944. The skeletal and dental development and variability of the gorilla. Human Biology. 61(1), 23-76.

Reichard, U., Sommer, V. 1997. Group Encounters in Wild Gibbons (*Hylobates lar*) Agonism, Affiliation, and the Concept of Infanticide. Behaviour. 134, 15-16, 1135-1174.

Remis, M. 1995. Effects of body size and social context on the arboreal activities of lowland gorillas in the Central African Republic. American Journal of Physical Anthropology. 97.4, 413-433.

Remis, M. J. 1999. Tree structure and sex differences in arboreality among western lowland gorillas (*Gorilla gorilla gorilla*) at Bai Hokou, Central African Republic. Primates. 40, 383-396.

Rein, T.R., et al. 2017. Adaptation to suspensory locomotion in *Australopithecus sediba*. Journal of Human Evolution. 104, 1-12.

Richmond, B.G. 1998. Ontogeny and biomechanics of phalangeal form in primates. Ph.D. Dissertation. State University of New York at Stony Brook. 9917470.

Richmond, B.G. 2003. Early hominin locomotion and the ontogeny of phalangeal curvature in primates. *American Journal of Physical Anthropology*. 36, 178-179.

Richmond, B.G. 2007. Phalangeal curvature and locomotor behavior in extant apes and early hominins. *American Journal of Physical Anthropology*. 133(3):907–915.

Richmond, B.G., Strait, D.S. 2000. Evidence that humans evolved from a knuckle-walking ancestor. Nature. 404, 382-385.

Richmond, B.G., Green, D.J., Lague, M.R., Chirchir, H., Behrensmeyer, A.K., Bobe, R., Bamford, M.K., Griffin, N.L., Gunz, P., Mbua, E. and Merritt, S.R. 2020. The upper limb of *Paranthropus boisei* from Ileret, Kenya. Journal of Human Evolution. 141, 102727.

Rogol, A.D., et al. 2000. Growth and pubertal development in children and adolescents: effects of diet and physical activity. The American Journal of Clinical Nutrition. 72, 2. 521S-528S.

Rohlf, F.J. 1990. Morphometrics. *Annual Review of Ecology and Systematics*. 21:299–316.

Rohlf, F.J. 1999. Shape statistics: Procrustes superimpositions and tangent spaces. Journal of Classification. 16(2):197–223.

Rohlf, F.J. 2001. Comparative methods for the analysis of continuous variables: geometric interpretations. Evolution. 55(11):2143–2160.

Rosas, A., Pérez-Criado, L., Bastir, M., Estalrrich, A., Huguet, R., García-Tabernero, A., Pastor, J.F. and De la Rasilla, M. 2015. A geometric morphometrics comparative análisis of Neandertal humeri (epiphyses-fused) from El Sidrón cave site (Asturias, Spain). Journal of Human Evolution. 82, 51-66.

Rose, M.D. 1983. Miocene hominoid postcranial morphology: Monkey-like, ape-like, neither, or both? In Ciochon, R.L, & Corruccini, R.S. eds, *New Interpretations of Ape and Human Ancestry*. New York, Plenum Press. 405-417

Rose, M.D. 1988. Another look at the anthropoid elbow. Journal of Human Evolution. 17(2):193–224.

Rose, M.D. 1993. Functional anatomy of the elbow and forearm in primates. In D.L. Gebo (Ed.), *Postcranial Adaptations in Nonhuman Primates* (pp. 70–95). Northern Illinois University Press.

Ruff, C.B. Burgess, M.L., Bromage, T.G., Mudakikwa, A. and McFarlin, S.C. 2013. Ontogenetic changes in limb bone structural proportions in mountain gorillas (*Gorilla beringei beringei*). *Journal of Human Evolution*. 65, 693-703.

Ruff C.B. 2003a. Ontogenetic adaptation to bipedalism: Age changes in femoral to humeral length and *strength proportions in humans, with a comparison to baboons. Journal of Human Evolution.* 45:317–349.

Ruff C. 2003b. Growth in bone strength, body size, and muscle size in a juvenile longitudinal sample. *Bone*. 33:317–329.

Ruff, C. Holt, B. and Trinkaus, E. 2006. Who's afraid of the big bad Wolff?:"Wolff's law" and bone functional adaptation. *American Journal of Physical Anthropology*: *The official Publication of the American Association of Physical Anthropologists*. 129(4), 484-498.

de Ruiter, D.J., Churchill, S.E. and Berger, L.R. 2013. Chapter 9: *Australopithecus sediba* from Malapa, South Africa, from "The Paleobiology of *Australopithecus*". 147-160.

Saers, J.P.P. 2023. Skeletal indicators of developmental changes in arboreality and locomotor maturation in extant apes and their relevance to hominin paleobiology. *Front. Eco. Evol.* 11, 1-19.

Sarringhaus, L.A., MacLatchy, L.M. Mitani, J.C. 2014. Locomotor and postural development in wild chimpanzees. *Journal of Human Evolution*. 66, 29-38.

Sarringhaus, L.A., MacLatchy, L.M. Mitani, J.C. 2016. Long bone cross-sectional properties reflect changes in locomotor behavior in developing chimpanzees. *American Journal of Physical Anthropology*. 160(1), 16-29.

Schmitz, R.W. Serre, D., Bonani, G., Feine, S., Hillgruber, F., Krainitzki, H., Pääbo, S. and Smith, F.H. 2002. The Neandertal type site revisited: Interdisciplinary investigations of skeletal remains from the Neander Valley, Germany. *Proc. Natl. Acad. Sci.* 99 (20), 13342-13347.

Senut, B. 1981. Humeral outlines in some hominoids primates and in Plio-Pleistocene hominids. American Journal of Physical Antrhopology. 56:275-283.

Simons, E.A. 2019. Ontogeny and phylogeny of catarrhine crania: an analysis of the evolution of ontogenetic shape change trajectories using geometric morphometrics. Ph.D. Dissertation. University of Oregon.

Simons, E.A., Frost, S.R. 2016. Constructing cranial ontogenetic trajectories: A comparison of growth, development and chronological age proxies using a known-age sample of *Macaca mulatta.* American Journal of Physical Anthropology. 161.2, 296-308.

Simons, E.A., Turley, K., Frost, S.R. 2018. Trajectory analysis among African hominoids can provide insights into genetic and epigenetic influences during ontogeny. American Journal of Physical Anthropology. 167(1):173–177.

Simons, E.A., Turley, K., & Frost, S.R. 2019. Phylogenetic perspectives on catarrhine talocrural joint phenotypic plasticity. Anatomical Record (Hoboken). 302(11):1977–1984.

Simons, E.A, Frost, S.R. 2021. Ontogenetic allometry and scaling in catarrhine crania. Journal of Anatomy. 238.3, 693-710.

Simpson, S.W., Latimer, B. and Lovejoy, C.O. 2018. Why Do Knuckle-Walking African Apes Knuckle-Walk? The Anatomical Record. 301.3, 496-514.

Singleton, M. 2015. Functional geometric morphometric analysis of masticatory system ontogeny in papionine primates. The Anatomical Record. 2981, 48-63.

Slowikowski, K. 2024. ggrepel: Automatically position non-overlapping text labels with 'ggplot2'. R package version 0.9.4. *https://github.com/slowkow/ggrepel*.

Slice, D.E. 2007. Geometric morphometrics. Annual Review of Anthropology. 36:261–281.

Stern, J.T. JR., Susman, R.L. 1983. The locomotor anatomy of *Australopithecus afarensis*. American Journal of Physical Anthropology. 60(3), 279-317.

Stratford, D.J. et al. 2017. Comments on 'The Age of Fossil StW573 ('Little Foot') an alternative interpretation of 26A1/10Be burial data. South African Journal of Science. 113, p. #a0213.

Stratovan Corporation. 2018. Stratovan Checkpoint [Software]. Version 2018.08.07. https://www.stratovan.com/products/checkpoint.

Sutherland, D.H., Cooper, L., Daniel, D. 1980. The Role of the Ankle Plantar Flexors in Normal Walking. Journal of Bone & Joint Surgery. 62, no. 3: 354-363.

Su, D.F., Jablonski, N.G. 2009. Locomotor behavior and skeletal morphology of the odd-nosed monkeys. Folia Primatologica. 80(3):189–219.

Susman, R.L. Stern, Jr, J.T. and Jungers, W.L. 1984. Arboreality and bipedality in Hadar hominids. Folia primatologica. 43(2-3), 113-156.

Susman, R.L., Stern, J.T. 1982. Functional morphology of *Homo habilis*. Science, 217; 931-934.

Tallman, M. 2010. Postcranial variation in Plio-Pleistocene hominins of Africa. City University of New York.

Tallman, M. 2016. Shape Ontogeny of the Distal Femur in Hominidae with Implications for the Evolution of Bipedality. PloS one. 11.2, e0148371.

Tarrega-Saunders, E.L.R., King, C., Roberts, A.M., & Thorpe, S.K.S. 2021. Knuckle-walking and behavioural flexibility in great apes. *Revue de Primatologie*.

Taylor, A.B. 1997. Scapula for and biomechanics in gorillas. Journal of Human Evolution. 33.5, 529-553.

Toussaint, M., Macho, G.A., Tobias, P.V., Partridge, T.C. and Hughes, A.R. 2003. The third partial skeleton of a late Pliocene hominin (StW 431) from Sterkfontein, South Africa. South African Journal of Science, 99, 215-223.

Tuttle, R.H. 1969. Knuckle-Walking and the Problem of Human Origins: Studies on the hands of great apes and man lead to reevaluation of theories on hominoid evolution. *Science.* 166(3908), 953-961.

Tuttle, R.H. 1972. Knuckle-walking and the origin of hominid bipedalism. *Folia Primatologica*. 18(3–4):161–176.

Tuttle, R.H. 1981. Knuckle-walking and the origin of hominid bipedalism. *American Journal of Physical Anthropology*. 55(2):175–181.

Turley, K., Frost, S.R. 2014. The appositional articular morphology of the talo-crural joint: the influence of substrate use on joint shape. *Anatomical Record*. 297(4):618–629.

Turley, K., White, F.J. and Frost, S.R. 2015. Phenotypic Plasticity: The Impacto of Habitat and Behavior (Substrate Use) on Adult Talo-Crural Appositional Articular Joint Shape Both Between and Within Closely Related Hominoid Species. Human Evolution, 30.

Turley, K., Simons, E.A., Frost, S.R. 2018. Trajectory analysis among African hominoids can provide insights into genetic and epigenetic influences during ontogeny. American Journal of Physical Anthropology. 167, 173-177.

Vaesen, K., Galliari, S., & Hélie, S. 2020. The biomechanical importance of the scaphoid-centrale fusion during simulated knuckle-walking and its implications for human locomotor evolution. Journal of Human Evolution. 143:102777.

Ward, C.V., Leakey, M.G. and Walker, A. 2001. Morphology of *Australopithecus anamensis* from Kanapoi and Allia Bay, Kenya. Journal of Human Evolution. 41:255-368.

Ward, C.V. 2002. Interpreting the posture and locomotion of *Australopithecus afarensis*: Where do we stand. American Journal of Physical Anthropology. 119, S35, 185-215.

Washburn, S.L. Lancaster, C.S. 1968. The evolution of hunting—Perspectives on the man evolution. Science review 1. 213-229.

Wheeler, P.E. 1991. The influence of bipedalism on the energy and water budgets of early hominids. Journal of Human Evolution. 21(2), 117-136.

Wiley, D.F., Amenta, N., Alcantara, D.A., Ghosh, D., Kil, Y.J., Delson, E., Harcourt-Smith, W., Rohlf, F.J., St John, K. and Hamann, B. 2005. Evolutionary morphing. In Proceedings IEEE Visualization 2005. 431-438.

White, F.J. 1996. *Pan paniscus*: 1973 to 1996: twenty-three years of field research. Evolutionary Anthropology. 5(6):161–167.

White, F.J., et al. 2020. Sex differences in bonobo (*Pan paniscus*) terrestriality: implications for human evolution. *Journal of Anthropological Sciences*. 98:5–14.

White, T.D., Suwa, G. 1987. Hominid footprints at Laetoli: Facts and interpretations. American Journal of Physical Anthropology. 72: 485-514.

Wickham, H. 2016. *ggplot2: Elegant Graphics for Data Analysis*. Springer, New York.

Young, N.M. 2003. A reassessment of living hominoid postcranial variability: implications for ape evolution. Journal of Human Evolution. 45.6, 441-464.

Zelazny, K. G. 2019. Morphological variation in the distal humerus of extant hominids and fossil hominins. Ph.D. Dissertation, Johns Hopkins University.

Zelditch, M.L., Swiderski, D.L., Sheets, H.D. 2012. Geometric Morphometrics for Biologists: A Primer (2nd ed.). Elsevier, Amsterdam.

Zipfel, B and Berger. L.R. 2010. New Cenozoic fossil bearing site abbreviations for the collection of the University of the Witwatersrand. *Palaeontologia africana*. 44. 77-80.

Zollikofer, C.P.E., and Ponce de León, M.S. 2010. The evolution of hominin ontogenies. Seminars in Cell & Developmental Biology. 21, 441-452.